Intelligent Novel MSW Management System for Biogas Control in Landfill

Ahmad Qasaimeh

A Thesis

in

Department of Building, Civil, and Environmental Engineering

Presented in Partial Fulfillment of the Requirements
for the Degree of Doctor of Philosophy at
Concordia University
Montreal, Quebec, Canada

August 2006

Your file Votre référence
ISBN: 978-0-494-23840-0
Our file Notre référence
ISBN: 978-0-494-23840-0

ABSTRACT

Intelligent Novel MSW Management System for Biogas Control in Landfill

Ahmad Qasaimeh, PhD.
Concordia University, 2006

Controlling greenhouse gases at landfill is a great point of concern. This research aims to control methane and carbon dioxide by applying novel intelligent MSW management system. The intelligent MSW management system (Intelligent QEJ Bricks) proposed in this research provides new ideas about: landfill operation, material for biogas collection, biogas transport modeling, biogas mass transfer optimization, design configuration, and automatic control system.

The operation of new system includes series of cells built subsequently with porous bricks that confines waste cells. This approach implies integrated operation system that combines waste disposal, biogas evacuation, and biogas control. Bricks are made up of hydrophobic recyclable material that might be available on waste disposal site. In this research, a recyclable hydrophobic polymer (Styrofoam) was tested at laboratory to check its functionality for biogas collection. The test procedure on polymer medium entails the following findings: the permeability, the conductivity and diffusion coefficients, the convective flowrate, and the diffusive flux through polymer medium for carbon dioxide and methane. The influence of parameters such as water content, porosity, temperature variation, pressure gradient, and concentration gradient on gas movement (diffusion and convection) was also analyzed.

Information obtained from the laboratory tests were formulated as knowledge bases. The fuzzy logic implicated knowledge bases and specific rules to have the output that

represents the gas transport rates in hydrophobic polymer medium for a wide range of various environmental parameters.

Genetic algorithm is used to optimize a transfer function that represents solutions for transfer rates for different ratios of biogas mixture. The mass and volume of biogas within the landfill time of service are determined for designing hydrophobic porous bricks for any ratio of CH_4:CO_2 in landfill.

After having the cells finished and closed the configuration of the new system satisfies confining the waste with hydrophobic porous walls that surrounds the waste and captures all available biogas generated at the landfill. The design includes a system of valves evacuating biogas from porous walls of the bricks. The process of evacuation might link the valves with a blower that is connected with a storage tank or an energy generator. The valves are controlled by fuzzy logic system that is fed by sensors-data acquisition system. The output of automatic intelligent fuzzy system is dependent on the input data from the sensor-data acquisition system.

ACKNOWLEDGEMENT

My great thanks go to Almighty Allah, whom I submit my continuous gratitude.

I wish to thank my supervisors: Dr. Maria Elektorowicz and Dr. Iwona Jasiuk for their guidance, time, and support.

I would like to acknowledge the NSERC (National Science and Engineering Research Council), the Faculty of Engineering and Computer Science Research Funds, and Concordia graduate fellowships for their financial support.

A great love and warm feelings submitted to my parents; to my mother, whom I need to spend hundreds of lives to award; to my father, the source of my strength. Never-ending thanks to my brothers, Ghazi, Mohammad, Omar. My virtual love to all my sisters (Aishah, Ghazia, Amal, Manal, Amal, Izdihar). My special appreciation conveyed to my friends (Montasir, Ameen, Malik) to M3en, Asim, Odat, Janaydeh and all friends in Montreal. To the spirit of my lovely sister Eman who left very fast may Allah bless you in Paradise. My great feelings to my wife and my son Laji they make my life different.

CONTENT

List of Figures

List of Tables

NOMENCLATURE

ρ:	Density of the fluid (kg/m^3)
φ:	Porosity of the landfill (m^3 of voids per m^3 of refuse)
μ:	Dynamic viscosity of the fluid (Pa.s)
ρ_b:	Bulk density (kg/ m^3)
ε_g:	Gas fraction in the porous pores
f_i:	Gas fugacity (Pa): a molecule tendency to flee from one phase to another
δ_{k3}:	Kronecker's delta: $\delta_{13} = \delta_{23} = 0$; $\delta_{33} = 1$ (dimensionless)
∇P:	Pressure gradient (N/m^2/m)
ρ_s:	Solid density (kg/ m^3)
θ_w:	Volumetric water content in the porous medium
$\overline{V}_i$:	Partial molar volume of i in the gas mixture (m^3/mol)
o:	Represents the CRI operator
U':	Represents the output (conclusion)
$A', B', ..., C'$:	Represents the inputs (observations)
AOM:	Average of maximums
C:	Concentration of the diffusing substance (kg/m^3)
COA:	Center of area
CRI:	Compositional rule of inference
C_T:	Total gas concentration in multi-phases (g/L)
C_w:	Gas concentration in porous porewater (g/L)

D_e:	Diffusion coefficient (m^2/s)
$D_{w,e}$:	Effective diffusivity coefficient of gas (m^2/s)
FDSS:	Fuzzy Decision Support System
F_g:	Mass transfer rate per unit area (kg/ s. m^2)
FIS:	Fuzzy Inference System Editor
g:	Acceleration due to gravity (m/s^2)
GA:	Genetic Algorithm
G_i:	Generation rate of the i^{th} component of the gas mixture (kg/day)
GUI:	Graphical user interface in the Fuzzy Logic Toolbox
H_c:	Henry's constant ($Pa.m^3/g$)
k:	Intrinsic permeability of the porous material (m^2)
K:	The conductivity coefficient (cm/s)
K_d:	Linear adsorption constant (m^3/kg)
MCOA:	Modified center of area (m^2)
M_i:	Molecular weight of gas i (kg/mol)
MSW:	Municipal solid waste
P_i:	Partial pressure of gas i (N/m^2)
R:	Universal gas constant (N.m/mol.°K)
r_a:	Rate of reaction for gain or loss
T:	Absolute temperature (°K)
U_k:	Advective velocity in the k^{th} direction (m/day)
Z:	Spatial coordinate (m)
Z_i:	Fugacity capacity (mol/m^3 Pa)

CHAPTER 1

Literature Review- Statement of the Problem

1.1. Introduction

The control of biogas, carbon dioxide and methane, in municipal landfills is an important issue due to the significance of these gases in terms of their pollution, hazards, and benefits.

Leachate and biogas are the two emissions that are characteristic of municipal solid waste (MSW) landfills (Manna et al. 1999). The anaerobic decomposition of landfilled MSW generates large amounts of gas composed of 50-60% CH_4 (by volume), 40-50% CO_2, and other trace gases such as nitrogen and volatile organic hydrocarbons (Kightley et al. 1995; Czepiel et al. 1996). Landfill gas is basically made up of half methane and half carbon dioxide, two potent greenhouse gases, as well as small amounts of hydrogen, oxygen, nitrogen and trace amounts of non-organic compounds and volatile organic compounds (Gardner et al. 1993). When released to the atmosphere, landfill biogas represents a threat to the environment, because both methane and carbon dioxide biogases are greenhouse gases. Methane is 21 times more powerful a greenhouse gas than carbon dioxide with a long lifespan of 150 years (Pacey 1986).

Landfills are estimated to account for approximately 25% of annual anthropogenic CH_4 emissions in the United States (Czepiel et al. 1996) and as much as 20% of the global anthropogenic CH_4 emissions (Nozhevnikova et al. 1993). Also; several of the produced

organic compounds present health hazards. Furthermore, methane is explosive when its volumetric concentration attains 5% to 15% in an air mixture. Safety and environmental concerns require that gas emissions be controlled at landfills (Nastev et al. 2001).

The landfill gas has been widely used as a fuel gas and hence landfill gas systems, especially in the western world, are developed to exploit this renewable source of energy (Shekdar 1997). A review by Richards and Aitchinson (1990) identified 242 sites in 20 nations where landfill gas was being tapped and used as a fuel with total energy contribution exceeding of 2.037 million tonnes of coal equivalent per annum.

There are two main ways to capture biogas emission from landfills. One option, like those in Northern Europe where there are many small and old landfills with low gas generation that is biologically uptaken (Jones and Nedwell 1993; Boeckx et al. 1996; Börjesson and Svensson 1997). Biological biogas uptake at landfills is apparently executed by biological methane oxidation by methanotrophs and carbon dioxide uptake by plants. Other option is gas collection and utilization, which could be very effective with a high gas generation. In this case, biogas can be collected by means of vertical and horizontal drain pipes and is employed to produce heat and energy. There are different technologies being studied to find the best handling of biogas collection (Andreottola and Cossu 1988; EMCON Associates 1980; El-Fadel 1991).

1.2. Biogas Capture in Landfill

Biogas in landfill is being captured by natural and engineered processes. The natural processes is represented by biological activities occurred in landfill such as bacterial methane oxidation and plant uptake for carbon dioxide at topsoil layer. The engineered processes are represented by different physical approaches of biogas extraction.

1.2.1. Biological Biogas Capture

1.2.1.1. Biological Methane Oxidation

While soils have not been considered as significant sinks for methane until recently, methane consumption has been reported in agricultural soils, forest soils, tundra, and bogs (Topp and Hanson 1991).

Recently, biological oxidation of CH_4 by bacterial methanotrophs has attracted much attention from the research community as an inexpensive waste gas treatment mechanism. Methane oxidizing activity, with a decrease in soil oxygen and an increase in microbial biomass, has been demonstrated in soils around leaks in natural gas pipes (Adams and Ellis 1969) and in landfill covers (Kightley et al. 1995; Whalen et al. 1990; Bogner et al. 1995). Methane oxidizing activity in soils is an event that could have a strong effect on CH_4 emissions control from sources such as municipal landfills, and the optimization of this process may give out an inexpensive strategy for controlling and utilizing emissions of this potent greenhouse gas.

Microbial oxidation in well-drained soils is the only identified biological sink for atmospheric CH_4 and accounts for 3% to 9% of total annual atmospheric CH_4 destruction

(Prather et al. 1996). This is similar in magnitude to the current atmospheric increase (Houghton et al. 1996). Accordingly, alterations of the soil sink strength are a significant determinant of the rate of change in the atmospheric CH_4 concentration (Prather et al. 1996) and absence of this sink will cause the atmospheric CH_4 concentration to increase at 1.5 times the current rate (Duxbury 1994). The control of aerobic methane oxidation is obviously related to the requirement for oxygen and methane. As a result, maximum oxidation rates are found where diffusion of oxygen from above and of methane from below is optimal for methanotrophs (King 1992; Sundh et al. 1995a; Sundh et al. 1995b).

Jia-ying et al. (2004) showed that methanotrophs oxidizes methane to carbon dioxide through sequential reactions catalyzed by a series of enzymes including methane monooxygenase, methanol dehydrogenase, formaldehyde dehydrogenase, and formate dehydrogenase. Methanotrophic bacteria cultivate aerobically on methane as a sole source of carbon and energy. The first two enzymes involved in methane oxidation are methane monooxygenase (MMO) and methanol dehydrogenase (MDH) (Anthony 1986). MMO oxidizes methane to methanol, and MDH catalyzes the oxidation of methanol to formaldehyde. *Methylosinus trichosporium* OB3b is a methanotrophic bacterium and contains two forms of MMOs: a soluble (sMMO) and a membrane-bound particulate (pMMO) whose syntheses depend on growth conditions (Murrell et al. 2000; Nielson et al. 1997; Takeguchi 2000).

Landfill gas is transported through soil layers in landfill top covers or in nearby areas before being released to the atmosphere. Whilst transported in the soil layers the biogas is mixed with atmospheric air, and the methane may hence be oxidized by the methanotrophic bacteria in the soil using oxygen from atmosphere. Methane oxidation is affected by different environmental factors such as: temperature, water content, nutrients, substrate, and oxygen concentrations (Hanson and Hanson 1996). In the following sections is the description of environmental factors effect on methane oxidation.

- Effect of Soil Moisture

Christophersen et al. (2000) showed that methane oxidation rate is a function of soil moisture content at different temperatures for the different soils. The optimum soil moisture content was different for each soil and depended on the temperature. Some soils had the lowest optimum soil moisture content and others had the highest. At lower temperatures the difference in oxidation rates with soil moisture content was reduced.

Methane oxidation rates decreased extensively after soil samples were dried below field moisture contents, increased to an optimum value as water was added, and decreased with sustaining water addition. The maximum oxidation rate occurred at moisture content of 15.4% (dry weight basis) (Stein and Hettiaratchi 2001). The texture and structure of soil will influence its moisture content in a manner that is site specific, depending on climatic variables such as temperature, solar flux, average wind speed and the type of vegetative cover (Stein and Hettiaratchi 2001). Methane uptake was controlled strongly by soil moisture, with reduced fluxes under conditions of very low or very high soil

moisture contents. The mineral soil Q10 (Q10 is the value for how many times the oxidation rate increases when temperature is increased 10°C at temperatures below the optimum temperature) of 1.11 for CH_4 uptake indicates that methane uptake is controlled primarily by physical processes (Bowden et al. 1998).

- *Effect of Temperature*

Christophersen et al. (2000) showed for all the soil investigations, the oxidation rate increased with increasing temperature. Predictably, optimum temperatures were not found in this experimentation. For all the soils the optimum temperature must be higher than 15°C, which was the highest temperature in these explorations. Most researchers found optimum temperatures around 30°C, which do seldom occur in temperate soils. Dunfield et al. (1993) found optimum temperatures for the methane oxidation around 25°C. As the temperature is increased, CH_4 oxidation increases exponentially to maximum and then decreases with continued temperature increase (Stein and Hettiaratchi 2001).

At high methane concentrations the oxidation becomes saturated, and the rate-limiting stage is the enzymatic action. Thus, the temperature response is something like parabolic: increasing rates with increasing temperature to a maximum and declining with continued temperature increase (Bailey and Ollis 1986). King and Adamsen (1992) investigated soil cores where the temperature was increased between 0°C and 30°C. The depth distribution of methane consumption and methane diffusion showed low sensitivity to changes in temperature. They observed methane consumption at -1°C, and they suggested that

methane consumption might occur at low temperatures on condition that the soil water remains liquid. Sommerfeld et al. (1993) showed that the soil microflora was active even when the soil was snow-covered and near 0°C and that methane consumption was taking place under that condition. In the 0-10°C range methane oxidation was about 13-38% of maximum activity. Priemé and Christensen (1997) observed methane oxidation to be active at low temperatures, down to 1°C in the field and -2°C in soil core experiments. Both in the field and in soil cores similar temperature responses of methane oxidation were measured. This indicated that temperature acts directly (i.e., via its effect on enzymatic processes and methane diffusion) on methane oxidation in the field. They suggested that the small temperature response of methane oxidation was partly a result of low substrate concentration.

- *Effect of Organic Matter Content and Methane Concentration*

Oxidation rates increased with increasing organic matter content. The optimum soil moisture content also increased with increasing organic matter content (Christophersen et al. 2000). Oxidation of methane in top covers of landfills has been observed on several occasions, and soil exposed to elevated methane concentrations can develop a high potential for methane oxidation (Whalen et al. 1990; Kightley et al. 1995; Boeckx et al. 1996; Czepiel et al. 1996; Börjesson and Svensson 1997; Bogner et al. 1997). Low initial methane concentrations resulted in low maximal oxidation rates (Boeckx and Van Cleemput 1996; Boeckx et al. 1996). The oxidation rates at low initial methane concentrations were much lower than oxidation rates at high initial methane concentrations, and the oxidation was performed by different kinds of bacteria (Bender

and Conrad 1992). Several researchers have shown that different species of bacteria are active at low and high methane concentrations (Bender and Conrad 1994; Kightley et al. 1995; Bogner et al. 1997).

- *Effect of Nitrogen Content*

There is a worldwide increase in atmospheric nitrogen (N) deposition on terrestrial and aquatic environments (Matthews 1994; Galloway et al. 1995). Methanotrophs are inhibited by high soil N; driving attention that the contemporary worldwide increase in atmospheric N deposition will decrease soil CH_4 oxidation. CH_4 oxidation by methanotrophic and methylotrophic bacteria occurs in aerobic soils and the magnitude and rate of oxidation are influenced by soil type, aeration, environmental parameters and Nitrogen availability (Topp and Pattey 1997; Le Mer and Roger 2001). Application of fertiliser has been shown to inhibit CH_4 oxidation in soil (Steudler et al. 1989; Hu¨tsch 1998; Tlustos et al. 1998; Kravchenko et al. 2002). Nitrogen content frequently shows low atmospheric CH_4 oxidation comparative to unfertilized controls (Steudler et al. 1989; King and Schnell 1994; Sitaula et al. 1995).

In two marshes, the vertical distribution of methane oxidation in the sediment and methane oxidation inhibition by ammonium was investigated by Van Der Nat (1997). In a slurry incubation experiment, he conducted tests for two sites different in their prevailing vegetation type, i.e., reed and bulrush, and in their heights above sea level. Inhibition of methane oxidation by ammonium was observed in all samples and depended on methane and ammonium concentrations. Increasing ammonium concentrations

resulted in more inhibition, and increasing methane concentrations resulted in less inhibition. Increasing atmospheric concentrations of CO_2 may increase emissions of N_2O by denitrification, and either increase or decrease the ability of soil to buffer atmospheric CH_4 depending on fertilizer application (Baggsa and Blum 2004).

- Effect of Leachate Recirculation, Metals, and Minerals

Leachate recirculation is one option for inexpensive leachate disposal (Kinman et al. 1987; Cureton et al. 1991), in reducing the cost of post-closure care and long-term liability (Diamadopoulous 1994; Westlake 1995; Reinhart and Al-Yousfi 1996). It could participate to improve leachate quality; reduce volume of leachate to be treated; and enhance gas production (Reinhart 1996; Sulisti et al. 1996; Mostafa et al. 1999; Warith et al. 1999). Chan et al. (2002) found that leachate recirculation reduced waste stabilization time and was effective in enhancing gas production and improving leachate quality, especially in terms of COD (Chemical Oxygen Demand). The results also indicated that leachate recirculation could maximize the efficiency and waste volume reduction rate of landfill sites. Leachate recirculation gives an aqueous environment that assists the supply of nutrients and biomass within the landfill that stimulates the degradation of municipal solid waste (El-Fadel 1999). Mobilizing nutrients and microorganisms in aqueous wastes improves mass transfer to prevent the development of inactive zones in landfill zones (Chugh et al. 1998).

Maurice (1999) showed that larger trees arise on plots irrigated with leachate, presumably due to the positive effect of water and nutrient supply. Methane oxidation levels between

50 and 950 mol/m^2.yr were observed. The positive relationship between soil methane oxidation capacity and tree existence is important for reduction of methane emission by landfill vegetation type. Optimizing methane oxidation using vegetation on topsoil could reduce the amount of methane released to the atmosphere (Maurice 1999). Leachate provides the soils with higher content of water, nutrient, and organic matter, it also provides metals. Heavy metals affect the growth, morphology and metabolism of microorganisms of soils through functional disturbance, protein denaturation, or the destruction of the integrity of the cell membrane (Baath 1989; Babich and Stozky 1980; Leita et al. 1995). In a laboratory incubation study, Mishra et al. (1999) showed that selected heavy metals in three rice soils were different in their effect on methanogenesis and methane-producing bacteria. Cd, Cu, and Pb inhibited CH_4 production in all soils. Zn stimulated CH_4 production in the alluvial soil, but inhibited it in laterite and acid sulfate soils. Cr effectively inhibited CH_4 production in the alluvial soil, but stimulated it in laterite and acid sulfate soils (Mishra et al. 1999).

In a laboratory study, Mohanty et al. (2000) showed that selected heavy metals differed in their effect on CH_4 oxidation in two soils for two water systems. The Cr significantly inhibited CH_4 oxidation in alluvial soil at 60% moisture capacity, while Cu stimulated the process. On the other hand, Zn inhibited CH_4 oxidation in both alluvial and laterite soils under saturated conditions.

The effect of inorganic redox substances (species of NO_3^-, Mn^{4+}, Fe^{3+}, and SO_4^{-2}) on methane production and oxidation in anoxic rice soil samples has vital effects. Sulfate

was the most inhibiting for methane production followed by Fe^{3+}, NO_3^-, and Mn^{4+} respectively. Laboratory studies showed that the addition of MnO_2 and K_2SO_4 enhanced aerobic methane oxidation in soil samples at 60% water content. Nitrate and Fe^{3+} motivated methane oxidation under anaerobic conditions and delayed it under aerobic conditions. Manganese (IV) delayed methane oxidation under anaerobic conditions, but enhanced it under aerobic conditions. On the other hand, SO_4^{-2} stimulated methane oxidation in soil equivalent medium under both aerobic and anaerobic conditions (Kumaraswamy et al. 2001).

There is substantial interest in methane monooxygenase (MMOs) of methanotrophic bacteria in soils, because these enzymes in methanotrophs oxidize methane to a potential fuel source, methanol, detoxifies trichloroethylene, and uses a greenhouse gas as a reactant (Sabastiãno et al. 2002). It is well known that sMMO expression in methanotrophs is repressed by copper ions [sMMO is expressed for concentrations lower than 0.86μmol/g dry cell weight (Barta and Hanson 1993) or, generally, when the copper concentration is lower than 1 μM (Burrows et al. 1984)]. Above this concentration, the particulate (membrane-bound) form of methane monooxygenase (pMMO) is produced (Nguyen et al. 1994). To overcome this natural regulation, a *M. trichosporium* OB3b mutant has been obtained that expresses sMMO in the presence of copper probably because of a deficiency in copper transport (Phelps et al. 1992). Transcription of soluble methane monooxygenase (sMMO) of methanotrophs is tightly regulated by low concentrations of copper ions [Cu^{2+} e.g., transcription is completely repressed at copper concentrations higher than 0.86 μmol/g dry cell weight] (Green et al. 1985). In a research

study, Jahng and Wood, (1996) showed sMMO inhibition by metal ions and different medium ingredients was investigated for the first time using sMMO purified from the type II methanotroph *Methylosinus trichosporium* OB3b. Cu(I) and Cu(II) decreased sMMO activity of *Methylosinus trichosporium* OB3b by inhibiting not only the reductase but the hydroxylase component as well. Ni (II) also inhibited both enzyme components, and Zn (II) inhibited sMMO by lowering the activity of the hydroxylase only. The Ni (II) and Zn (II) aggregated the reductase component of sMMO, and the later precipitated the hydroxylase component. Cu (II) caused the reductase to precipitate (Jahng and Wood 1996).

- *Uncertain Environmental Factors*

Field studies in temperate forests have shown a chronological illustration of CO_2 and CH_4 fluxes (Castro et al. 1994; Peter John et al. 1994; Castro et al. 1995) that corresponds strongly with seasonal changes in soil moisture and temperature. Temperature is considered the primary predictor of CO_2 fluxes, not surprisingly; moisture also influences soil respiration rates (Groffman et al. 1992). Moisture usually exerts strong control over CH_4 uptake rates, although inclusion of both moisture and temperature in models can increase predictive capabilities. Lessard et al. (1994) suggested that the strong relationship between moisture and CH_4 uptake may mask relationships between temperature and uptake, thus it has been difficult to determine the relative importance of these factors. Steinkamp et al. (2001) showed significant seasonal differences in the magnitude of CH_4 oxidation rates at experimental sites with high rates during summer, relative low rates during winter and intermediate rates during spring and autumn. Hellebrand and Scholz (2000) showed results that the temperature was the main reason

for the seasonal change of the methane uptake. Whereas the uptake dropped near to zero during the winter period, the uptake rates reached values up to 0.6 mg CH_4 /m^2.d (25 μg CH_4 /m^2.h) in the summer. Lessard et al. (1994) used field studies to determine the relative importance of moisture and temperature in controlling flux rates is difficult because soil temperature and moisture usually vary seasonally in temperate ecosystems. Soil temperatures are usually highest by late summer, but strong evapotranspiration potentials usually reduce soil water even if precipitation stays relatively constant. Thus, it is not a straightforward exercise to determine if maximum rates of soil respiration or CH_4 uptake in late summer, for example, are due to high temperatures, lower soil moisture, or an interaction of both factors.

1.2.1.2. Biological Plant Uptake of Carbon Dioxide

Measurements of CO_2 in the atmosphere, which began in Maunaloa (Hawaii) in 1958, indicated clearly that the concentration of CO_2 in the atmosphere is increasing rapidly (Keeling *et al.* 1982). The ice core studies showed that the CO_2 concentration was about 205 μmol/ mol some 20,000 years ago. Pre-industrial value was 280 μmol/ mol during the past 10,000 years. Whereas before 1900, the CO_2 concentration in the atmosphere was 290 μmol/ mol. Maunaloa studies also observed that from 1958 to 1982 there was an increase of 1.0 μmol/ mol CO_2 per year. The 1958 value of atmospheric CO_2 was 316 μmol/ mol and in 1995 (Collette 1995) and the present concentration (Kimball 1997) were recorded as high as 360 and 370 μmol/ mol respectively. Thus the concentration of CO_2 in the atmosphere is likely to be doubled (600 μmol/ mol) by the middle of 21st century (Houghton et al. 1990). Recent studies suggest that boreal forests may play major

role in regulating the climate of the northern hemisphere and in global carbon cycling (Bonan et al. 1992). In North America, the Boreal ecosystem atmosphere study program has investigated carbon and energy exchange in two regions of Canada (Sellers et al. 1995).

Short rotation woody crops fix carbon dioxide from the atmosphere and store carbon both above and belowground as biomass. Moreover, the harvested portions of the trees displace other products that are made from non-renewable fossil fuels (Tuskan and Walsh 2001). One of the ways to decrease greenhouse emissions in the future is to plant fast growing woody crops on unproductive land thereby sequestering carbon and displacing fossil fuels by harvesting woody biomass for bio-energy, or by storing carbon in long-lived woody products (Tuskan and Walsh 2001). Short rotation poplar and willow crops deployed as phytoremediation buffer systems would qualify for carbon uptake, and if planted at large scales would contribute greatly to atmospheric carbon dioxide gas reduction (Isebrands and Karnosky 2001).

- Examples of CO_2 Plant Uptake

Plants in their juvenile phase can benefit more than mature ones of optimal growing conditions. Transplant production in greenhouses offers the opportunity to optimize growing factors in order to reduce production time and improve transplant quality. Carbon dioxide and light are the two driving forces of photosynthesis. Carbon dioxide concentration can be enriched in the greenhouse atmosphere, leading to heavier transplants with thicker leaves and reduced transpiration rates (Tremblay and Gosselin

1998). The almost entirely juvenile tissues of seedlings are all expanding, and could be utilizing and diluting the enhanced photosynthate production in an enriched CO_2 atmosphere (Lindhout and Pet 1990). Hence, the greatest advantage of CO_2 enrichment would be realized in the vegetative growth of young plants (Kimball 1983). As leaf tissues formed early in seedling culture begin to mature, starch accumulation begins to slow photosynthetic rates and relative growth rate (Thomas et al. 1975).

The potential benefit from CO_2 augmentation of the greenhouse atmosphere has been known for a long time (Hand 1994; Enoch 1990), and they are particularly important for roses (Urban 1994; Baille et al. 1996). The response of "Parfum de Rose" to CO_2 augmentation is rapid: it takes only 2 months to observe a sharp yield increase.

The net primary production of maturing loblolly pine (*Pinus taeda*), on a site of moderate soil fertility, increased by 25% in the two years following the onset of a 200 ppm CO_2 enrichment in a 'Free Air CO_2 Enrichment' FACE experiment (DeLucia et al. 1999). A parallel longer-term study produced a larger stimulation of tree growth of up to 34% over the first three years of enrichment (Oren et al. 2001). It is particularly interesting; therefore, that carbon allocation to reproduction is strongly stimulated in loblolly pine after three years of CO_2 enrichment (LaDeau and Clark 2001). After this period, trees growing in the enriched CO_2 were twice as likely to be reproductively mature, and produced three times as many cones and seeds, than control trees. In contrast, flowering and seed set in grasslands, where species may have deterministic life cycles, were stimulated (Smith et al. 2000).

C_4 and C_3 species increased total biomass significantly in elevated CO_2 by 33% and 44% respectively and higher carbon assimilation rates were found in both C_3 and C_4 grass 33% and 25% respectively (Wand et al. 1999). Carbon dioxide enrichment increased transplant leaf area, shoot and root dry weight and decreased the leaf area ratio of celery (*Apium graveolens* L.) transplants (Tremblay et al. 1987). Study on the characterization of CO_2 responsiveness in *Brassica oxycamp* hybrid and its parents *B.oxyrrhina* and *B.campestris* showed that the response of *B.oxycamp* hybrid to elevated CO_2 was significantly positive in respect to photosynthesis and growth, similar to that of its parent *B.campestris*. Hybrid *B.oxycamp* and *B.campestris* with greater sink potential responded significantly, whereas, *B.oxyrrhina* with poor sink size did not respond to CO_2 enrichment (Uprety et al. 1998).

Woodrow et al. (1987) demonstrated that CO_2 affects both source metabolism and partitioning to sinks (stems, roots and leaf carbohydrate) in tomato plantlets. They found that CO_2 enrichment produced heavier transplants desirable for successful field establishment without elongation growth. Dry matter accumulation in shoot and root was increased as well as leaf dry weight (by 81 % over control). Transpiration rates were reduced under CO_2 enrichment conditions by 34%. Increased leaf dry weight accumulation and specific leaf weight (SLW) under CO_2 enrichment suggests that more carbohydrate may be available to the plant for future growth. Apparently, the ratio of total sugars to amino acids in the leaf is shifted in favor of sugar content. In a study with tree seedlings, Luxmoore et al. (1986) suggest that CO_2 enrichment may increase sucrose translocation in roots and facilitate the mobilization of N and C compounds to new root primordia. Increased net leaf photosynthesis rate and decreased transpiration rate under

CO_2 enrichment are well documented (Woodrow et al. 1987). One of the most important effects of CO_2 enrichment is the increase in water efficiency (Wong 1979), which leads to drought tolerance. Actually, rising CO_2 concentration reduces the transpiration of plants by 20% to 40% (Mortensen 1987). Radoglou et al. (1992) reported an increase in water use efficiency of bean (*Phaseolus vul garis* L.) leaves as a result of increased assimilation rate and decreased stomatal conductance at higher ambient CO_2 concentrations. In cotton (*Gossypium arborcum* L.), stomata conductance after 40 d of CO_2 enrichment took 5 d to reach normal levels in non-enriched conditions. In short, CO_2 enrichment of vegetable transplants shortens the nursery period and modifies photosynthate allocation to the diverse parts, leading to sturdier, higher quality plants. This, together with the fact that CO_2 enriched plants make a more efficient use of water may impact favorably on the plant's ability to overcome transplanting stress (Sasek et al. 1985). The relative increase in net assimilation rate due to an increase in CO_2 concentration from 200 to 1000 ppm was almost as great at the lower as at the higher light level studied. The light compensation point is lowered by increased CO_2 concentration (Mortensen 1987). Fierro et al. (1993) demonstrated interactive effects of CO_2 and light enrichment on tomato and pepper transplants. If either were applied 3 weeks before transplanting tomatoes and peppers, they increased accumulation of dry matter in shoots by 50%. Fierro et al. (1993) results suggested that it is more important to achieve optimal light conditions first, and then make use of CO_2 enrichment.

- *CO_2 Plant Uptake Mechanism*

Plants and other photosynthetic organisms convert carbon dioxide into energy rich organic molecules, which are the precursors of carbohydrates. These molecules are either used by the organism directly, or are passed into the food chain to be utilized by non-photosynthetic organisms (Paradise and Cyr 1995). The complete photosynthetic process may be summarized by the following equation:

$$nCO_2 + nH_2O \longrightarrow (CH_2O)n + nO_2$$

Carbon dioxide serves as substrate to photosynthetic carbon assimilation. There is concomitant decline in photo-respiratory activity and alteration in stomatal aperture. It was reported that C_3 plants (wheat, rice, oilseeds, pulses, etc.) respond to elevated CO_2 since elevated CO_2 reduces oxygenase activity of RuBP carboxylase oxygenase enzyme in plants. C_4 plants (sorghum, maize, sugarcane, etc.) show little or no photosynthetic response to elevated CO_2 because C_4 pathway is not competitively inhibited by O_2 and is completely CO_2 saturated. However, there is no consensus on the quantitative effects of increased CO_2 in plant processes and growth due to differences in response at different stages of growth, species of crops and because of growth limiting environmental factors (Uprety et al. 2000a).

The key enzyme for CO_2 fixation is rubisco. Its activity depends on the ratio of the O_2 and CO_2 concentration in the atmosphere. The major effect of CO_2 enrichment is the shift in balance between the carboxylation and oxygenation activity of rubisco, this effect is important at low and high light levels. Kimball (1983) stated that, on average, yields of crops should increase by 33% with a doubling of CO_2 concentration in the earth's

atmosphere. Although these estimates have been developed for plants over their complete life cycles, enhanced growth and dry matter accumulation are correlated with higher net photosynthetic rates in young vegetative tissues under CO_2 enrichment as well.

Studies on the response of rice cultivars Basmati-1 and Pusa-677 to the elevated CO_2 showed increase in growth, photosynthesis, and seed yield (Uprety et al. 2000b). The increased photosynthesis and greater accumulation of sugar contributed significantly to the accelerated development of leaves and tillers in both cultivars. The response of rice cultivars to the elevated CO_2 with reference to their stomatal characters showed a marked increase in the stomatal resistance, stomatal index, size of guard cells, stroma, and epidermal cells (Uprety et al. 2002).

- *Parameters Affecting CO_2 Plant Uptake*

Ecosystem responses to CO_2 enrichment and climate change are expressed at different levels: biochemical and stomatal processes at the leaf level, growth processes at the plant level, and water budget and carbon - nitrogen cycling at the ecosystem level. Predicted responses of net primary production and N mineralization to CO_2 enrichment and climate change are, therefore, complex. Responses to individual climate factors were often modified by responses to other factors, through interaction among processes at the same and different levels of organization (Coughenour and Chen 1997). The final outcome of ecosystem responses to CO_2 enrichment and climate change is dependent on the relative importance of these different processes. The relative enhancement of net primary production by CO_2 enrichment was greater at high temperature in the C_3 grass species,

and greater under ambient temperature conditions in the C_4 grass. Most previous studies revealed that a CO_2-doubling generally caused greater increases in growth at higher temperatures (e.g. Cure 1985), although Sionit et al. (1981) reported that the CO_2 response of okra had stimulatory effects on growth at lower temperature, and Coleman and Bazzaz (1992) reported that the effects of CO_2 enrichment on final biomass of a C_4 annual forb was positive at low temperature and negative at high temperature. Chen et al. (1994) found that the relative enhancement of CO_2 enrichment on an aquatic plant was strongly temperature dependent, and that the maximum relative effects of CO_2 were reached at a low temperature. These different responses suggest that the effects of elevated CO_2 and temperature may interact in a seasonal environment and that this interaction is species specific (Hunt et al. 1991).

The responses of N mineralization to elevated CO_2 were negative or near neutral except for the C_3 grass species system at high precipitation. Reduced N mineralization under elevated CO_2 may be ascribed to reduced litter quality (Strain and Bazzaz 1983). However, N mineralization in the *P. smithii* system was increased by doubling CO_2 under wet conditions. Increased N mineralization under elevated CO_2 was also observed in an open top hamper study of *Populus granditenta* (Zak et al. 1993). They found up to five-fold increases in N mineralization. They suggested that elevated CO_2 would increase belowground carbon inputs, which would increase microbial biomass and their activity and thus decomposition and mineralization rate. Decomposition and mineralization could be greater under elevated CO_2, in spite of decreased residue quality, because decomposition and mineralization, being donor-controlled processes, tend to increase

with net primary production (Hunt et al. 1991; Coughenour and Chen 1997). Interactions among biochemical, ecophysiological and ecosystem processes appear to be significant. To reasonably estimate ecological effects of CO_2 enrichment and climate change, a model must couple biochemical, ecophysiological and ecosystem processes. Ecosystem models that ignore physiological and ecophysiological responses are incapable of predicting responses to elevated CO_2 and climate change (Coughenour and Chen 1997). On the other hand, ecophysiological models that do not couple soil water and nitrogen cycling would be not able to represent the feedbacks of biogeochemical processes such as N mineralization. In natural ecosystems, many plant species coexist competitively. There are hundreds of plant species representing C_3, C_4 and CAM photosynthetic pathways in Colorado shortgrass steppe. CO_2 enrichment and climate change differently affect many plant and ecosystem processes. It has been hypothesized that different responses of C_3 and C_4 species to CO_2 enrichment and climate change could change the competitive balance between these species in a future CO_2 enriched atmosphere (Arp et al. 1993).

Trees treated with both nitrogen fertilizer and elevated CO_2 showed a three-fold increase in growth over controls. The photosynthetic rates of plant species within a grassland community also showed little positive response to CO_2 enrichment (Lee et al. 2001) observed after at least three years of fumigation (Oren et al. 2001). The stimulation of carbon sequestration in the vegetation and litter of forest trees was paralleled in grassland where CO_2 was enriched by 240 ppm over a six-year period (Niklaus et al. 2001). The elevated CO_2 increased the rate of photosynthesis, promoted greater foliage, more number of siliqua and increased root growth. The carbon need to satisfy the demand for

these newly generated sinks was met from new photosynthates produced during the high CO_2 exposure. Plants accumulated increased metabolic reserves in terms of sugars and starch to significantly enhance metabolic flexibility to respond to adverse moisture stress (Uprety et al. 1995). The main constraint to growth occurs when the plant is unable to photosynthesize at the potential rate, governed by the amount of incoming solar radiation. This will normally occur when one of the substrates for photosynthesis (carbon, water, nitrogen) is limiting (Agren 1985).

- Plant Uptake of CO_2 in Landfill

The landfill industry makes use of a potentially valuable, environmentally beneficial and sustainable utilization of restored landfill sites. The biomass produced at restored landfill sites from short rotation coppice (SRC) trees, such as willow and poplar, may have a number of uses: as a fuel for electricity generation plants; for the production of charcoal; as a soil amendment for clay caps; or simply as a carbon sink for atmospheric CO_2 (Cannell et al. 1987).

Present municipal solid waste landfills generate biogas that is flared on site to destroy noxious contaminants and water is extracted from leachate to be drained away. However, biogas could alternatively be a cheap fuel for winter heating and could provide horticultural greenhouses with abundant carbon dioxide to boost plant growth all year long (Jaffrin et al. 2003).

In the research of Chan et al. (1997), two landfill sites in Hong Kong (Shuen Wan and Junk Bay StageI) were chosen as the field sites and three sites (Yuen Chau Kok, Tai Po and Lok Wo Sha) were chosen as reference sites. The vegetation survey classified the plants under woody plants, herbs and grasses groups. Seventeen species of vascular plants were found at the reference sites; whereas 25 and 20 species, respectively, were found at the two-landfill sites. The gross average coverage of plants at the reference sites (57.8%) was lower than that at the two-landfill sites (70.3%, 61.4%). Tree cover on the landfill sites was dominated by two species: *Acacia confusa* and *Leucaena leucocephala,* which seemed suited for growth and were abundant on landfill sites. Therefore, completed landfill sites can be good habitats, which support a variety of plants and animals, provided that the plants can phytoremediate landfill gas and leachate contamination (Chan et al. 1997).

1.2.2. Physical Biogas Capture

1.2.2.1. Biogas Extraction

- Biogas Collection Systems

In landfills, gas is collected using network of collection pipes and wells. The gas collection efficiency in landfills is between 40-90 % (Augenstein and Pacey 1991). Biogas is collected by means of some vertical and horizontal drain pipes and is then burned in flares or employed to produce heat and energy (EMCON Associates 1980). The designs for gas abstraction systems include different types of well configurations such as vertical, horizontal, hybrid, etc (Leach 1990). The landfill gas collection system consists of vertical extraction well, transport pipe network, blower for passive gas collection or

pumping for active collection, monitoring equipment, and flare stack (Park and Shin 2001).

Landfill gas can be collected by either a passive or an active collection system. Passive gas collection systems (Figure 1.1) use existing variations in landfill pressure and gas concentrations to vent landfill gas into the atmosphere or a control system. The collection wells are typically constructed of perforated or slotted plastic and are installed vertically throughout the landfill to depths ranging from 50% to 90% of the waste thickness. Vertical wells are typically installed after the landfill, or a portion of a landfill, has been closed. A passive collection system may also include horizontal wells located below the ground surface to serve as conduits for gas movement within the landfill (ATSDR 2001).

Active Gas Collection (Figure 1.2) is considered a good means of landfill gas collection (EPA 1991). An active collection system composed of extraction wells connected to header pipe to a pump that delivers gas for energy recovery (Wheless and Wiltsee 2001). An active system consists of extraction well, header pipe, vacuum, condensate removal, and burner (Baggchi 2004, Baggchi 1994). However, wells in the active system should have valves to regulate gas flow and to serve as a sampling port. Sampling allows the system operator to measure gas generation, composition, and pressure (ATSDR 2001).

"The Environmental Protection Agency, State, and local regulators use assumed gas collection efficiencies to calculate landfill emissions in regulating and setting policies for landfills. These assumed efficiencies are usually around 75%. A thorough review of gas

system operators' experiences and of researcher's efficiency determination methods and their results is required to better assess actual collection efficiencies." (Los Angeles County Sanitation Districts 2005)

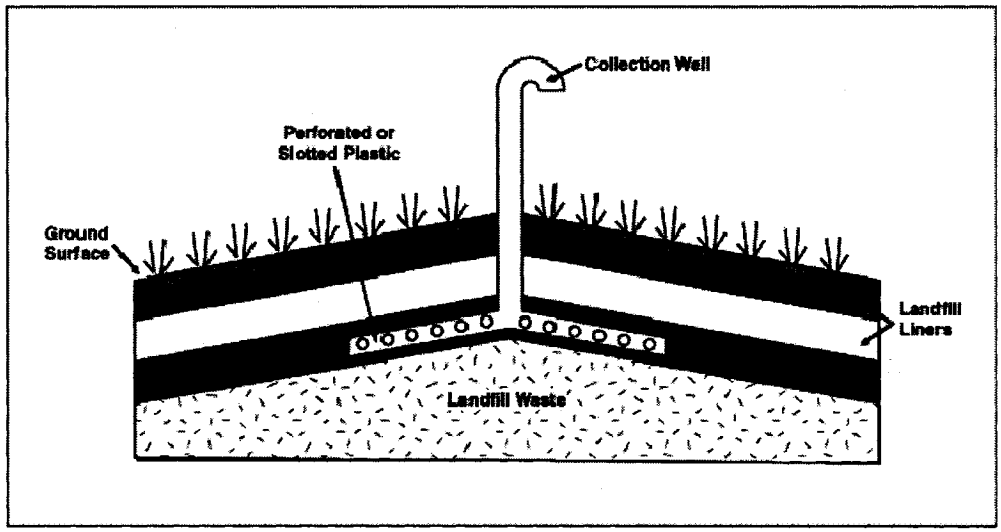

Figure 1.1 Passive Gas Collection System (ATSDR 2001)

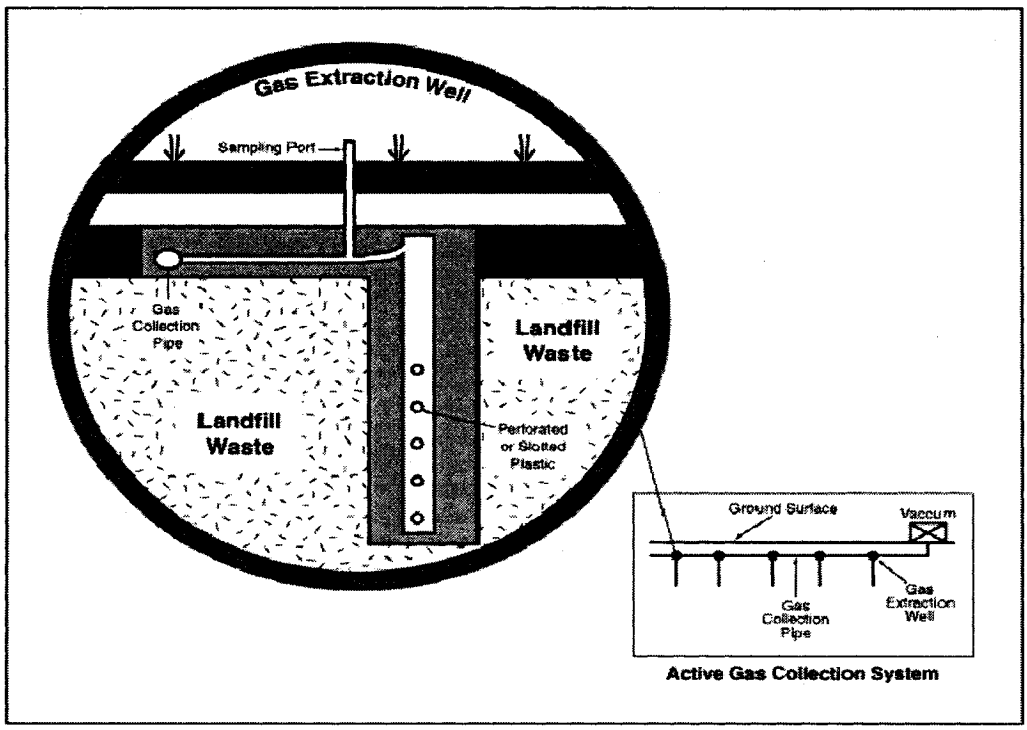

Figure 1.2 Active Gas Collection System (ATSDR 2001)

- Biogas Control Methods

There are two common methods of conducting a control to gas migration: using very low permeability materials to resist gas flow, and using highly permeable materials to allow the gas to vent to the surface. Among combination of those methods the following could be summarized:

- Trench filled with granular backfill acts as passive system to collect gas from boundaries.
- Trench backfilled with gravel and an impermeable membrane installed along the back wall of the trench to trap the gas to be more effective interceptor.
- A gravel trench with vertical perforated pipe to collect gas within trench passive collection system.
- A gravel trench with horizontal and vertical perforated pipes to collect gas within the trench (McBean et al. 1995).

Current methods of forming a gas resistant barrier usually involve the excavation of a trench and backfilling with either a low permeable material such as bentonite, or the inclusion of a gas resistant membrane. Vent trenches are normally constructed using trenches backfilled with either gravel or geocomposite venting media to promote gas flow to the surface. An alternative method is to provide a series of discrete vent wells at regular spacing or using vertical permeable curtain. These methods allow the gas to exhaust directly to atmosphere without any dilution in the system (Wilson and Shuttleworth 2002). The Vent System provide preferential pathway (route of least resistance) to atmosphere as shown in Figure 1.3 (Permavoid Ltd 2002).

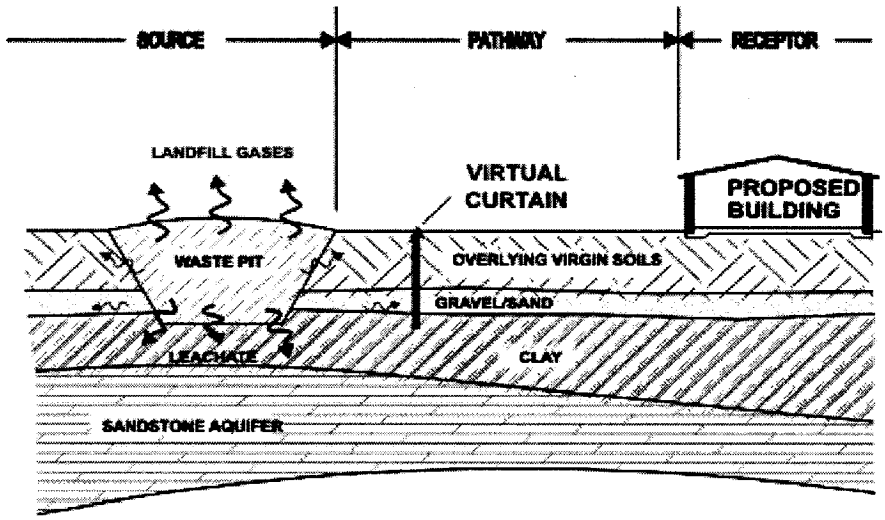

Figure 1.3 Vertical Permeable Venting Curtain for Gas Control

- Biogas Collection Layers

There are other processes of gas collection such as collection layers. Tire shreds have been used as landfill gas collection material at municipal solid waste landfills (Augestein et al. 1997). GeoSyntec (1998a) for the California Integrated Waste Management Board provided a summary of recommended procedures for use of tire shreds as landfill gas collection material at municipal solid waste landfills, including horizontal landfill gas collection layers, horizontal trenches and vertical boreholes. Tire shreds have a compressibility that is several orders of magnitude greater than materials typically used for landfill gas collection such as gravel, sand, or crushed rock (GeoSyntec, 1998b). Consideration should be given to using a properly selected geotextile as a separation between the tire shreds and soil materials. The geotextile would prevent soil from

migrating into the relatively large voids between the tire shreds (GeoSyntec 1998a). According to intrinsic permeability values, it is found that grain size fractions of 0.1-2 mm, 0.6-1.2 mm (sand) and 0.1-56 mm (natural soil), are inappropriate for the application as gas collection layer materials, as they demonstrated lower values than a sample of solid waste (Huber and Wohnlich 1999). As the mentioned grain size fractions of sand and natural soil belong to materials, which are commonly used for constructing the foundation layer of landfill cover systems (Fox, 1996), these layers can not serve at the same time as gas collection layers. The coarse materials (grain size fraction of 16-32 mm of gravel, crushed lime stone, crushed granite, and crushed basalt) were proved to be the most suitable for constructing gas collection layers, since it indicates high intrinsic permeability (Huber and Wohnlich 1999).

- Biogas Collection Covers

There are other methods of gas collection such as collection covers, which are used other than application in landfill, but could give good analogy of incorporated processes and/or materials to apply in landfill.

McGrath and Masonnn (2004) in their application to assess biogas production from anaerobic waste stabilization pond treating farm dairy wastewater, they used floating gas collection cover was constructed of fiber-reinforced polypropylene geomembrane fabric (J. P. S. Elastomerics, Westfield, NC, USA), supported on a 2m by 2m framework fabricated from 25mm diameter, and foam filled 110mm diameter polyvinylchloride pipe and fittings.

Manure lagoons can be covered by floating polyethylene liners on the liquid surface allowing for the cost-effective construction of anaerobic digesters which use microorganisms to ferment and process waste producing methane gas. The polyethylene cover prevents vector migration out of the lagoon preventing odors, vapors and gasses from entering the atmosphere. They also prevent rainwater dilution. The most desirable effect of the polyethylene cover is to create an inflatable methane gas reservoir (Kriofske 1998).

The XR-5 cover by ETP Inc, AL USA, is a proven material for biogas collection. It is strong, tough, and it is highly resistant to biogas. Its low gas permeability makes it ideal for the collection of biogas and for use as a floating cover material. Poly-log-floats are used to buoy the cover and to form pass-ways for the collection of the biogas. Rainwater drainage is provided by the use of thru-cover drains. The cover's unique design allows it to act as a gas storage container at times of peak production (Engineered Textile Products, ETP Inc. 2004).

A large employer in upper State Maine, USA, expanded their food processing capability. As part of that expansion, they needed to build an anaerobic digester that would retain heat in the cold climate of Maine, and be able to collect the biogas produced. Lemna, MN, USA used LemTec™ Modular Insulated Cover System a turnkey to biogas design (Lemna Technologies Inc. 2004).

Geomembrane Technologies Inc. GTI, NB, Canada produces Gas Collection Covers that are floating cover systems used to collect gases from wastewater treatment lagoons, sludge ponds, aeration systems, flow equalization tanks and pretreatment tanks. In the case of anaerobic digestors, GTI cover systems are used to capture biogas. GTI cover system includes reduction of process heat loss/gain, elimination of water evaporation and prevention of sunlight penetration. Features can include insulation, automatic rainwater removal, baffles, sample ports and hatches. These durable, UV protected covers are strong enough to safely support foot traffic, light vehicles and snow loads (Geomembrane Technologies Inc. GTI 2004).

The Canadian French-fry manufacturer, needed to replace an old (competitor's) insulated gas collection cover that was prone to failure due to migrating solids (grease bergs) that ripped the gas collection membrane. The design of the old cover made it next to impossible to remove the grease bergs and to repair the damaged cover. The insulated gas collection cover by Lemna replaced the old one. The new gas collection cover has the ability to remove sections of the cover to dispel solids when required (Lemna Technologies Inc. 2004).

A dairy in Pennsylvania had a wastewater tank that was generating odors. Lemna Technologies proposed the installation of LemTec™ Gas Collection Cover System. This system provides effective odor control by completely covering the water surface with a single layer membrane. Channels are created beneath the cover for gas to flow for

collection. Channels above the cover provide for rainwater removal (Lemna Technologies Inc. 2004).

Scotford and Williams (2001) investigated the effectiveness of a floating plastic cover to reduce ammonia emissions from slurry lagoon. They measured ammonia emissions from both an uncovered lagoon and covered lagoon. The ammonia emissions were measured using hoods. Each hood was fitted with an inlet pipe and outlet pipe. Air was forced into the hood using a fan that gave a superficial air velocity across the measured surface. The ammonia flux was measured into and out of the hoods. The floating plastic cover prevented nearly 100% of these emissions.

1.3. Biogas Transport at Landfill

At the landfill, organic matter decomposition due to anaerobic processes produces methane and carbon dioxide (biogas) that leads to increase in pressure, corresponding partial pressures and concentrations, which in turn enhance biogas migration in porous media in/and around landfill. Biogas migration occurs by two major transport mechanisms: convection and diffusion. The gas pressure and concentration are variable during the time within geo-environmental systems. These changes create pressure gradients leading to gas convection, as well as concentration gradients that lead to gas diffusion.

1.3.1. Biogas Production and Migration

The MSW at landfill undergo biochemical processes that are consisted of three phases: hydrolysis, acidification, and methanogenesis. The first and most important part in the biodegradation process of organic material in sanitary landfill is the hydrolysis, which is likely to be the rate-limiting step for methane production from solid waste (McCarty et al. 1986). First-order kinetics is used to represent the hydrolysis of refuse constituents:

$$\frac{dC_{si}}{dt} = -K_{hi}\, C_{si} \qquad \text{As} \qquad C_{(S)i} + H_2O \longrightarrow C_{(aq)i} \tag{1.1}$$

where: K_{hi} is first-order hydrolysis rate constant of refuse constituent i (day^{-1}), $C_{(S)i}$ is solid organic carbon concentration of refuse constituent i (kg/m^3), and $C_{(aq)i}$ is aqueous organic carbon concentration of refuse constituent i (kg/m^3).

The second phase of the biochemical process is the acidification, where carbon dioxide and acetate are produced from the biodegradation of organic matter. In this phase, the pH value has important effect on the methanogens (El-Fadel et al. 1996). The third phase is the methanogenesis, where the acetic acid is converted to methane and carbon dioxide.

The mass balance coupled with the Monod formula is used to describe the microbial growth within landfill:

Mass balance:

$$C_{(X)} = C^{g}_{(X)} - C^{d}_{(X)} \tag{1.2}$$

Monod formula:

$$\frac{dX}{dt} = \frac{\mu_{max} S}{K_s + S} X \qquad (1.3)$$

where:

$C_{(X)}$ is net formation rate of carbon concentration (kg/m^3.day),

$C^g_{(X)}$ is generation rate of carbon concentration (kg/m^3.day),

$C^d_{(X)}$ is depletion rate of carbon concentration (kg/m^3.day),

(dX/dt) is rate of microbial growth (kg/m^3.day),

μ_{max} is maximum rate of substrate utilization (day^{-1}),

X is microbial concentration (kg/m^3),

S is substrate concentration (kg/m^3), and

K_S is half saturation constant (kg/m^3) (El-Fadel et al. 1996).

The most commonly used reaction rate equation in engineering practice for gas production estimation is:

$$\frac{dS}{dt} = -\frac{k_m}{K_s} XS; \qquad S << K_s \qquad (1.4)$$

where:

dS/dt: rate of substrate utilization (kg/m^3.day)

k_m : maximum utilization coefficient (day^{-1})

X: is microbial concentration (kg/m^3)

S: substrate concentration (kg/m^3)

K_S: half saturation constant (kg/m^3)

The above equation implies an environment capable of supporting biological activity in accordance with substrate availability (Popov and Power 1999). A necessary condition in applying this kinetic model to the decomposition of organic matter in a sanitary landfill is that the organic matter is limiting for the rate determining by methanogenic bacteria (McCarty 1965). Although the rate determining nature of methanogenic bacteria has been studied in great detail for applications to anaerobic digestion, it is difficult to directly apply this information to organic decomposition in sanitary landfills because of the undefined nature of the landfill environment (McCarty 1965).

The Scholl Canyon model estimates the energy potential at landfill. This simple model is widely used in the landfill gas industry in Canada and United States (US EPA 1996). This model is consistent with Environment Canada and IPCC climate change protocols for calculating greenhouse gas emissions inventories. The Scholl Canyon Model can be written as the following:

$$G_i = kL_o M_i (e^{-kt_i})$$

Where:

Gi is methane generation rate at year t_i, in the i^{th} section (m^3 of CH_4/year)

k is methane generation rate constant (yr^{-1})

L_o is methane generation potential (m^3 of CH_4/tonne of refuse)

M_i is mass of refuse landfilled, in the i^{th} section (tonne)

t_i is age of the refuse (yr)

There are values of 'k' reported for each Province in Trends In Canada's Greenhouse Gas Emissions (Jaques et al, 1997), *ki* is the decay rate constant each year was estimated to be close to the average constant for Canada $k = 0.01$.

The gas pressure and composition vary during the life of the landfill. The methane and carbon dioxide generation increases the pressure gradients leading to the gas advective flow. The concentration gradients lead to the gas diffusion. The generated heat also influences gas migration because of its effect on the thermodynamic properties of the fluids. Following the path of least resistance, gas will migrate either vertically to the atmosphere or laterally beyond landfill boundaries in surrounding geological formations. In the latter case, gas eventually reaches the atmosphere (Nastev et al. 2001).

1.3.2. Convective Biogas Transport

In convective flow, the gas moves due to pressure gradient. To equalize pressure, gas travels from a region of higher pressure to a lower one. In landfill, the primary driving force for gas migration is pressure differential. Falling pressures tend to draw gas out of the landfill and increase the gas concentration near the surface layers. Temperature changes can also give rise to pressure differences and lead to gas migration (Bouazza and Vangpaisal 2003).

The convection of fluids in porous media is described by the following formula, in which the generalized expression for a single-phase fluid is given as:

$$Q = KA\nabla\frac{P}{\rho g} = \frac{K}{\rho g}A\nabla P \tag{1.5}$$

where Q is the flow rate in m^3/s, ∇P is the pressure gradient in $N/m^2.m$, A is the cross sectional area in m^2, ρ stands for the density of the fluid in kg/m^3, g denotes the acceleration due to gravity in m/s^2 (Didier et al. 2000). The conductivity coefficient K (m/s) is a function of the properties of both soil and fluid in accordance with the following equation (Carman 1956):

$$K = \frac{k\rho g}{\mu} \tag{1.6}$$

where k is the intrinsic permeability of the porous material in m^2, μ is the dynamic viscosity of the fluid in Pa.s. Based on equation (1.6), it is possible to rewrite equation (1.5) as follows:

$$Q = \frac{k}{\mu}A\nabla P \tag{1.7}$$

For one-dimensional flow the above equation becomes:

$$Q = \frac{k}{\mu}A\frac{dP}{dx} \tag{1.8}$$

The integration of equation (1.8) is possible for compressible fluid provided that the temperature stays constant during the flow. It is expected that both dynamic viscosity and kinematic viscosity should vary greatly with changes in temperature (Didier et al. 2000).

In reality, it seems that dynamic and kinematic viscosities increase only by 3% and 7% respectively between 15 °C and 25 °C (Soltani 1997).

1.3.3. Diffusive Biogas Transport

In diffusive flow, gas movement occurs when a gas is more concentrated in one region than another. Gas diffuses into the less concentrated region, thus the molecules move in response to a partial pressure gradient or concentration gradient of the gas (Bouazza and Vangpaisal 2003). Diffusion is a generic transport process, encountered in fluids, by which molecules that can move randomly are redistributed until equilibrium is reached when concentration becomes uniform (Aubertin et al. 2000). The main diffusion equation, known as Fick's first law, can be written as follows for the gas flux:

$$F_g = -D\frac{\partial C}{\partial Z} \tag{1.9}$$

where F_g is given as a mass transfer rate per unit area (kg/ s. m^2); C is the concentration of the diffusing substance (kg/m^3); Z is the spatial coordinate (m) measured perpendicularly to the unit cross sectional area; D is the diffusion coefficient (m^2/s); the negative sign in Eq. (1.9) indicates that flux occurs in the opposite direction to the concentration increase. When Eq. (1.9) is rewritten in terms of partial pressure gradients (e.g. Hillel 1980; Fredlund and Rahardjo 1993) one can establish a parallel between Fick's first law and the formulas used for advection transport. Crank (1975) used an equation for one-dimensional flux in an isotropic non-reactive medium as described below:

$$\frac{\partial C}{\partial t} = D\frac{\partial^2 C}{\partial Z^2} \tag{1.10}$$

which is the usual form of Fick's second law. More general expressions can also be developed for anisotropic or heterogeneous media and for reactive materials that consume or generate a diffusive element (Crank 1975; Hillel 1980).

1.3.4. Multicomponent Gas Transport

In isobaric systems, gas transport occurs by diffusion, whereas in non-isobaric systems gas transport occurs by advection and diffusion. The equation of mass conservation accounting for gas in a porous media can be written as:

$$\partial \frac{[C]_T}{\partial t} + \frac{\partial N}{\partial x} + r_a = 0, \tag{1.11}$$

where:

$$N = -D_{w,e} \frac{\partial [C]_g}{\partial x} \tag{1.12}$$

and

$$[C]_T = (\rho_b K_b + \theta_w + \varepsilon_g H_c)[C]_w \tag{1.13}$$

where, C_T: total gas concentration in multi-phases (g/L), C_w: gas concentration in porous porewater (g/L), K_d: linear adsorption constant (m^3/kg), ρ_b: bulk density (kg/ m^3), ε_g: gas fraction in the porous pores, θ_w: volumetric water content in the porous medium, H_c: Henry's constant, $D_{w,e}$: the effective diffusivity coefficient of gas (m^2/s), r_a: rate of reaction for gain or loss (Valsaraj 1995).

The concentration of gas mixture in multimedia phase can be calculated directly as the following:

$$C_i = f_i Z_i \quad (1.14)$$

Where, C_i: gas concentration (mol.m^{-3}), Z_i: fugacity capacity (mol.m^{-3}. Pa^{-1}) which is different from medium to another as it is shown in Table 1.1, and f_i: gas fugacity (Pa): a molecule tendency to flee from one phase to another,

To calculate the fugacity for certain gas under certain conditions, the following expression can be used:

$$\ln\left[\frac{f_i}{p_i}\right] = \int_0^P \left(\frac{\bar{v}_i}{RT} - \frac{1}{P}\right) dP \quad (1.15)$$

where: p_i is the partial pressure of i in the gas mixture at final pressure P, f_i is the fugacity for the component i in the gas mixture, $\overline{V}_i$ is the partial molar volume of i in the gas mixture (Valsaraj 1995).

Table 1.1 Definition of Fugacity Capacity for Environment Compartments

Compartment	**Definition of Z (mol.m^{-3}.Pa^{-1})**
Air	1/RT
Water	$1/H_c$
Soil/Sediments	$K_d \rho_s/H_c$
Biota	$K_b \rho_b/H_c$

The following equation of mass conservation gas diffusion-convection in a porous media can be written:

$$\varphi \frac{\partial C_i}{\partial t} = -\frac{\partial (U_k C_i)}{\partial x_k} + \frac{\partial}{\partial x_k}(D_{ik} \frac{\partial C_i}{\partial x_j}) + G_i \qquad (1.16)$$

where: φ is porosity of the landfill (m^3 of voids per m^3 of refuse), C_i is concentration of the i^{th} component of the gas mixture (kg/m^3), U_k is advective velocity in the k^{th} direction (m/day), D_{ik} is diffusion coefficient of gas i in the k^{th} direction (m^2/day), x_k is k^{th} direction (m), and G_i is generation rate of the i^{th} component of the gas mixture (kg/day) (El-Fadel et al.1996).

Since the Reynolds number characterizing the flow of gases generated in sanitary landfills is typically smaller than 1, the velocity field can be described by the generalized form:

$$U_k = -\frac{k}{\mu_M}(\frac{\partial P}{\partial x_k} - \delta_{k3}\rho g) \qquad (1.17)$$

where: k is permeability of the landfill (Darcy), μ_M is viscosity of the gas mixture (N.day/ m^2), P is total pressure inside the landfill (N/m^2), ρ is density of the gas mixture (kg/m^3), δ_{k3} is Kronecker's delta: $\delta_{13} = \delta_{23} = 0$; $\delta_{33} = 1$ (dimensionless), and g is acceleration due to gravity (m/day^2) (El-Fadel et al.1996).

The total pressure when two or more different gases are present is equal to the sum of the individual partial pressures of the different gases. Hence, the total pressure can be given by:

$$P=\sum_{i=1}^{n} P_i \tag{1.18}$$

$$P_i=\frac{R}{M_i} C_i T \tag{1.19}$$

where: R is universal gas constant (N.m/mol.K), T is absolute temperature (K), P_i is partial pressure of gas i (N/m^2), M_i is molecular weight of gas i (kg/mol), and C_i is concentration of gas i (kg/m^3).

1.3.5. Porosity and Water Content Effect on Gas Transport

For the biogas transport in porous media, porosity and water content are very important factors due to their effect on the coefficient of diffusion and coefficient of conductivity and subsequently their effect on the overall transport.

For the effect of porosity and water content on diffusion coefficient, the water-induced linear reduction (WLR) model based on the Marshall (1959) model is describing the effect:

$$\frac{D_p}{D_0} = \frac{\varepsilon^{2.5}}{\Phi} \tag{1.20}$$

Where: $\phi = \varepsilon + \theta$

Where D_P is the gas diffusion coefficient in soil, D_0 is the gas diffusion coefficient in free air, ε is the soil air-filled porosity (cm^3 soil air/ cm^3 soil), ϕ is the soil total porosity (cm^3 /cm^3), θ is the volumetric water content (cm^3 /cm^3) (Moldrup et al. 2000).

As it is seen from the equation (1.20) when the water content increases then diffusion decreases, and as the porosity increases diffusion increases. And hence, increasing porosity and decreasing water content will increase diffusion coefficient and subsequently increasing gas diffusion flux.

The problems of water flow in vadose zone such as filtration and drainage are described by assuming that water is the only liquid phase, the water is incompressible, the air phase is continuous, and that the pressure is atmospheric. These conditions are represented by Richards equation for 3-D (Richards 1931):

$$\frac{\partial}{\partial x}(K_x(\psi)\frac{\partial \psi}{\partial x}) + \frac{\partial}{\partial y}(K_y(\psi)\frac{\partial \psi}{\partial y}) + \frac{\partial}{\partial z}(K_z(\psi)(1+\frac{\partial \psi}{\partial z})) = C(\psi)\frac{\partial \psi}{\partial t}$$

where:

$K(\psi)$ is unsaturated hydraulic conductivity (LT^{-1}), $C(\psi)$ is specific moisture capacity (L^{-1}), and ψ is pressure head (L)

For the effect of porosity and water content on gas conductivity coefficient, the following equation represents the coefficient of conductivity of gas in porous media as a function of gas properties, media properties and water content (θ):

$$K(\theta) = \left(\frac{k\rho g}{\mu}\right) k_r(\theta) \tag{1.21}$$

Where k is intrinsic permeability of the medium, ρ is the density of gas, g is gravitational constant, μ is gas dynamic viscosity, $k_r(\theta)$ is gas relative permeability (dimensionless, ranges from 0 to 1) (Stephens 1996).

The intrinsic permeability (k) of the medium as a property of the medium is dependent on the medium porosity as shown in the following formula from Kozeny-Carmen equation:

$$k = \frac{1}{180}\frac{\varepsilon^3}{(1-\varepsilon)^2} d_p^2 \tag{1.22}$$

where d_p is diameter of solid particle, ε is porosity (Reible 1999). In addition, the gas relative permeability ($k_r(\theta)$) is dependent on the water content in the porous medium as it is shown in Figure 1.4

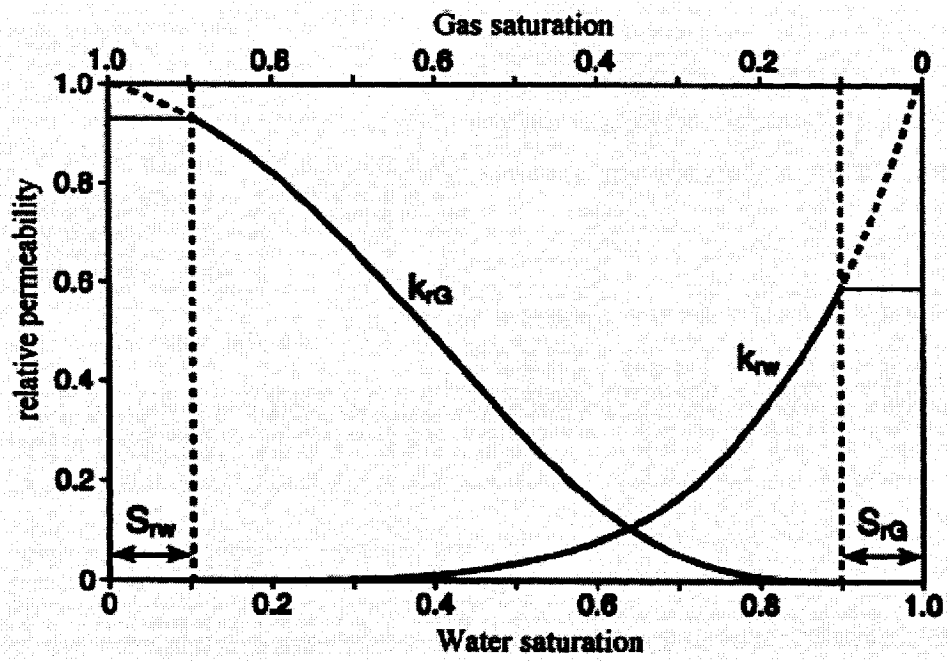

Figure 1.4 Schematic Relative Gas Permeability (K_{rG}) and Relative Water Permeability (K_{rw}) with Respect to Gas and Water Saturation, where (S_{rG}) is Residual Gas Saturation, and (S_{rw}) is Residual Water Saturation (Scanlon et. al 2002)

It is seen from the Figure 1.4 that when the water content increases then gas relative permeability (k_{rG}) decreases, and equation (1.22) shows that when the porosity increases the intrinsic permeability (k) increases. Increasing porosity and decreasing water content will increase conductivity coefficient and subsequently increasing convection flux.

It is worthy to state that the transfer of biogas through a porous media is the limiting factor in any landfill gas collection system (Manley 1997). The reached landfill gas collection rates are still very poor; Schachermayer et al. (1999) estimated an average gas collection rate of 15 %. The porous media involved in the collection systems require reconsideration. A new material and/or new collection system would improve collection

rate. Particular attention should be paid for decrease of moisture effect and increase of porosity.

1.3.6. Modeling of Biogas Migration

For biogas modeling, numerical models of varying degrees of complexity have been presented to simulate landfill gas migration. Group of models simulated gas migration beyond lateral landfill boundaries, and treated the landfill as a constant linear source. Using this approach, Moore et al. (1979) have simulated landfill gas migration through a soil represented as an aggregation of parallel capillary tubes of variable radius. The simultaneous diffusion of two gas components was simulated, including the effects of off-site venting wells. Using instead a continuum approach to represent the porous medium, Mohsen et al. (1980) developed a symmetric finite element model. With the model, the depth of an off-site venting trench was varied to assess its impact on gas migration. Metcalfe and Farquhar (1987) developed a two-dimensional finite element model that solves the advection–dispersion equation. The viscosity and the diffusion coefficients depend on the gas mixture, and retardation factor accounts for the dissolution of carbon dioxide (Nastev et al. 2001).

Another group of numerical models simulated gas generation and migration within the landfill only, as well as gas emission to the atmosphere. Findikakis and Leckie (1979) presented a one-dimensional finite difference advection–diffusion model including an exponential gas production equation. Several simulations evaluated the effects of various degradable fractions of the refuse on gas production, and the temporal distribution of gas-phase pressures and concentrations of three gas components. Predicted pressure and

concentration profiles were confirmed with monitoring data from Palos Verdes and School Canyon landfills, California. El-Fadel et al. (1989) used the same migration model, but included a more complex gas production model based on sequential biological growth and where degradation of organic matter was represented by a complex system of first order equations accounting for different carbon sources. Finally, Lang and Tchobanoglus (1989) developed a three-dimensional finite element model to solve the advection–dispersion equation for trace gases in a gas mixture of constant density and viscosity. A retardation factor was included to account for the sorption and chemical/biological transformation of trace gases. The impact of landfill cover and horizontal extraction wells on atmospheric gas emission was investigated (Nastev et al. 2001).

As to the literature, all biogas modeling processes are complex models and needed some assumption for simplicity. Major part of modeling depended on numerical and finite element modeling, which needs many parameters to describe the problem classically and without flexibility. These models are classical formulas and have complicated procedures and extensive approaches. The complexity of the biogas transport in porous media can be solved using natural language modeling that takes the real data and real expert from the field to the artificial computing with simple flexible natural language, and herein fuzzy logic modeling is being proposed.

1.4. Fuzzy Logic

1.4.1. Introduction

Fuzzy logic is a superset of conventional logic that has been extended to handle the concept of partial truth, truth-values between "completely true" and "completely false". It was introduced by Lotfi Zadeh of UC/Berkeley in the 1960's as a mean to model the uncertainty of natural language. Fuzzy Logic is a departure from classical two-valued sets and logic, which uses "soft" linguistic (e.g. large, hot, tall) system variables and a continuous range of truth-values in the interval [0, 1], rather than strict binary (True or False) decisions and assignments (Bonde 2000). Zadeh says that rather than regarding fuzzy theory as a single theory, we should regard the process of "fuzzification" as a methodology to generalize any specific theory from a crisp (discrete) to a continuous (fuzzy) form. Thus recently researchers have also introduced "fuzzy calculus", "fuzzy differential equations", and so on (Kantrowitz et al. 1993).

Fuzzy logic is a model-free estimator that approximates a function through linguistic input-output associations. The fuzzy system is a rule-based approach that is applied to solve many types of problems, especially where a system is uncertain and hard to model (Bonde 2000).

Fuzzy logic is derived from fuzzy set theory dealing with reasoning that is approximate rather than precisely deduced from classical predicate logic. It can be thought of as the application side of fuzzy set theory dealing with well thought out real world expert values for a complex problem (Klir 1997).

In classical set theory, a subset U of a set S can be defined as a mapping from the elements of S to the elements of the set {0, 1}:

$U: S \longrightarrow \{0, 1\}$

this mapping may be represented as a set of ordered pairs, with exactly one ordered pair present for each element of S. The first element of the ordered pair is an element of the set S, and the second element is an element of the set {0, 1}. The value zero is used to represent non-membership, and the value one is used to represent membership.

The truth or falsity of the statement:

x is in U

is determined by finding the ordered pair whose first element is x. The statement is true if the second element of the ordered pair is 1, and the statement is false if it is 0 (Kantrowitz et al. 1993). For example, the measure of temperature has to be transformed into a "high" or "low" value with a respective degree of membership, before being processed by the inference engine.

The fuzzy interval is an uncertain set $\tilde{A} \subseteq R$ with a mean interval where elements possess the membership function value $\mu_A(x) = 1$. As in fuzzy numbers, the membership function must be convex, normalized, at least segmentally continuous.

For any set S, its characteristic function $f_S(x)$ describes whether or not an element x is an element of the set S. Where $f_S(x) = 1$ if true, and $f_S(x) = 0$ if false.

In Boolean logic:

$$f_S(x) = \begin{cases} 1, \text{ if } x \in S \\ 0, \text{ if } x \notin S \end{cases}$$

In Fuzzy logic, $\mu_S(x)$ describes the membership function of S, or the degree to which x is a member of the set S, this is known as the degree of truth:

$$\mu_S(x) = \begin{cases} 1, \text{ if } x \text{ is totally } \in S \\ 0, \text{ if } x \text{ is not } \notin S \\ 0 < \mu_S(x) < 1, \text{ if } x \text{ is partially } \in S \end{cases}$$

For the universe X and given the membership degree function $\mu \rightarrow [0,1]$ the fuzzy set A is defined as:

$$\tilde{A} = \{(x, \mu_A(x)), x \in X$$

The membership function $\mu_A(x)$ quantifies the grade of membership of the elements x to the fundamental set **X**. The value 0 means that the member is not included in the given set, 1 describes a fully included member. The values between 0 and 1 characterize fuzzy members fuzzy members (Fig. 1.5) (Wikipedia (2006).

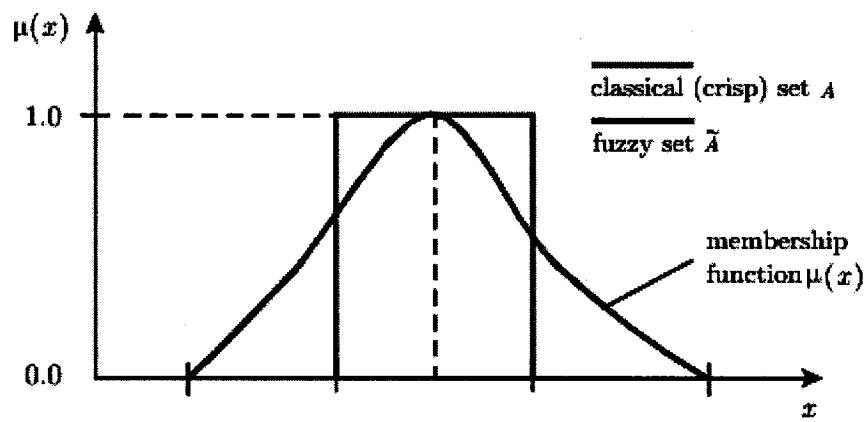

Figure 1.5 Fuzzy Set Compared with Classical Set

1.4.2. Fuzzy Inference System

A fuzzy inference system is a system that uses a collection of fuzzy membership functions and rules, instead of Boolean logic, to reason about data.

In contrast to ordinary (crisp) rules, fuzzy rules allow the partial and simultaneous fulfillment of rules. This means that, instead of the usual case in which a rule can either be applied or not, partial applicability is also possible. This allows for cases in which different rules with different consequences can be applied to the same premise (Borri et al 1998).

A typical fuzzy system consists of a rule base, membership functions, and an inference procedure (Bonde 2000). The general inference process proceeds in fuzzification, inference, and defuzzification process (Kalaykov 2000):

- Fuzzification

Fuzzification is the process that changes the crisp value to fuzzy value using membership function. The membership functions defined on the input variables are applied to their actual values, to determine the degree of truth for each rule premise (Gulley and Roger 1995).

- Inference

The truth-value for the premise of each rule is computed, and applied to the conclusion part of each rule. This results in one fuzzy subset to be assigned to each output variable for each rule. MIN or PRODUCT is used as inference rules. In MIN inference, the output

membership function is clipped off at a height corresponding to the rule premise's computed degree of truth (fuzzy logic AND). In PRODUCT inference, the output membership function is scaled by the rule premise's computed degree of truth (Kantrowitz et al. 1993). AND represents the intersection or MIN between two sets, expressed as:

$$\mu_{A \cap B} = \min[\mu_A(x), \mu_B(x)]$$

OR represents the union or MAX between two sets, expressed as:

$$\mu_{A \cup B} = \max[\mu_A(x), \mu_B(x)]$$

NOT represents the opposite of the set, expressed as:

$$\overline{\mu_A} = [1 - \mu_A(x)]$$

A fuzzy inference process is shown in the demonstration below. For two inputs X and Y, and one conclusion Z with the following rules (Roger J 2006):

Rule 1: if X is A_1 and Y is B_1 then Z is C_1
Rule 2: if X is A_2 and Y is B_2 then Z is C_2
One can say a fact: X is A` and Y is B` then Conclusion: Z is C`

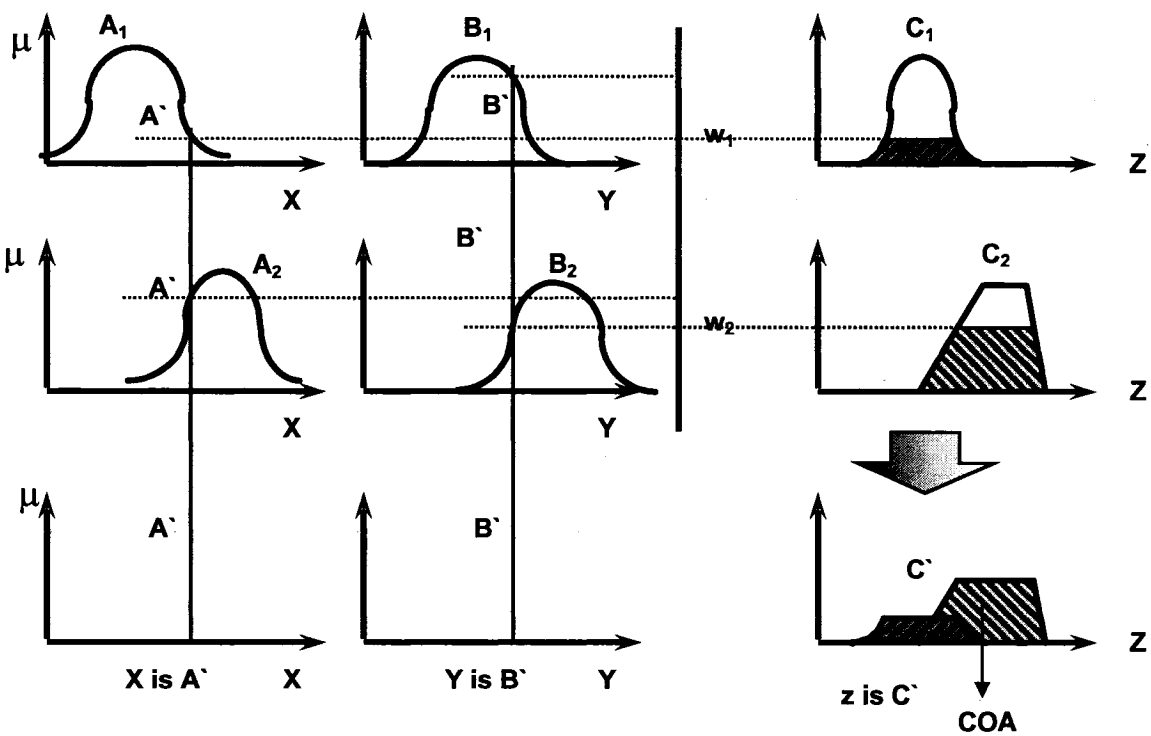

- *Defuzzification*

Defuzzification is used when it is useful to convert the fuzzy output set to a crisp number. Three of the more common techniques of defuzzification are the centroid, maximizer, and weighted average methods. In the *centroid* method, the crisp value of the output variable is computed by finding the value of the center of area (COA) of the membership function for the fuzzy value. In the *maximum* method, one value by which the maximum output of the variable values is selected. In the *weighted average* method, it averages weighted possible outputs (Kartalopoulos 1996).

1.4.3. Fuzzy Decision Support Systems

Fuzzy decision support systems (FDSS) comprise rule-based approach to decision making using fuzzy logic techniques, based on the compositional rule of inference (CRI). This approach is used to handle uncertain knowledge. Such knowledge can be collected and delivered by a human expert like decision-maker or designer. The CRI may be written in the following form:

$$U' = (C' \times ... \times B' \times A') o\, R$$

where: U' represents the output (conclusions); $(A', B', ..., C')$ represents the inputs (observations); the symbol o represents the CRI operator; R represents the global relation that aggregates all rules (knowledge base) (Balazinski and Jemielniak 1998). Fuzzy rule-based systems are being applied to solve many types of real-world problems, especially where a system is difficult to model. Human operator or expert controls these systems. A typical fuzzy system consists of a rule base, membership functions, and inference procedures. Three defuzzification methods are usually available, i.e. center of area

(COA), average of maximums (AOM), and the modified center of area (MCOA). The knowledge base consists of two components: the linguistic term base (database) and the fuzzy production rule base. The database is divided in two parts: fuzzy premises and fuzzy conclusions. Knowledge bases can be built up manually based on results from experimental tests and computations, or it can be generated automatically using genetic algorithm (Baron 1998; Balazinski et al. 2000). FDSS uses knowledge bases to support the final decision.

1.4.4. Fuzzy in Environmental Systems

Like all natural systems, environmental systems are complex, particularly when we consider their evolution over time and space, and their internal and external exchange systems. Great precision and certainty is usually needed when modeling the process of evaluating an environmental system. The oversimplification of a modeling system has always been seen as a great risk in the evaluation process (Pearce, 1993) since environmental systems are usually characterized by high complexity.

Compared to traditional modeling, fuzzy systems provide a robust tool which can directly handle the linguistic models of human interpretation of environmental systems. They are able to handle categories without requiring a prescribed functional structure. Since they are able to handle categories, fuzzy rule-based systems are able to represent knowledge completely through a number of rules which is smaller than in the traditional systems (Yager et al., 1994). As a result, the rule-based system is simplified without risking oversimplification. In real life and reasoning, problems defined by purely mathematical

or analytical modeling can often give a false impression of accuracy. The gain in simplicity, computational speed, and flexibility of fuzzy models does not imply a loss in accuracy. Furthermore, the size of a fuzzy rule set may be adjusted to match the amount and accuracy of data (Bardossy et al., 1993).

It is sometimes necessary when evaluating environmental systems to deal with parameters that cannot be described through numerical representations. In this case, it is possible to build a rule-based algorithm which formalizes the cognitive rules needed to supply membership values. This would extend the concept of the membership function to general algorithms which would associate one element of the universe of discourse with a degree of membership. Further extension along these lines might entail the use of a neural network (Borri et al 1998).

Fuzzy logic has an advantageous effect on modeling of environmental engineered systems. Fuzzy logic, for example, was used to assess the best conditions required for constructed wetland to serve as a sink of metal removal; it is also used to generate the main information on the behavior of metals (mercury) in wastewater/water in relation to its uptake by plants and adsorption to sediments (Elektorowicz and Qasaimeh 2004; Elektorowicz et al. 2002). In hazy natural cases where there are plenty of parameters, these complicated systems can be managed by the application of the fuzzy logic approach. For example, the technical information system (conducted at Inland Water Institute, NRC, Winnipeg, Manitoba) can be installed overall the constructed wetland in order to collect information for the conditions of the wetland components. As a link

between design and natural conditions, the data collected could be used as an input feed to the Genetic Algorithm Fuzzy Decision Support System that automatically provides design decision whenever the conditions vary (Qasaimeh 2003).

Qasaimeh et al. (2006a) proposed a new management system to control biogas transport in landfill. Biogas convective and diffusive transport was modeled using fuzzy logic approach. The biogas evacuation process from the system was controlled using intelligent fuzzy logic approach (Qasaimeh et al. 2006b).

1.5. Summary - Problems with Biogas in Landfill

The literature in the previous sections highlighted important issues associated with biogas at landfill. Methane and carbon dioxide are vital in terms of their pollution, hazards, and benefits. They are greenhouse gases and contribute to the phenomena of global warming. On the other hand, methane and carbon dioxide have been widely used as a source of energy; and therefore it is important to collect and control their emissions.

In conventional landfills, the biological biogas capture is associated with low biogas concentrations; however for high biogas concentrations, the physical collection and control processes need new approaches for more efficiency. As shown in Figure 1.6, gas could migrate in the nearby areas through liner joints or cracks due to liner failure by pressure build up, inactive zone obstruction, heterogeneous gas transfer, etc. The following problems are associated with biogas at conventional landfills:

- Due to different management, the gas collection efficiency, in average, for landfills is between 40-90 % (Augenstein and Pacey 1991).
- The landfill gas collection rates are still doubtful; in some conditions it could be very poor, for example Schachermayer et al. (1999) estimated an average gas collection rate of 15 %.
- The transfer of biogas through solids toward gas collection system is a limiting factor (Manley 1997).
- Transfer of biogas through landfill is complex and uncertain due to:
    1. multi transport (convection-diffusion)
    2. multi gas components
    3. multi media (porous media: solid, air, water)
    4. variable affecting environmental conditions

- Modeling of biogas transport in porous media is complex.
- Migration of biogas at landfill is unexpected and uncontrollable.

Thus, a new Intelligent MSW Management System for Biogas Control in Landfill is needed.

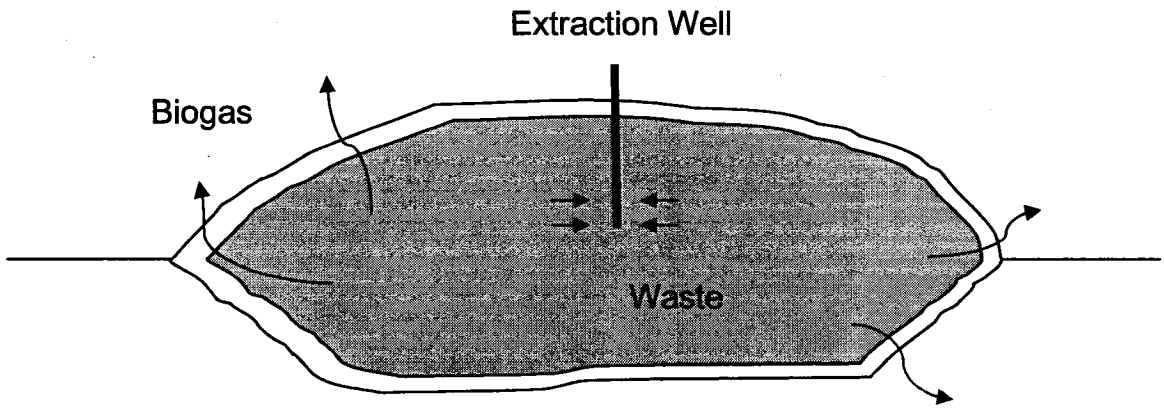

Figure 1.6 Conventional Landfill Profile.

CHAPTER 2

Objectives and Methodology

2.1 Objectives

The main objective of this work is to provide a new intelligent MSW management system for biogas control in landfill.

To achieve the main objective of this research, the following sub-objectives should be accomplished:

- To provide a new waste management and operation system for better accommodation for biogas transport;
- To provide a new material medium for more efficient biogas collection;
- To develop an automatic control system for biogas collection;
- To provide a new landfill construction design that is able to implement an intelligent control for biogas collection.

2.2 Methodology

2.2.1 Novel Intelligent MSW Management System: Intelligent QEJ Bricks

The proposed new MSW management system includes the following:

a. Implementation of new construction design configuration that confines the waste and collects the gas produced;

b. New cell construction and operation including series of cells with prefabricated confinements in the form of porous "bricks" built sequentially to form a wall confining the waste (Figure 2.1);
c. Integrated operation system that combines waste disposal, biogas evacuation, and biogas control;
d. Implementation of new material for better control of biogas transport;
e. Artificial Intelligence modeling for biogas transport;
f. Genetic Algorithm optimization for biogas mass transfer;
g. Intelligent fuzzy automatic control system for optimization the biogas evacuation processes.

Consequently, the new MSW management proposed in this research provides new ideas about: landfill operation, material medium and tests to verify its functionality as a permeable medium for biogas collection, biogas transport modeling, biogas mass transfer optimization, design configuration, and automatic system for the gas extraction control.

2.2.1.1. Operation System

To fulfill the research objectives, a system with new operation and waste management is proposed. The proposed operation system is built gradually when the waste is being disposed. Different than conventional disposal at landfill, waste is put between "bricks" that are perforated containments filled up on- place with porous material or prefabricated directly from porous material. To maintain the integrity of the system, cells are constructed at chronological order (more details in Chapter 3). Figure 2.1-b shows the

gradual construction of the landfill using porous "bricks". To maintain the stability of the structure each brick can be reinforced to the other down- or- up brick by key knobs that fit to keyholes. Crossing the horizontal "bricks" to perpendicular "bricks" satisfies more stability (Figure 2.1).

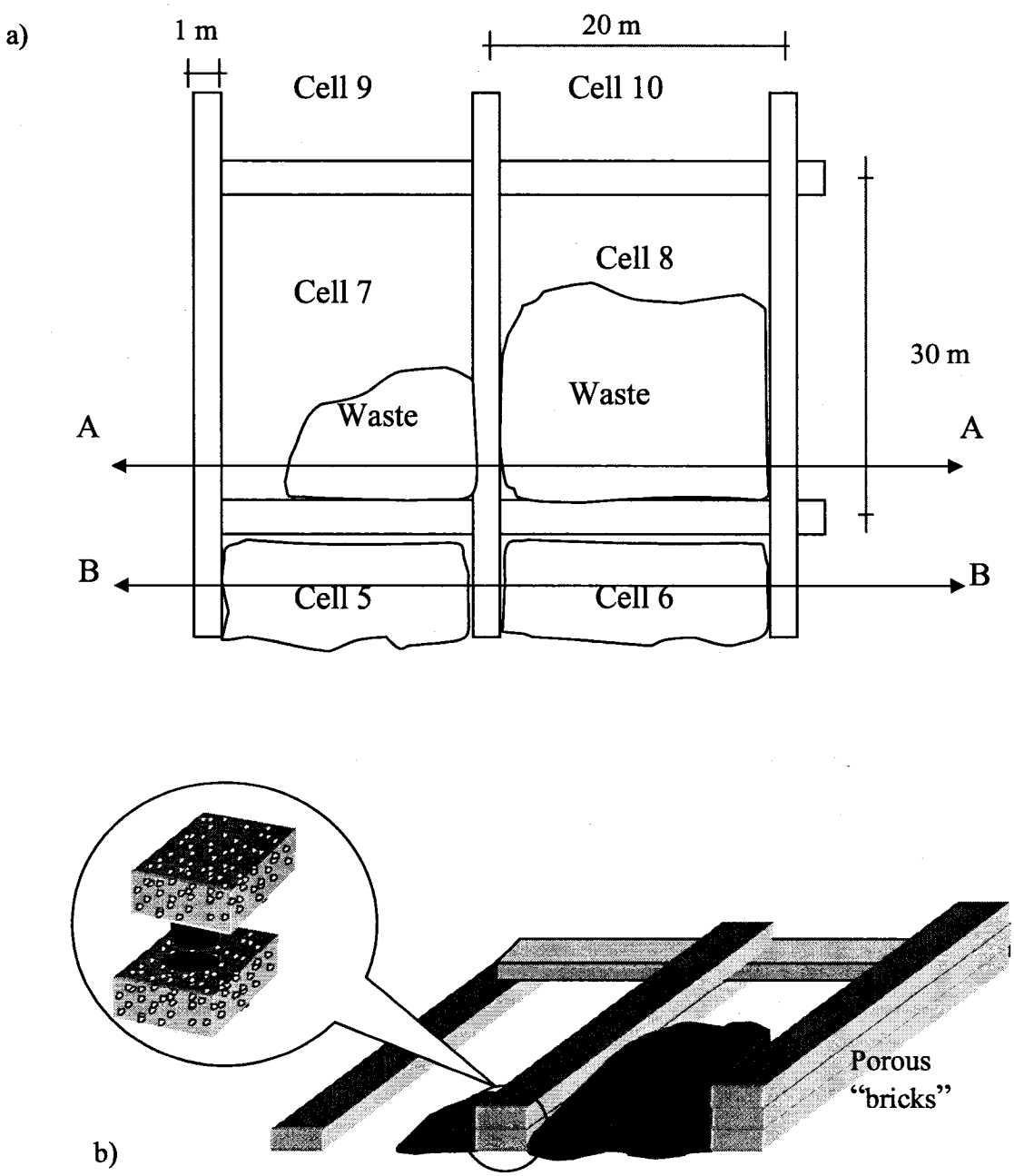

c)

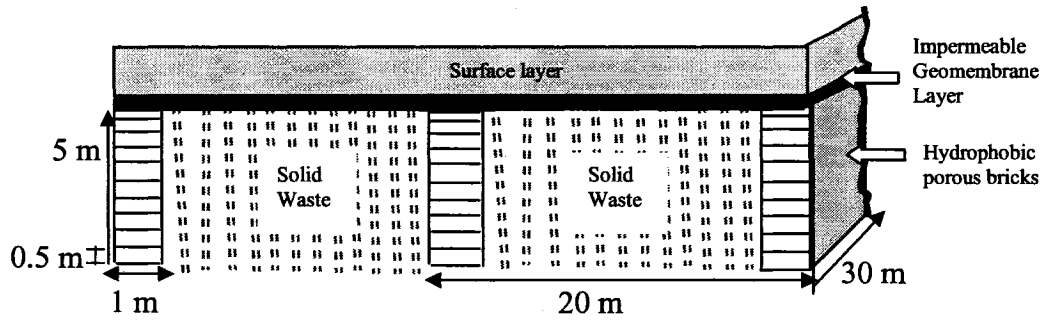

Figure 2.1 Example of Design and Operation of Intelligent QEJ Bricks: a) plan view; b) side view at cross section A-A for cells 7 and 8 under operation; c) side view at cross section B-B for finished cells 5 and 6

2.2.1.2. QEJ Brick Material

As described in Chapter 1 (section 1.3.5), the porosity and water content are vital factors affecting the biogas transport in porous media, then, it was concluded that increasing the porosity and decreasing the water content provide more efficient biogas transport (convection and diffusion). Consequently, the proposed medium in this research should respond to the following criteria:

- Negligible water content (more permeable)
- No microbial growth inside (no clogging)
- High porosity (more air filled voids that normally)
- Light and easily reformed material
- Cheap and recyclable material

Subsequently, a hydrophobic porous polymer seems ideal medium for Intelligent QEJ bricks formation.

The hydrophobic medium might be a material such as polymers (e.g. polystyrene (PS), polyethylene (PE)). To fulfill sustainable development principles, polymers used for hydrophobic medium can also be formed from recyclable materials available on the landfill dump. Another source of sustainable materials for bricks' formation is wasted polymers during wrong polymerization processes taking place occasionally in the factory.

In this research, a recyclable hydrophobic polymer medium (Styrofoam) was tested at laboratory to verify its functionality as a permeable medium for biogas collection. Therefore the test procedure on polymer medium entailed the following:

- Finding the permeability of polymer, conductivity coefficient, and diffusion coefficient of carbon dioxide and methane within the polymer medium;
- Finding carbon dioxide and methane convective flow rate and diffusive flux through polymer medium;
- Finding the influence of parameters (water content, porosity, temperature variation, pressure gradient, concentration gradient) on gas transport (diffusion and convection).

The Experimental Procedures

Referring to the objective of the research, biogas capture and control is the main issue. The experimental procedure entails tests that check the biogas relevant processes that affect its collection and control. Styrofoam material that forms the QEJ bricks should be tested to check its permeability and functionality for conveying the biogas by diffusion and convection transport. Therefore, series of tests have to be conducted to determine the coefficients of permeability, diffusion, and conductivity for Styrofoam medium.

A. Permeability Test on Different Material Media

The QEJ bricks system was represented by Styrofoam material. To show the functionally of this material to convey gas in comparison to other materials, a permeability test was conducted on four samples: landfill cover soil (from CESM landfill), sand (0.05 mm), coarse crushed basalt (6 mm), and hydrophobic Styrofoam chips (2 mm particle@10 mm chip) (Tab. 2.1). For the permeability test, the material filled in a glass cylinder (20 cm long and 8 cm diameter). The material was packed without compaction (porosity 95%). Air was convected through the material medium pack as shown in Figure 2.3. Water U-tube manometer was connected to the medium to measure the head loss of air pressure through the media as an indication of medium permeability.

Air was convected through each material medium for different air flow rates. The head loss was recorded for each flow rate in each medium. The tests were conducted on standard room conditions at bench scale. Tests were replicated three times for each flow rate for each medium.

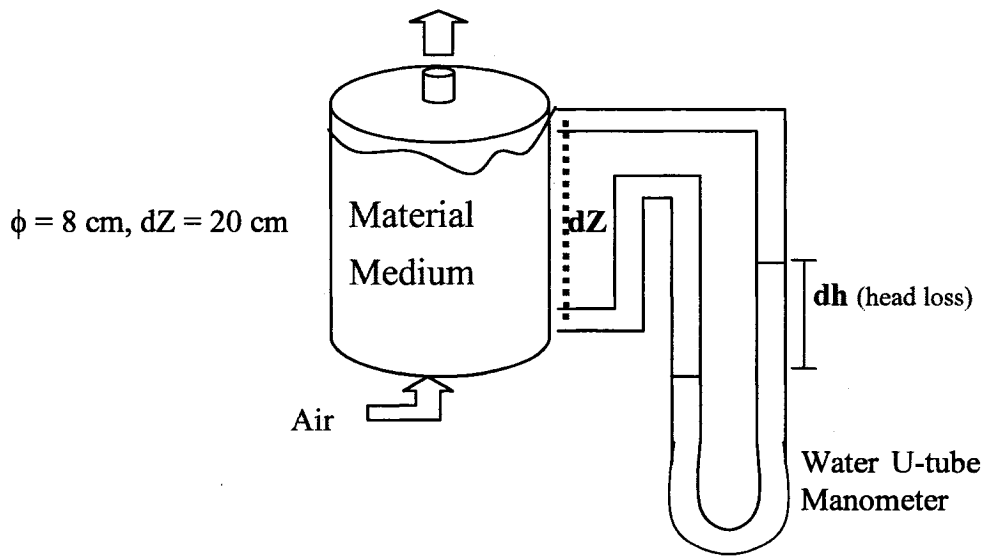

Figure 2.3 Scheme of the Experimental Setup for Permeability Test

Table 2.1 Physical Properties of the Material Used for Permeability Test

Material	**Composition**	**Void Ratio (% v)**	**Specific Gravity (SG)**	**Available Water Percent by Volume (%v)**
Sand	Fine Sand	38	1.65	8
Cover soil	Silty Loam	52	1.30	20
Road stone	Coarse crushed basalt (6 mm aggregate)	80	1.96	4
Hydrophobic Styrofoam	Polystyrene (2 mm particle@10 mm chip)	95	0.05	Negligible

B. Test of Gas Diffusion within Hydrophobic Styrofoam Medium

This test aims to find the coefficients of diffusion of methane and carbon dioxide within the Styrofoam polymer medium. Consequently, a simulation was done using a Styrofoam chips (1cm) packed without compaction (95 % porosity) in a plastic box (30 cm ×15 cm ×10 cm) with multi ports for gas entrance and sampling. Sensors and data acquisition system were connected to the system (Figure 2.4). To detect methane diffusion in polymer medium, sensor (Combustible Gas Detector VQ548ZD / e2V Technologies - UK) and required electrical Wheatstone bridge circuit were built and connected to the 6-channel data logger system (Field Portable Computer - Field Works Inc) with Microsis-R6 data acquisition system. For carbon dioxide detection, infrared gas sensor (IR11BD / e2V Technologies - UK) was used. Gas samples were introduced to sensors to check the sensors response to methane and carbon dioxide. The scope within data acquisition system recorded the voltage signals from sensors and then a gas concentration calibration was done. Different gas concentrations were recorded to calibrate voltage signals to gas concentrations. Sensors were able to detect as minimum as 1 % volume of biogas and sensitive to provide as low as 20 milli-volts signal.

Both Methane (from gas line-1000mL) and carbon dioxide (from cylinder-1000mL) were diffused together through the Styrofoam polymer medium, as shown in Figure 2.4, to find methane and carbon dioxide coefficients of diffusion through polymer medium. The process was done at different temperatures. The temperature of polymer medium was controlled by having the box with medium pack submerged in the water bath (BLUE M) at different temperatures (0, 15, 25 °C). The process repeated three times for each

temperature for both methane and carbon dioxide. Each time sensor-data acquisition system recorded the concentration (dC) with the time (dt) for given distance (dZ) (Figure 2.4). Therefore, the diffusion coefficient (D) of methane and carbon dioxide within the polymer medium were found for different temperatures according to the following equations:

$$F_g = -D\frac{\partial C}{\partial Z} \tag{2.1}$$

and

$$F_g = \frac{\partial C}{\partial t} \times \partial Z \tag{2.2}$$

The above-described process was repeated at room temperature with different Styrofoam medium porosity [85 %, 90 %, 95 %(no compaction)]. The porosity was changed by varying the compaction degree, and it was calculated based on the pack weight, volume and bulk density according to the following equation:

$$\eta = 1 - D_b/D_p \tag{2.3}$$

where η is porosity, $D_b = W_s/V_t$ is the bulk density (W_s weight of polymer medium , V_t total volume of polymer with voids), D_p particle density. Each test is repeated three times at each porosity value.

Identified different water volumes (0.2, 0.3, 0.5 %) were added to Styrofoam pack to check water content effect on biogas diffusion coefficients.

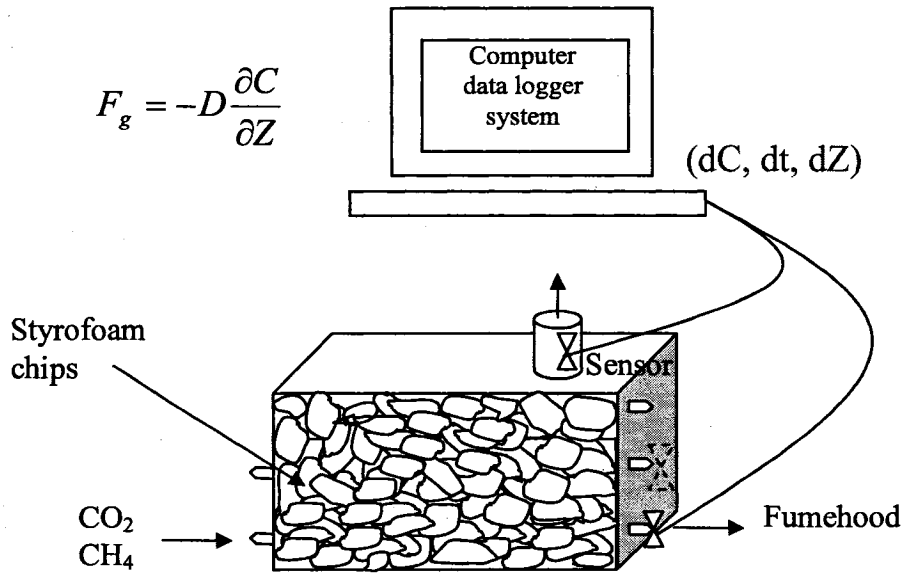

Figure 2.4 Scheme of the Experimental Setup for Gas Diffusion Test

In order to find diffusion flux, a test was done at 25 °C temperature, at 95 % polymer medium porosity, at negligible water contents for different biogas concentration gradients (0, 0.25, 0.5, 0.75, 1 kg/m^3.m). The gradients were adjusted by varying volumes of biogas by several folds and keeping fixed distance for biogas transport. This process was repeated three times for each biogas gradient.

C. Test of Gas Convection Transport within Hydrophobic Styrofoam Medium

In order to obtain medium permeability and biogas conductivity through the medium, a gas conductivity test was conducted. A simulation was done using a Styrofoam chips packed without compaction (95 % porosity) in a glass cylinder (8 cm diameter, 20 cm height) with entrance and exit port. Water U-tube manometer and flowmeter (TF) were used to record the pressure gradient and biogas flow rates respectively (Figure 2.5).

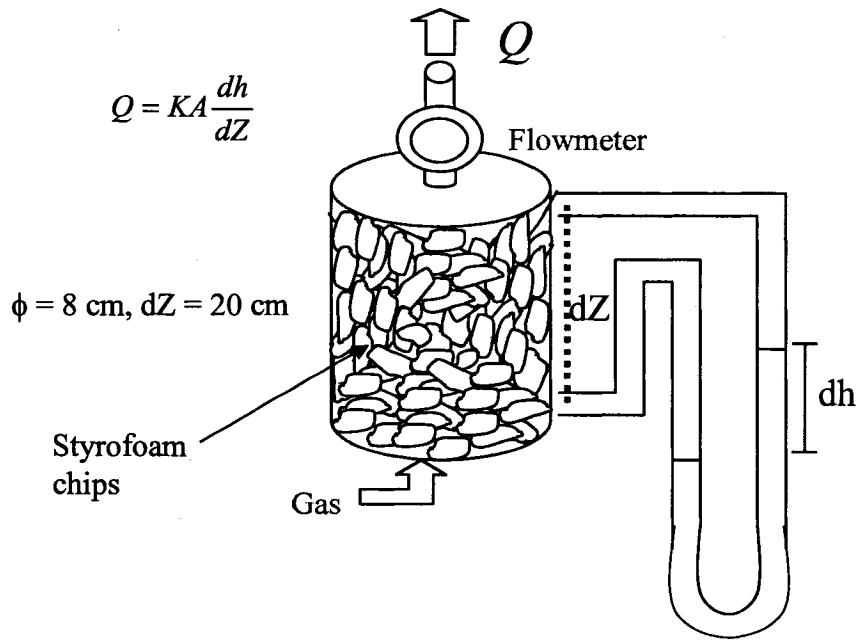

Figure 2.5 Scheme of the Experimental Setup for Styrofoam Medium Conductivity Test

The coefficient of permeability is a property of the medium regardless of gas passes through. To find the coefficient of permeability for the Styrofoam polymer medium, the permeability test using air passing through polymer medium was applied. However, the coefficient of conductivity is a function of medium properties (permeability) and gas properties, and it can be found as shown in Figure 2.5 from the equations (2.4) and (2.5):

$$Q = KA\frac{dh}{dZ} \tag{2.4}$$

$$K = \frac{k\rho g}{\mu} \tag{2.5}$$

where K is the coefficient of gas conductivity within the polymer medium, k is the intrinsic permeability of the polymer medium, μ is the dynamic viscosity of the gas, ρ is the gas density.

To find the coefficients of conductivity for biogas within the Styrofoam polymer medium, methane and carbon dioxide together were convicted through the polymer medium as shown in Figure 2.5. The process was done at different temperatures (0, 15, 25 °C). The temperature was controlled by having the medium pack submerged in water bath (BLUE M) at different temperatures. The process repeated three times for each temperature for both methane and carbon dioxide. Each time flowmeter and manometer recorded the flow rates (Q) and the pressure head (dh) for given distance head (dZ) and area (A), and hence coefficients of conductivity of methane and carbon dioxide within the polymer medium were found for different temperatures (Figure 2.5).

The above mentioned procedure was repeated for different porosities (85, 90, 95 %) at room temperature.

Different water volumes (0.2, 0.3, 0.5 %) were added to Styrofoam pack to check its effect on biogas conductivity coefficients.

For convection flow rates, the test was done at 25 °C temperature, at 95 % polymer medium porosity, and negligible water contents for different biogas pressure gradients (0, 0.25, 0.5, 0.75, 1 $N/m^2.m$).

Collected information about parameters (temperature variation, pressure gradient, and concentration gradient) were generated to obtain their effect on polymer-gas conductivity coefficient, gas convection rates, gas diffusion coefficient, and gas diffusion flux through the porous Styrofoam polymer medium. Table 2.2 summarizes procedure, and setup components of experimental gas diffusion and conductivity tests.

Table 2.2 Setup and Experimental Items for Gas Diffusion and Conductivity Tests

	Gas Diffusion Test	***Gas Conductivity Test***
Apparatus used	Polymer medium pack you used word cylinder, Sensors, Data acquisition system Microsis	Polymer medium pack you used word box, Flowmeter, Manometer
Gas used	CH_4 (*from gas line*) CO_2 (*from cylinder*)	CH_4 (*from gas line*) CO_2 (*from cylinder*)
Medium used	Hydrophobic porous polymer (*Styrofoam*)	Hydrophobic porous polymer (*Styrofoam*)
Parameters tested	Temperature variation Water content Porosity Concentration gradient ($\Delta C/\Delta X$)	Temperature variation Water content Porosity Pressure gradient ($\Delta P/\Delta X$)
Coefficients calculated	Diffusion coefficient	Permeability coefficient Conductivity coefficient
Rates calculated	Diffusive flux	Convective flow rate

2.2.1.3. Fuzzy Logic Modeling for Biogas Transport in Polymer Medium

Data obtained from the laboratory tests about diffusion and conductivity coefficients, biogas diffusion and convection transport, as well as affecting parameters were formulated as knowledge bases (input- output).

The inputs-outputs were fuzzified from crisp values to fuzzy value by formulating membership functions assigning values in the range of (0-1) describing the inputs and the outputs premises. The next step was to infer the input fuzzy values by fuzzy rules and operators (e.g. max - min) to the output values. After the inference process completed, the values were defuzzified from fuzzy to crisp values again using average or centriod operators (Figure 2.6).

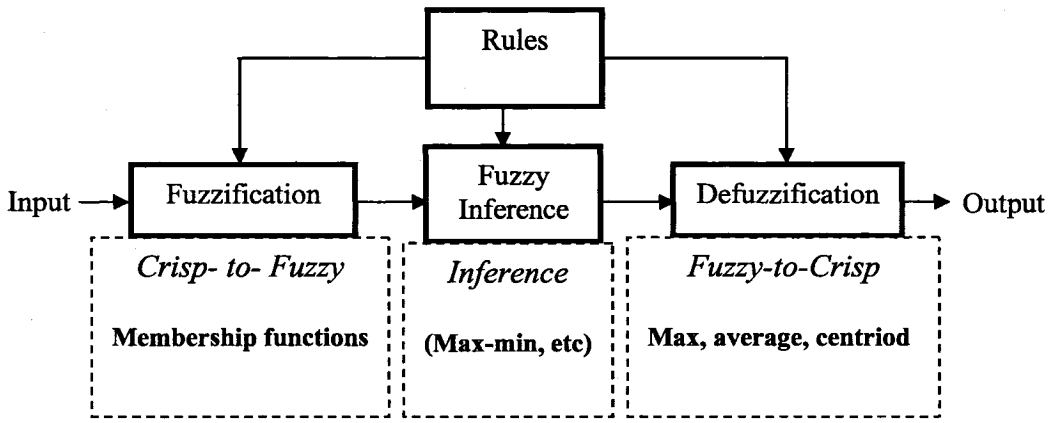

Figure 2.6 Fuzzy Logic Processes: fuzzification, inference, defuzzification

In this research, Fuzzy Logic Toolbox (Matlab 6.5) is used to build fuzzy model of biogas transport in hydrophobic polymer. The Fuzzy Logic Toolbox uses Mamdani fuzzy inference system in this research.

The fuzzy logic implicated biogas inputs (concentration gradient, pressure gradient, and temperature premises) to biogas outputs (biogas diffusion and convection transport) by specific rule bases in order to estimate the defuzzified output result that describes the CO_2 and CH_4 diffusion and convection in hydrophobic porous polymer media in landfill for a wide range of input premises.

Fuzzy input-output premises and rules were built manually based on results from experimental tests, and expert of model maker. With manually built fuzzy model, calibration takes place repeatedly until the correlation between the experimental data and fuzzy modeled data were very high and the squared difference was minimal. Verification of model was done on set of data other than data used in calibration.

2.2.1.4. Genetic Algorithm Optimization for Biogas Mass Transfer in Polymer Medium

In this section, genetic algorithm was used to optimize a transfer-function that represents solutions for mass transfer rate for different ratios of biogas mixture in polymer medium in landfill. Biogas ratios were assigned to inputs and mass transfer rates were assigned to outputs. By genetic algorithm, mass transfer rates were determined for design of the

hydrophobic porous polymer for any ratio of biogas mixture in landfill through the time of service.

The experimental setup of diffusion test (point B at the experimental procedures in the section 2.2.1.2) was used to obtain data for mass transfer for biogas transport at different pressure gradients for different biogas ratios. Genetic algorithm was used to optimize the obtained data for a micro-scale unit to find biogas mass transfer rate (dm/dt) in the porous hydrophobic polymer medium. Genetic algorithm was used to characterize the dynamics of input-output data by identifying a dynamic transfer function.

Genetic algorithm was applied by means of TransGA 1.0 (©Angel Martin 2002) for optimizing the micro-scale biogas transfer rates in the porous hydrophobic medium for any biogas ratio at different pressure gradients.

The transfer function was obtained by fitting a dynamic input-output data to the input-output solutions. As shown in Figure 2.7, input-output data were encoded to chromosomes (1, 0 digits). These chromosomes were subjected to genetic processes as crossover and mutations. Then a process of evaluation took place. The evaluation process entailed an objective function that evaluated the squared difference between experimental and calculated values. After the chromosomes were evaluated, they were either selected for more iteration or decoded to the solutions. The selection process was performed on non-optimal chromosomes by keeping the most promising individuals based on their

fitness. The decoding process was performed on optimal chromosomes to obtain optimal solutions and required optimal transfer function.

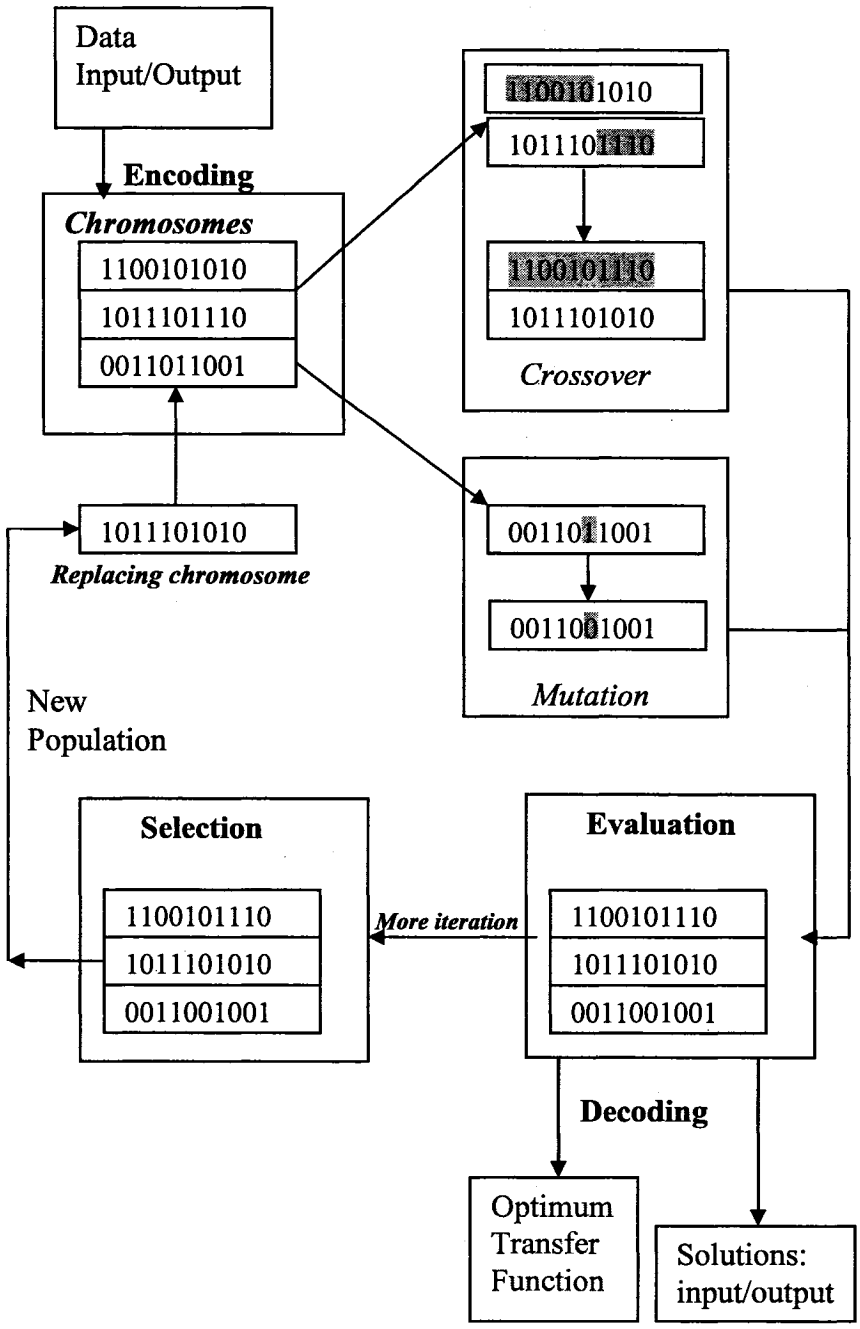

Figure 2.7 Genetic Algorithm Processes and Optimization

2.2.1.5. Intelligent Fuzzy Control Approach for Biogas Evacuation in the QEJ Bricks Management System

QEJ Bricks Management System satisfies confining the waste with hydrophobic porous walls that surround the waste and capture all available biogas generated at the landfill. Biogas evacuated from the porous walls has to be stored for further utilization. In conventional landfills, the extraction systems collect biogas roughly depending on classically connected pressure gauges, pumps, pipes and valves that are managed at nonflexible bases (Baggchi 2004, Park and Shin 2001). Different than classical methods, the evacuation system in the QEJ bricks management system is intelligent and dynamic. At the collection ports, the valves are connected with meters and /or sensors. These meters are connected to data acquisition system that is supplying information (concentration, pressure, volumetric flow rates) for fuzzy logic control system, which in turn controls the valves back depending on the acquired inputs.

CHAPTER 3

Intelligent "QEJ Bricks" Waste Management System

3.1 Introduction

Intelligent "QEJ bricks" is a novel management system (originated by Qasaimeh, Elektorowicz, and Jasiuk) as a new system for controlling biogas at landfill. Different than conventional disposal at landfill, waste is put between bricks that are perforated containments filled up on-place or prefabricated at a factory with porous hydrophobic polymer. These bricks might be made up of recyclable material (e.g. styrofoam) available on the dumping area. QEJ bricks are utilized to provide a porous medium for biogas collection. Since the material is hydrophobic, it does not contain water in the voids providing more space for gas transport.

3.2. Operation System

3.2.1 QEJ Bricks Fabrication

QEJ bricks can be formed either on site or in factory. At a landfill, there are many sources of plastic and hydrophobic materials available at the dump. Styrofoam is one of the hydrophobic materials that can be reused for QEJ brick production. There are two scenarios suggested; the first is that empty, perforated, and light bricks-containments from plastics are produced in factory in a way that can be easily transported, stored and joined together on landfill (Figure 3.1). Once bricks are installed in trenches or in a cell, they are filled with shredded recyclable hydrophobic material (e.g. Styrofoam). In the case of Styrofoam, a size of 1 cm Styrofoam chip is recommended based on the preliminary tests. The second scenario is to use recyclable hydrophobic material in the

factory for reforming it with a porosity of 95% (as of recommendation from preliminary tests) (Figure 3.2). In this case entire bricks are transported and stored and installed in the field.

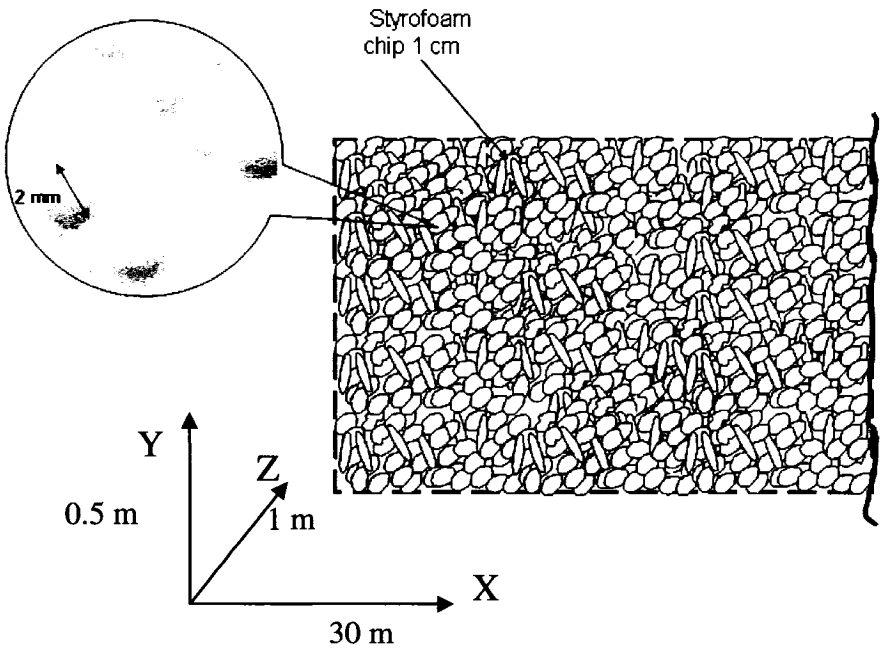

Figure 3.1 Side Cross Section of QEJ Brick (prepared on site with Styrofoam chips filled in prefabricated hydrophobic perforated containment)

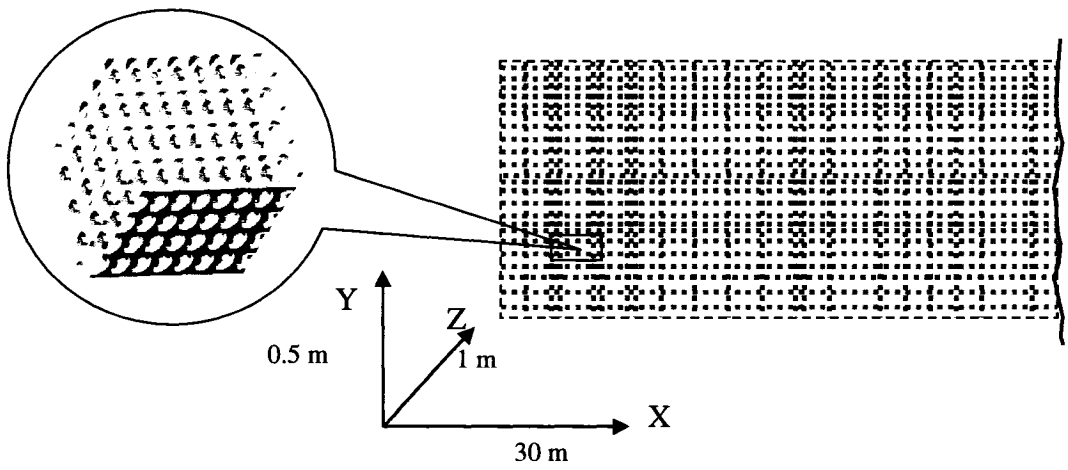

Figure 3.2 Side Cross Section of QEJ Brick (reformed from styrofoam chips at factory)

3.2.2. Landfill Operation with QEJ Bricks

In the QEJ bricks management system, the waste is put and compacted between hydrophobic bricks installed in landfill trenches or cells as shown in Figure 3.3. Starting with one brick then adding another brick over the first one forming wall of bricks rises as the height of waste rises up.

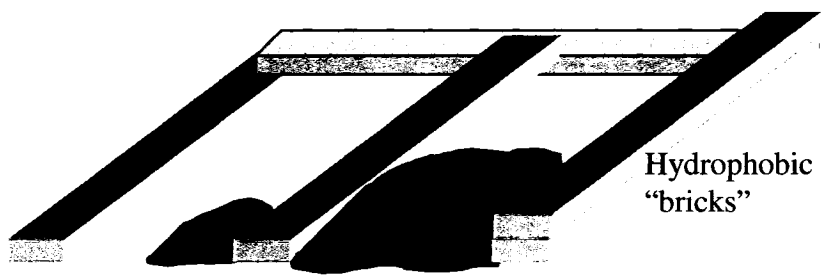

a)

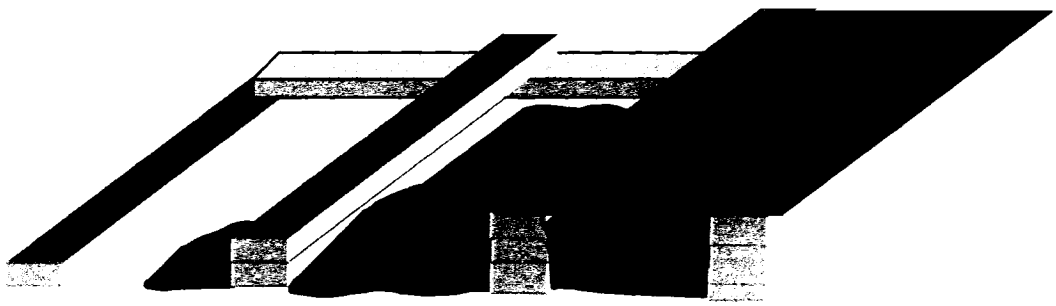

b)

Figure 3.3 Landfill Operation with QEJ Bricks: a) initial operation for two cells; b) finished first cell and chronological operation for subsequent cells

The process of building the bricks is chronological as the confining bricks are built with sequential order. In more details, the profile of waste is declining from the first operated cell towards the subsequent cells; this process maintains structure stability and consecutive order of aerobic processes that will be replaced by anaerobic processes after step of time. Figure 3.4 shows the waste profiles during the QEJ bricks operation. Profiles A and B are previous past operations, C is the current profile showing the chronological order of spreading waste and building bricks, D is the future profile, and E is the future geomembrane profile once cells are finished and closed.

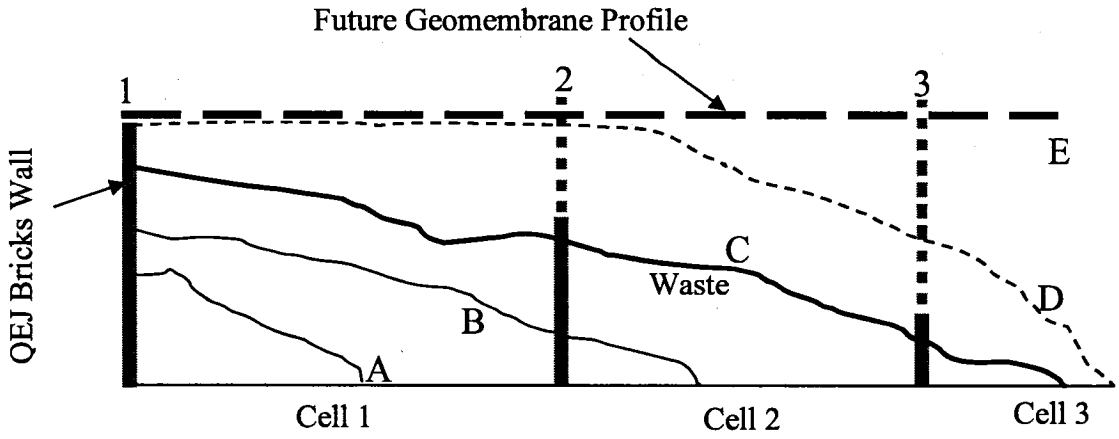

Figure 3.4 Landfill Profiles while QEJ Bricks Operation: A and B are previous past profiles, C is the current profile, D is the future profile, E is the future geomembrane profile

3.3. Waste Stabilization

During operation of landfill cells, there will be successive aerobic and anaerobic processes, which are important for waste stabilization, waste degradation, and biogas generation. Figure 3.5 shows the contours of successive anaerobic processes during operation. The role of hydrophobic bricks is to provide good distribution of air through the medium for aerobic processes that will be replaced gradually by anaerobic processes when cells are being operated.

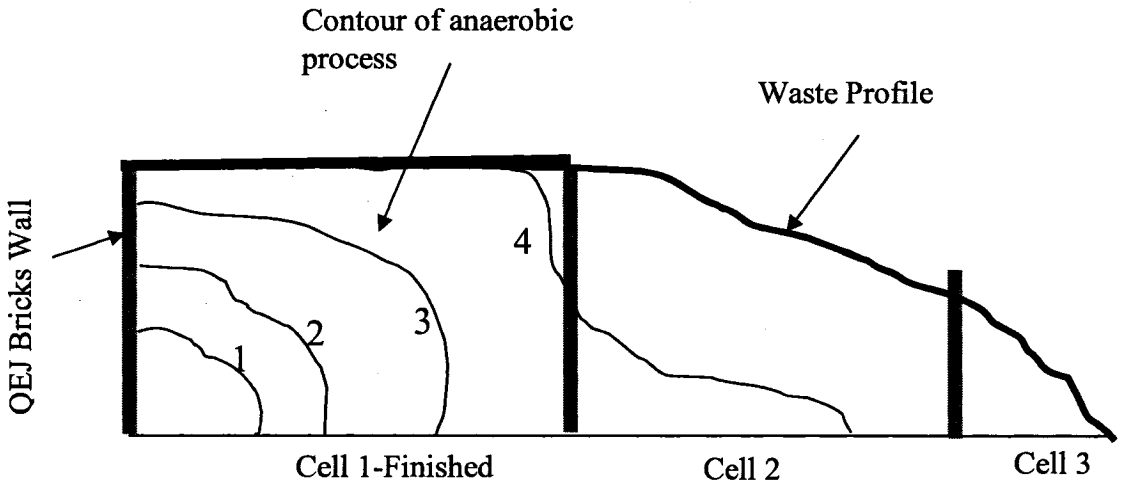

Figure 3.5 Propagation of Anaerobic Processes: anaerobic contours 1, 2, 3 for previous waste profiles (A, B, C in Fig 3.4) respectively, contour 4 for current waste profile (D in Fig 3.4)

During the operation of each QEJ bricks cell, the process is not different than conventional processes including the daily cells, lining, and leachate collection system. The waste will be stabilized by aerobic processes with time. After the cell is finished, it will be sealed with geomembrane. The system could be adapted to various landfill disposal systems including biocell with the leachate recirculation (Figure 3.6).

Each filled cell will be connected to valves and piping system in order to send biogas to a storage area through the intelligent valve system. The cell might also be connected with leachate collection tanks for leachate recirculation through pipes penetrating the geomembrane to the waste for more biogas production in biocell (Figure 3.6).

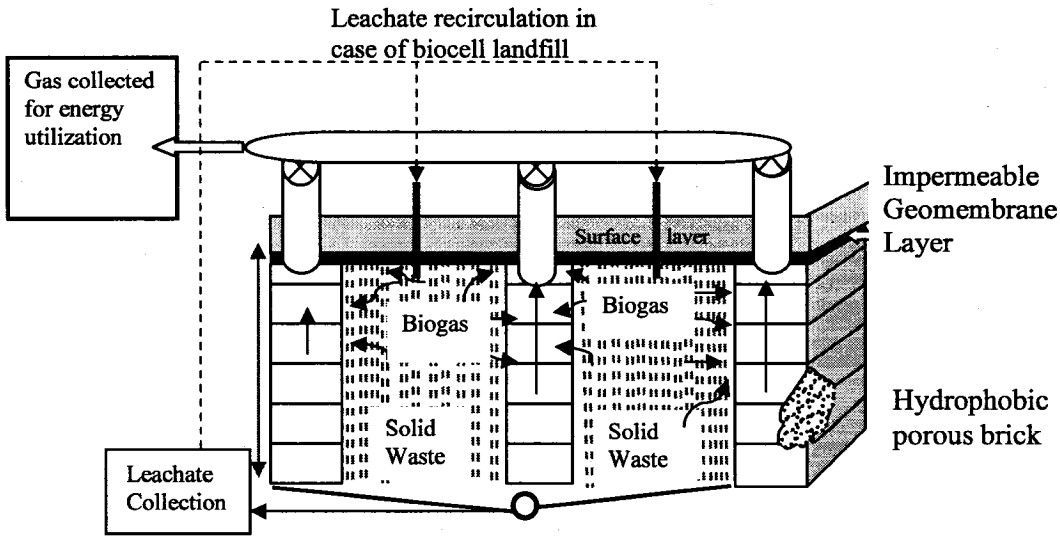

Figure 3.6 QEJ Bricks Management System with Biogas Collection (and leachate recirculation in a case of biocell)

Furthermore, for the closed cells under anaerobic processes, biogas produced begins to move in the least resistant pathway toward the areas of less pressure and concentration. Biogas transfers fast and smoothly through the homogenous and neatly filled waste where there is no pressure build up, no inactive zone obstruction, and no heterogeneous gas transfer. Biogas tends to transport toward the permeable evacuated QEJ bricks and then they are collected at ports. Gas collection processes are controlled by intelligent fuzzy control system (Figure 3.7). The valves at gas collection ports are linked to sensors/meters, data acquisition system, and fuzzy logic control system. The data acquisition system takes information from sensors/meters at landfill about biogas pressures, concentrations, and flow rates. Then it provides data as input to fuzzy control system that automatically uses the input data to provide a signal to control valve opening

depending on information collected from the data acquisition system, and consequently controlling biogas evacuation processes with efficient biogas transfer through the waste and the bricks in landfill toward storage and utilization.

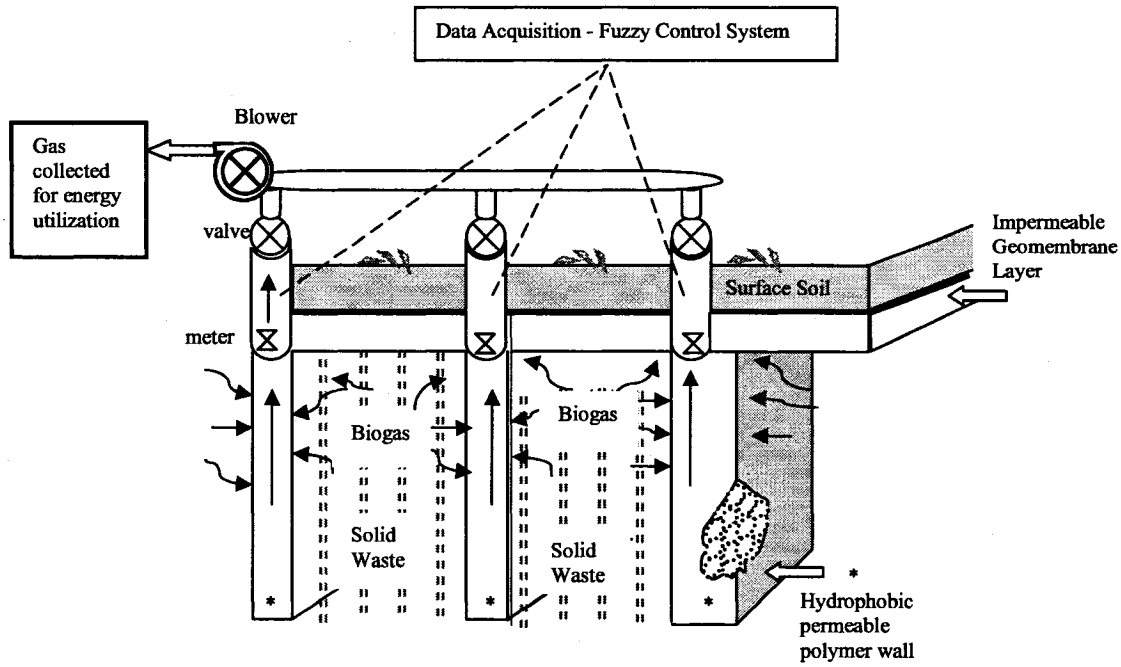

Figure 3.7 Intelligent QEJ Bricks Management System

3.4. Structure Stability and Design of the QEJ Bricks System

The intelligent QEJ bricks management system is stable structure due to firm construction of the QEJ bricks. As shown in Figure 3.8, the system is constructed with bricks such a way that the loads on the structure are balanced.

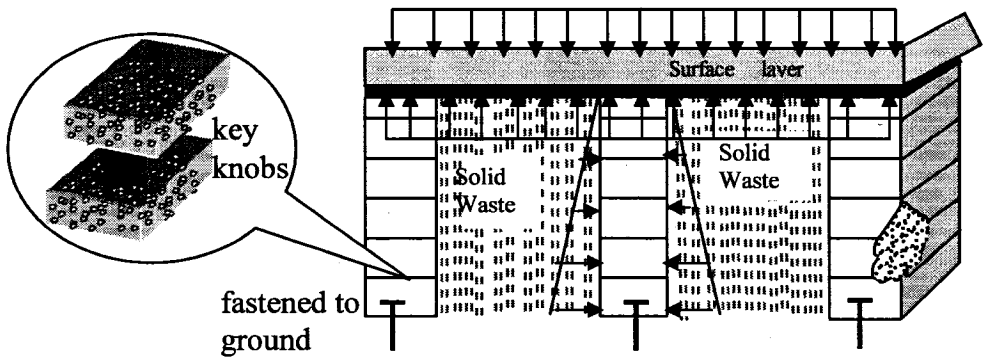

Figure 3.8 Waste Load Distribution on QEJ Bricks Structure

The base bricks are anchored to the ground (Fig 3.8). Each brick is fixed to the upper and lower brick by key knobs (30 cm diameter) entering fitted holes to integrate bricks. The longitudinal and lateral bricks are crossed, and that gives the structure the stability even if a differential settlement takes place. At fabrication level, the bricks should be designed to withstand acting loads on bricks and knobs. In addition, reinforcement to the structure could be added if additional loads are expected.

At level of design, the bricks are expected to carry normal stress (σ_n), shear stress (σ_t), and bending stress (σ_b). The worst case considering the ultimate stresses is that the bricks are subjected to loading for one side only. The analysis for calculating the stresses subjected to the bricks and consequently the required material strength can be specified. Having a wall of bricks as shown in the demonstration below; the load distribution and stress analysis per unit length of the brick (Z = 1m) can be characterized as the following sample example:

For block A

N= **Q*X** (Q: weight of upper loads/m)
T= **0.5*L*(F/3)** (F: lateral refuse stress)

σ_n = normal stress
σ_n = **Q*X/(X*Z)**
σ_t = shear stress
σ_t = **[0.5* L*(F/3)]/ [π/4 D^2]**
σ_b = bending stress
= MC/ I

M = 0.5*L*(F/3)*(L/3)
= 0.055 L^2 F

σ_b = ([0.5*L*(F/3)*(L/3)]*[D/2])/I
I = π D^4/64

σ_b = **(1.78 F L^2)/ (π D^3)**

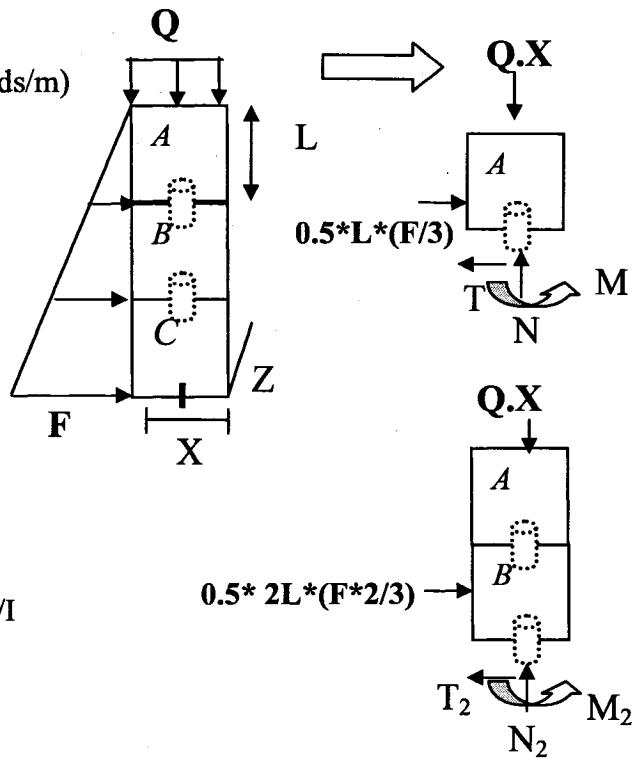

For block B

N_2 = N = **Q.X**
T_2 = 0.5* 2L*(F 2/3)
= **2/3 L*F**

σ_n = **Q*X/(X*Z)**
σ_t = **2/3 L*F/[π/4 D^2]**

M_2 = 0.5*2L*(F*2/3)L 2/3
M_2 = 2/3 2/3 L^2 F

σ_b = (2/3 2/3 L^2 F)(D/2)]/ [π D^4/64]
σ_b = **14.22 FL^2 / (π D^3)**

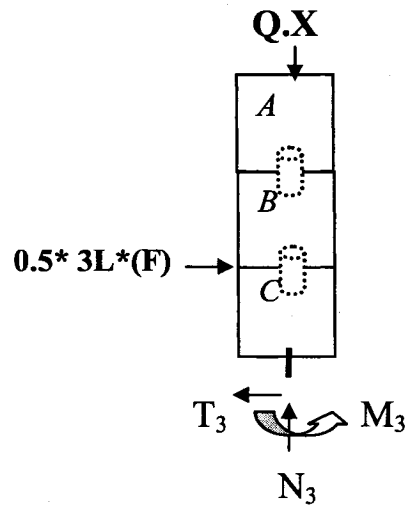

For block C

N3 = N = **Q*X**
T3 = 0.5* 3L(F)
= 1.5 LF
= **1.5 LF**

σ_n = **Q*X/(X*Z)**

$\sigma_t = 1.5\ L*F/[\pi/4\ D^2]$

$M_3 = 1.5\ L*F\ (L)$
$= 1.5\ L^2\ F$

$\sigma_b = [(1.5\ L^2\ F)\ (D/2)]/\ [\pi\ D^4/64]$
$\sigma_b = 48\ L^2\ F\ /\ (\pi\ D^3)$

Here is an illustration of numerical analysis for the design shown in Chapter 2 (Fig. 2.1)

for unit length of the brick (Z = 1m) where the following were specified:

Topsoil depth d = 0.5 m
Waste depth h = 5 m
Brick width X = 1 m
Brick length Z = 1 m
Rode diameter D = 0.3 m
$\rho_{soil} = 1300\ kg/m^3$
$\rho_{waste} = 600\ kg/m^3$
$g = 9.8\ m/s^2$

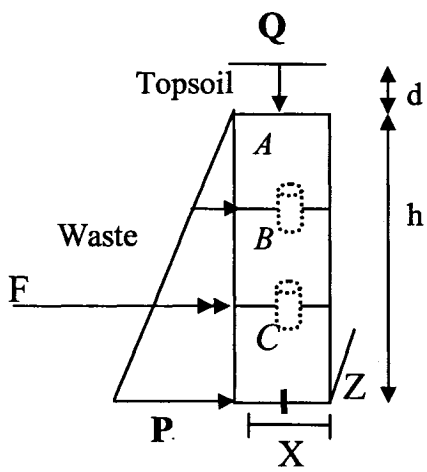

$Q = \gamma\ V = \rho\ g\ (X.Z.d)$
$= 1300(9.8)(1)(1)(0.5)$
$= 6370\ N$
$\sigma_n = Q/(X*Z)$
$= 6370/(1)(1) = 6.37\ kPa$

$P = \gamma\ h = \rho gh = 600(9.8)(5)$
$P = 29400\ N/m^2$
$F = 0.5\ \rho g\ h^2(Z)$
$F = 0.5(600)(9.8)(5)^2(1)$
$= 73.5\ kN$

$\sigma_t = 73.5\ /[\pi/4\ D^2]$
$= 73.5\ /[\pi/4\ (0.3)^2]$
$= 1.04\ MPa$

$M = F\ (h/3) = 73.5\ (5/3) = 122.5\ kN.m$

$\sigma_b = M\ (D/2)/\ [\pi\ D^4/64]$
$\sigma_b = 122.5*10^3\ (0.3/2)/(\ \pi\ (0.3)^4/64)$
$= 46.2\ MPa$

The analyses for the stresses within the bricks structure give information, compared with material strength, for structure design and construction. The amount of the waste and the size of the landfill will play the major role determining the scenario of design for cell dimensions, number of cells, and number of lifts.

3.5. Advantages of Intelligent QEJ Bricks Management System

Intelligent QEJ Bricks confines the waste with a new trend that provides a proper waste disposal, control of the generated biogas, permeable medium for conveying gas to collection storage, and a control in biogas evacuation processes.

Intelligent QEJ Bricks system is also a state of the art method of reusing recyclable material at the dump. As the bricks are hydrophobic, they contain no water, more air voids, for more permeable medium for biogas collection. Successive aerobic and anaerobic processes in the system increases waste degradation and stabilization, especially when there is leachate recirculation in a case of biocell.

Prospective advantages of Intelligent QEJ Bricks management system include:

- Integrated operation system that combines waste disposal, biogas evacuation, and biogas control.
- Fast decomposition and biological stabilization of the waste
- More biogas generation
- Smooth and fast transfer of biogas from waste to the bricks
- Lower waste toxicity and mobility due to both aerobic and anaerobic conditions

- Good candidate to apply for bioreactor landfill
- Application of "reuse and recycle" solid waste management

U.S. EPA developed the solid waste management pyramid, which ranked the most preferable ways to address solid waste management. Source reduction, which includes reuse, was the listed as the best approach, followed by recycling. These two approaches are applied in Intelligent QEJ Bricks management system in addition to enhanced gas uptake and better control of greenhouse gas emission.

The Styrofoam reused in bricks has to be tested to find it's functionally to serve as porous medium for conveying and collecting biogas and this will be the focus of the following chapter.

CHAPTER 4

Investigation of Biogas Transport in Hydrophobic Porous Polymer Medium

4.1 Introduction

In voids within the porous media, gas moves by diffusion due to concentration gradient and/or by convection due to pressure gradient. The following equation of mass conservation for gas diffusion-convection in a porous media can be written:

$$\frac{\partial C_i}{\partial t} = \frac{\partial (U_k C_i)}{\partial x_k} + \frac{\partial}{\partial x_k}(D_{ik} \frac{\partial C_i}{\partial x_j}) \tag{4.1}$$

where: C_i is concentration of the i^{th} component of the gas mixture (kg/m^3), U_k is convection velocity ($U_k = \frac{K}{\rho \times g} \nabla P$) in the k^{th} direction (m/s), K is conductivity coefficient (m/s), ∇P is the pressure gradient (N/m^2.m), ρ stands for the density of the fluid (kg/m^3), g denotes the acceleration due to gravity in (m/s^2), D_{ik} is diffusion coefficient of gas i in the k^{th} direction (m^2/day), and x_k is the distance in the k^{th} direction (m).

As it is described in Chapter 1 (section 1.2.4), the porosity and the water content are vital factors affecting the biogas transport in porous media, and it is concluded that increasing the porosity and decreasing the water content provides more permeable medium for biogas transport.

In this chapter, the hydrophobic polymer medium used in the research is brought to tests that entail the properties of both the polymer and the biogases that move through it. The porous hydrophobic polymer medium used in this research repels water (negligible water content), contains more than 95 % air (high porosity), and provides highly permeable medium for gas transport.

The movement of biogas in the porous hydrophobic polymer is to be characterized and investigated under variable parameters that affect medium and gas properties and in turn affect the gas transport.

4.2 Methodology

As the methodology described in section 2.2.1.2, gas diffusion test gives information about gas diffusion coefficient in polymer medium and the convection test gives information about gas conductivity coefficient and medium permeability. Methane (from gas line) and carbon dioxide (from cylinder) transported through the polymer medium by diffusion and convection within variable parameter: temperature, porosity, water content, concentration gradient, and pressure gradient. Collected information about parameters was recorded to obtain their effect on gas convection and gas diffusion through polymer medium.

The permeability test was conducted on four samples: landfill topsoil (from CESM landfill), fine sand, coarse crushed basalt, and Styrofoam chips (material properties are described in Table 2.1).

4.3 Performance Tests Results

The new proposed medium in this research has to be checked to find its performance to act on landfill for biogas collection. As it was described in section (2.2.1.2) permeability test using air passing through different media was applied to check the media permeability, which is a property of the medium regardless what gas passes through. When analyzing results obtained from the permeability test, polymer medium showed high permeability since it has minimal head loss as shown in Figure 4.1. The polymer medium is hydrophobic and porous; thus it has high porosity and negligible water content. The average coefficient of conductivity of air in polymer is 3.29 cm/s as it is calculated from average slope of volumetric flow rate vs. pressure head gradient, as it is shown in Figure 4.2, and thus polymer coefficient of permeability is 5.4×10^{-8} m^2, which is highly permeable. These coefficients show that the polymer material is highly permeable medium for biogas collection. These results show that the proposed hydrophobic medium is an excellent choice especially when using recyclable hydrophobic polymer as Styrofoam available on landfill.

Subsequently, series of tests on coefficients of conductivity and diffusion were carried out to assess the medium performance for conveying biogas by convection and diffusion under variable parameters (temperature, porosity, and water content). Figure 4.3 shows the effect of temperature variation on the coefficients of conductivity and diffusion for methane and carbon dioxide in the porous hydrophobic polymer medium.

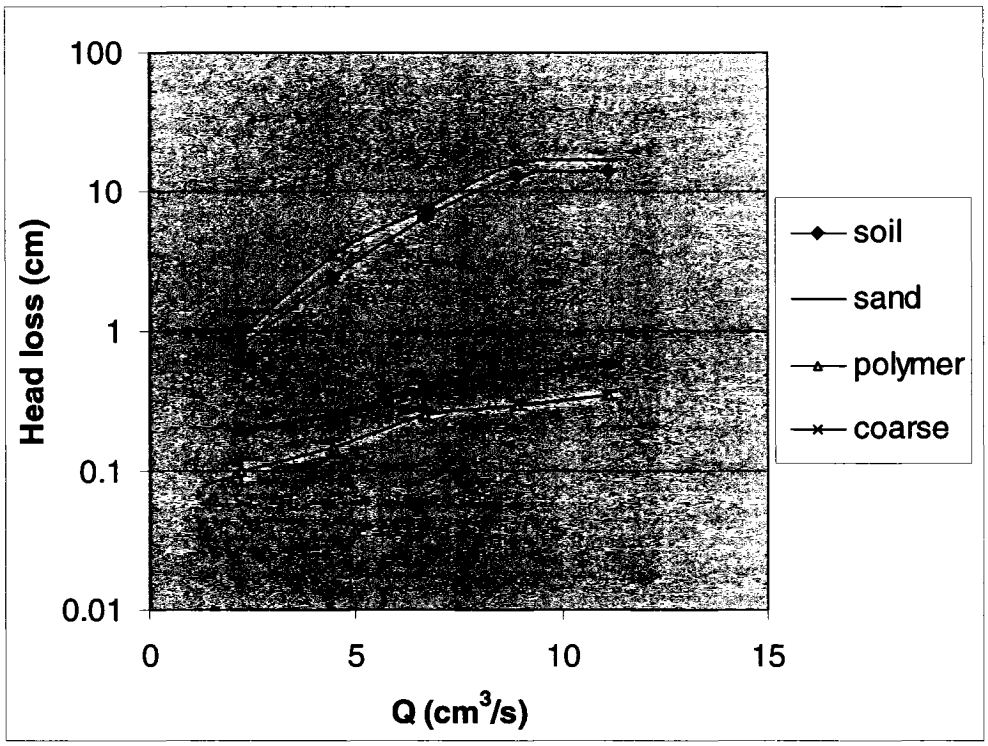

Figure 4.1 Head Loss vs. Air Flow Rate within Different Media (at 25 °C and 1 atm)

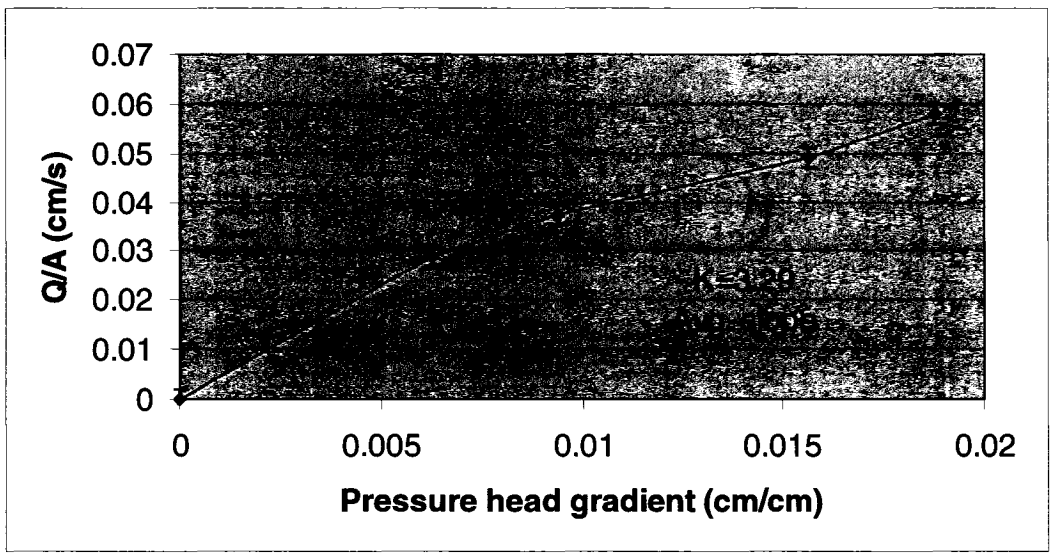

Figure 4.2 Volumetric Flow Rate vs. Pressure Head Gradient and the Average of Coefficient of Air Conductivity (Avg. Slope) within Hydrophobic Polymer (Styrofoam polymer medium at room temperature and atmospheric pressure)

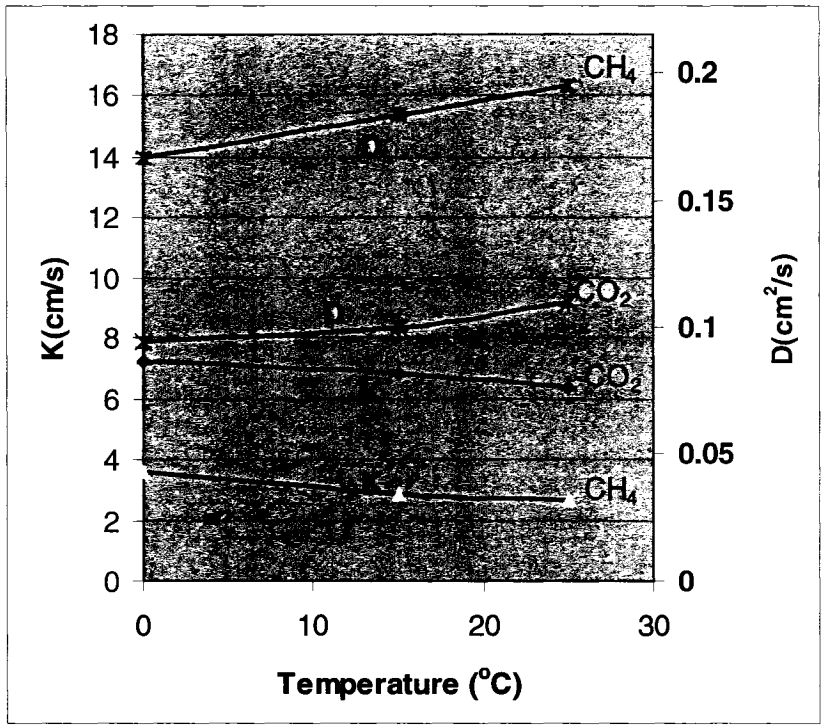

Figure 4.3 Effect of Temperature Variation on Coefficient of Conductivity (K) and Coefficient of Diffusion (D) (at atmospheric pressure) for Biogas in Hydrophobic Medium.

Figure 4.3 shows that diffusion coefficient of methane is higher than that of carbon dioxide, for example at 15 °C the diffusion coefficient of methane is 1.8 times higher than that of carbon dioxide. On the other hand the coefficient of conductivity of methane is less than that of carbon dioxide because methane is more viscous than carbon dioxide, for example at 15 °C the conductivity coefficient of methane is less 2.3 times than that of carbon dioxide. In addition, as the temperature increases the coefficient of diffusion increases for both methane (from 0.17 to 0.19 cm^2/s) and carbon dioxide (from 0.09 to 0.11 cm^2/s) when the temperature increases from 0 °C to 25 °C. However, as the temperature increases the coefficient of conductivity decreases for both methane (from 4

to 2.5 cm/s) and carbon dioxide (from 8 to 6 cm/s) when the temperature increases from 0 ^{o}C to 25 ^{o}C; because gas viscosity increases when temperature increases.

As it was expected, the results showed that by increasing porosity the coefficient of conductivity is increasing for CH_4 and CO_2 but with higher gradient of CO_2 (Fig. 4.4).

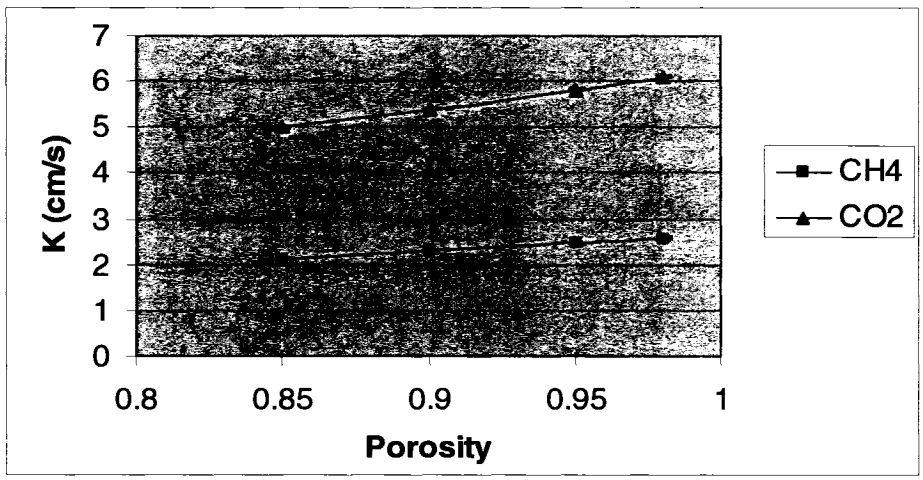

Figure 4.4 Coefficient of Conductivity for Gases in Polymer Medium for Different Porosity (at room temperature and atmospheric pressure).

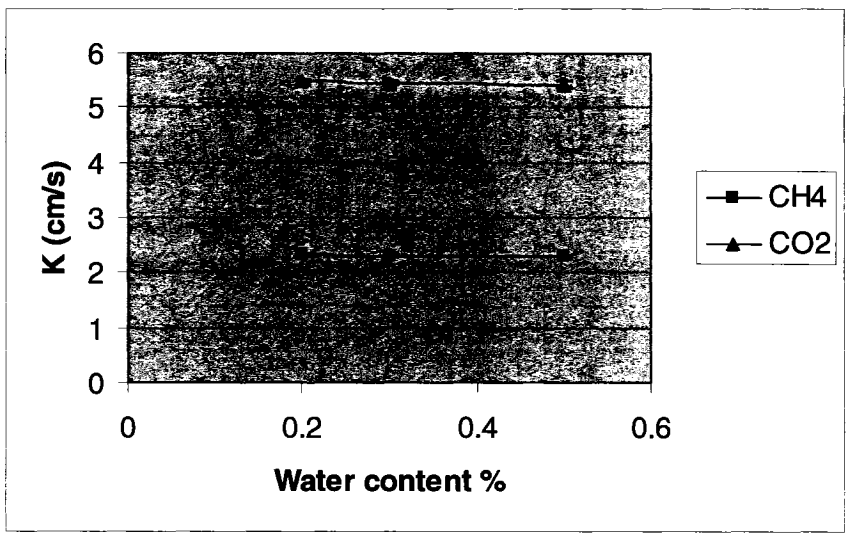

Figure 4.5 Coefficient of Conductivity for Gases in Polymer Material for Different Water Content (at room temperature and atmospheric pressure).

On the other hand, as the water content increases in the polymer medium, the coefficient of conductivity decreases for both methane and carbon dioxide (Figure 4.5)

As the porosity of the polymer medium increases between 0.85 and 0.95, the coefficient of diffusion increases for methane between 0.17 and 0.22 (cm^2/s) and for carbon dioxide between 0.1 and 0.12 (cm^2/s) (Figure 4.6). On the other hand, as the water content increases in the polymer medium from 0.1 to 0.5%, the coefficient of diffusion decreases for both methane and carbon dioxide with 0.01 (cm^2/s) (Figure 4.7).

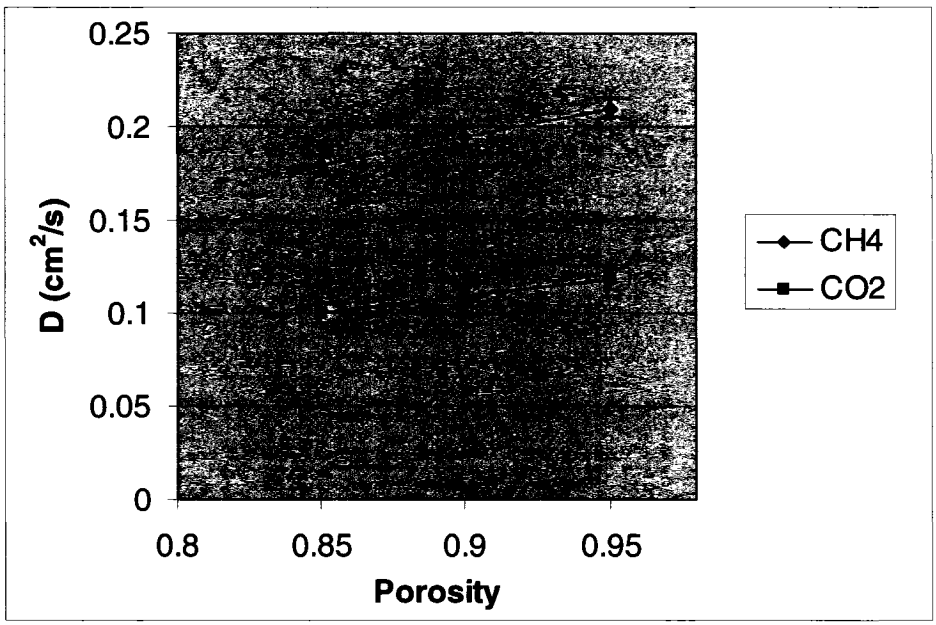

Figure 4.6 Coefficient of Diffusion for Gases in Polymer Material for Different Porosity (at room temperature and atmospheric pressure).

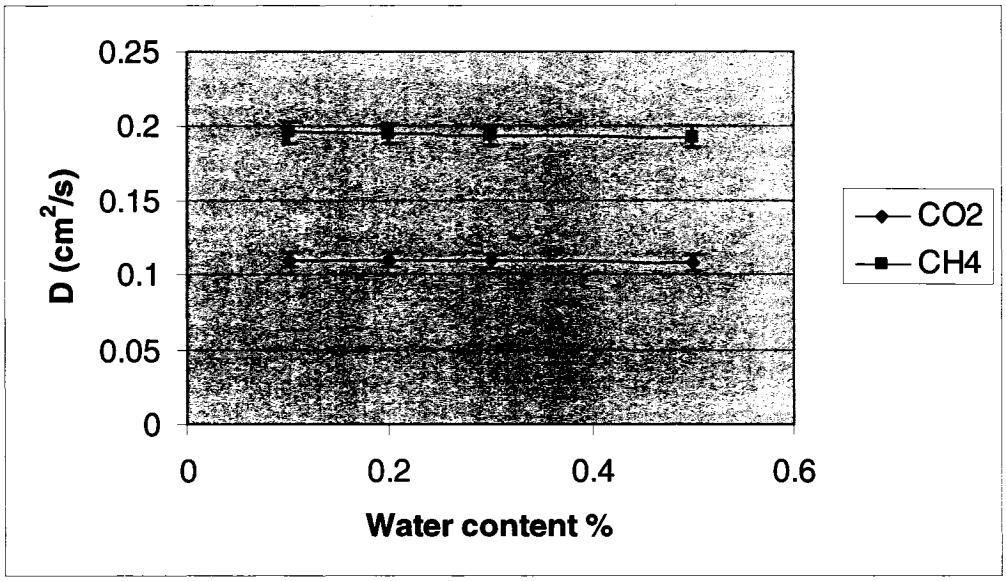

Figure 4.7 Coefficient of Diffusion for Gases in Polymer Material for Different Water Content (at room temperature and atmospheric pressure).

It can be seen from the Figures 4.3 to 4.7 the effect of temperature, porosity, and water content on the coefficient of conductivity and diffusion, and subsequently their effect on the convection and diffusion transport, since diffusive flux and convective flow rate depend on diffusion and conductivity coefficients respectively. For the hydrophobic polymer used in this research, porosity is kept at the level of 95 % air voids, and the water content is negligible because of polymer hydrophobicity. This water content is negligible compared to other soil water content. Consequently, there are three vital parameters that affect the biogas transport: the temperature (0, 15, 25 ^{o}C), biogas concentration gradient (0, 0.25, 0.5, 0.75, 1 kg/m^3.m), and pressure gradient (0, 0.25, 0.5, 0.75, 1 N/m^2.m).

Series of evaluations based on experimental data shown in Figure 4.3 and above-mentioned parameter ranges were performed to assess the biogas transport in polymer medium based on equation (4.1). The diffusion of biogas calculated from the experimental data can be seen in Figure 4.8 that shows the flux of biogas via concentration gradient at different temperatures.

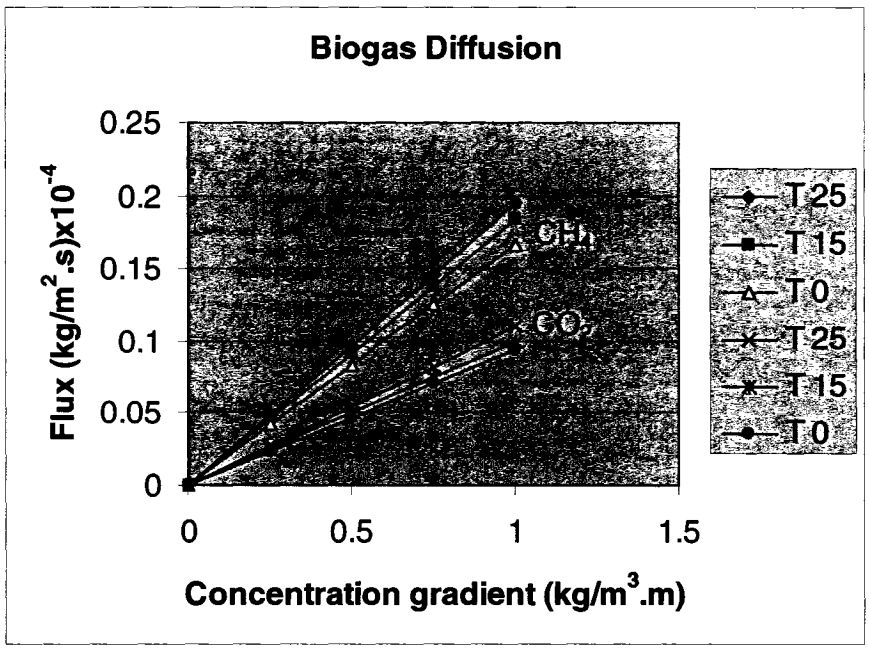

Figure 4.8 Flux of Biogas vs. Concentration Gradient and Different Temperatures for the Biogas Diffusion in Hydrophobic Polymer Medium (at atmospheric pressure)

Once there is a pressure gradient, biogas moves under convection, and hence gas flow rate is a function of conductivity coefficient. Figure 4.9 shows the calculated flow rates of biogas versus pressure gradient and different temperatures in the hydrophobic permeable polymer medium. There is a higher biogas flow rate at lower temperatures when it is moving due to convection. On the contrary, there is a higher biogas flux at higher

temperatures when it is moving due to diffusion. The average ratio of methane transport rate to carbon dioxide transport rate is 1.8 for diffusion and 1.3 for convection.

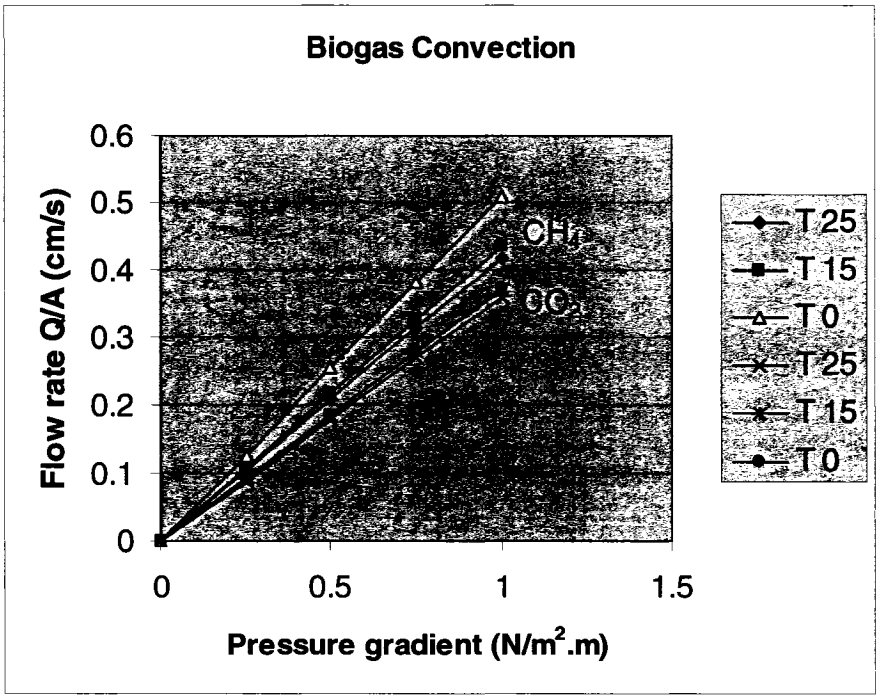

Figure 4.9 Flow of Biogas vs. Pressure Gradient and Different Temperatures for The Biogas Convection in Hydrophobic Polymer Medium (at atmospheric pressure)

4.4 Conclusion

Results obtained from the permeability test on polymer medium showed high permeability since it has minimal head loss due to high porosity (95 % air voids) and negligible water content (hydrophobic polymer medium).

The coefficient of diffusion of methane is higher than that of carbon dioxide. On the other hand the coefficient of conductivity of methane is lower than that of carbon dioxide. As

the temperature increases, the coefficient of diffusion increases for both methane and carbon dioxide. On the other hand, as the temperature increases the coefficient of conductivity decreases for both methane and carbon dioxide. Temperature affects the coefficients of conductivity and diffusion. The temperature and the concentration gradient affect the biogas flux by diffusion. The temperature and the pressure gradient affect the biogas flow by convection; biogas flow rate is higher at lower temperatures. On the contrary, biogas flux is higher at higher temperatures when it is moving due to diffusion. Methane transport rate is higher than carbon dioxide in both transport processes (diffusion and convection). The analysis showed that biogas convection and diffusion depend on temperature, pressure and concentration gradients. These analyses are based on series of experimental data evaluated for standard points of ambiguous parameters. In reality much more expanded range of parameters is expected; therefore a new intelligent approach is necessary to assess expected relationships between variable parameters and biogas transport, and hence, a fuzzy logic approach has been proposed.

CHAPTER 5

Fuzzy Modeling of Biogas Transport in Hydrophobic Polymer Medium

5.1. Introduction

Fuzzy logic is a rule-based approach that approximates a function through linguistic input-output associations. Fuzzy rule-based systems are applied to solve many types of problems, especially where system is ambiguous and difficult to model (Bonde 2000).

A fuzzy expert system is a system that uses fuzzy membership functions and rules, instead of Boolean logic, to reason about data. A fuzzy system consists of a set of premises such as I_1 and I_2 that are formulated as A_i and B_i respectively in the form of fuzzy norms with membership functions μ_i, and a consequence O formulated as C_i membership functions. Fuzzy sets and fuzzy operators are the subjects and verbs of fuzzy logic. The if-then rule statements are used to formulate the conditional statements that comprise fuzzy logic. A single fuzzy if-then rule assumes the form:

If I_1 is A_1 and I_2 is B_1 ... then O is C_1

A typical fuzzy system consists of a rule base, membership functions, and an inference procedure (Bonde 2000). The general inference process proceeds in fuzzification, inference, and defuzzification process (Kalaykov 2000).

The fuzzy logic system entails inference of inputs to outputs by statement rules. The fuzzy system consists of membership functions for input and output premises, fuzzy logic

operators, and if-then rules. The fuzzy inference system can be explained in the following example:

For two input premises I_1 and I_2 with one output O, if I_1 is 1.4 and I_2 is 0.8 then the output O_1 can be demonstrated as the following:

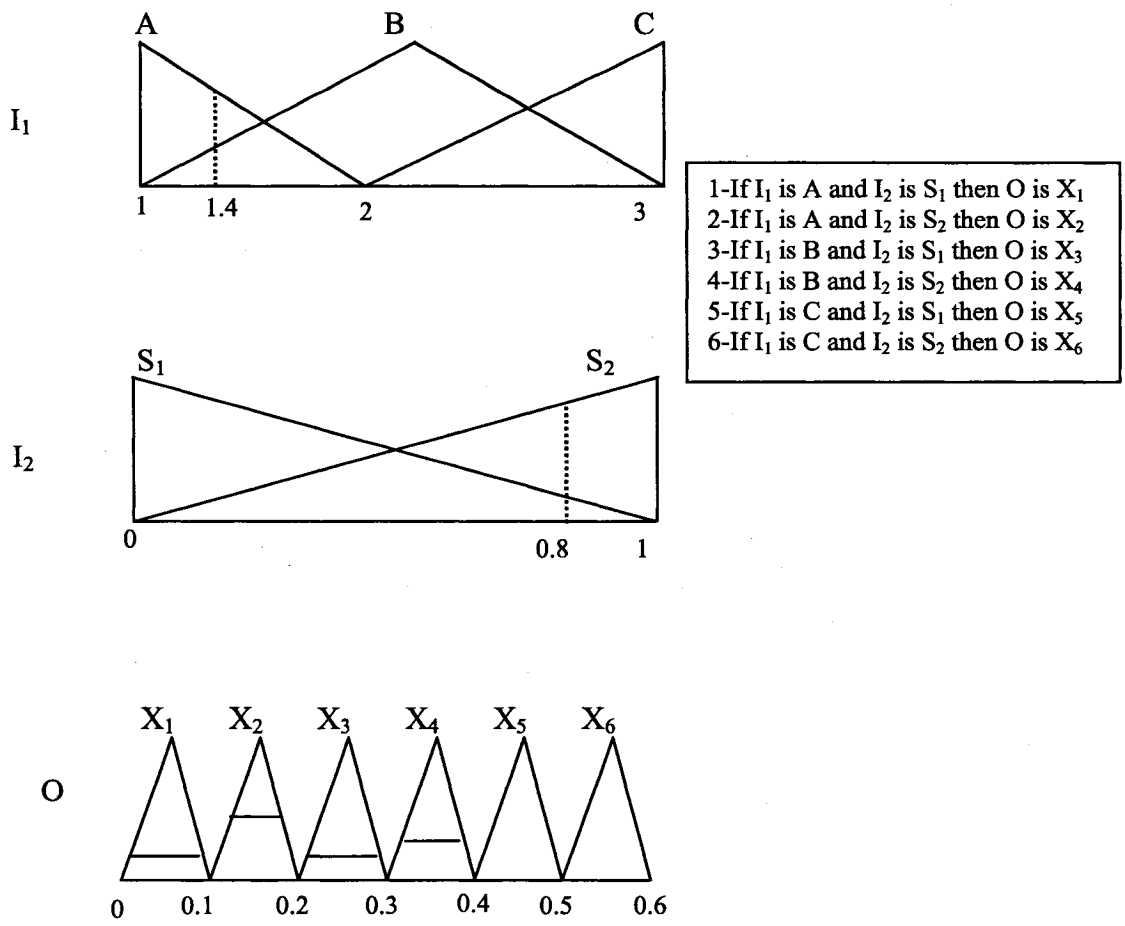

By applying the first rule, the following could be achieved:

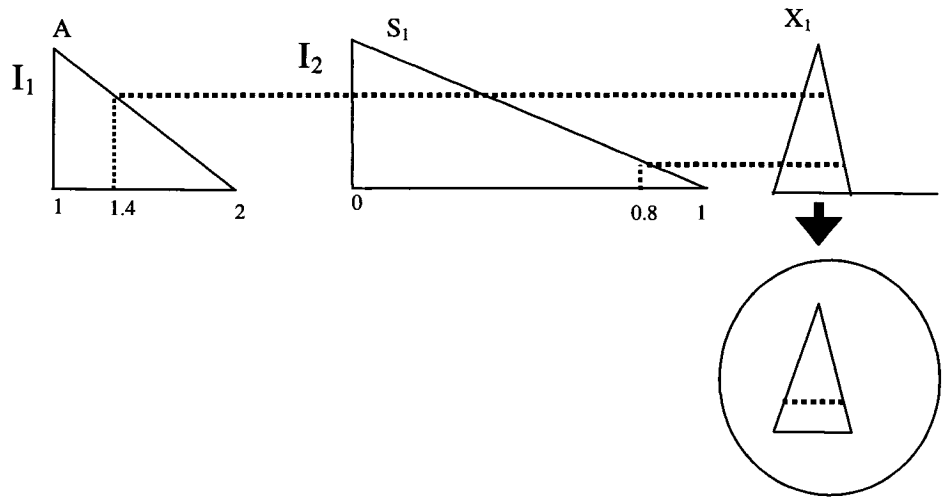

The entire inference process for all rules including aggregation and defuzzification can be seen in Figure 5.1, where the output O_1 obtained equals to 0.208

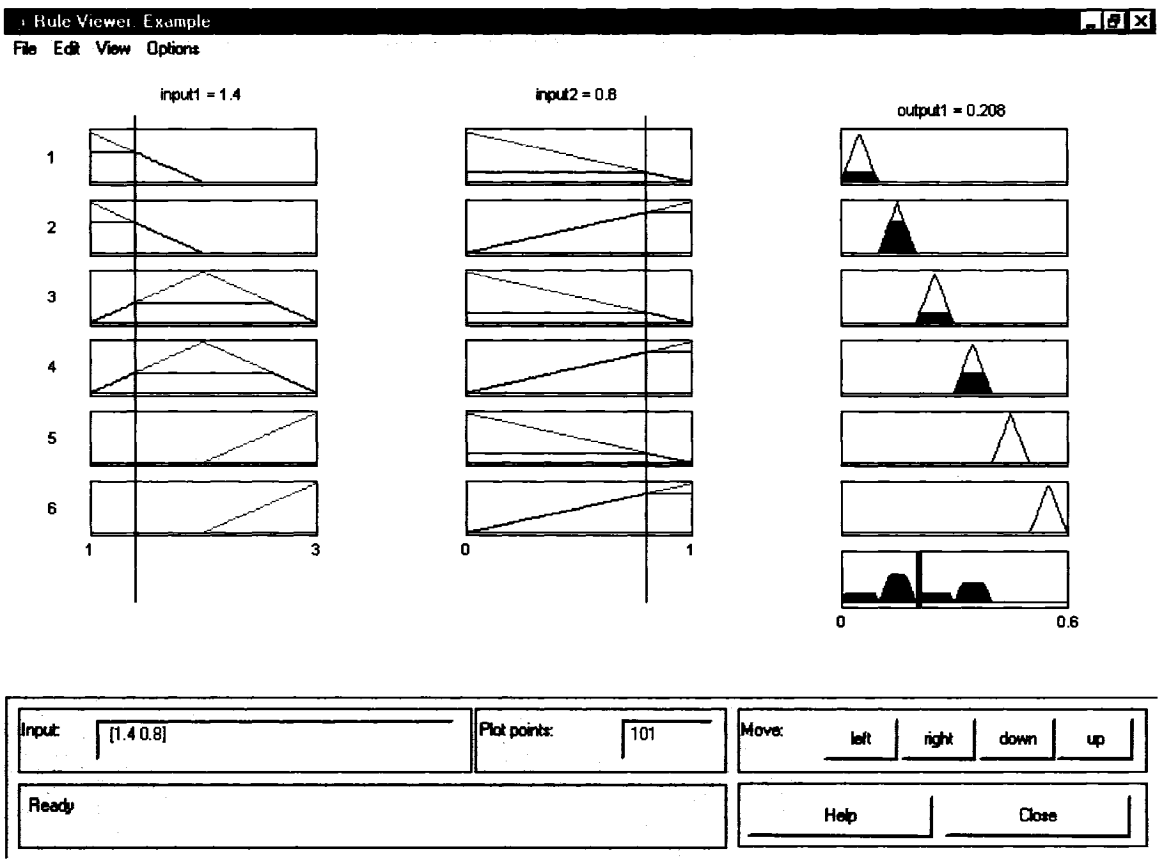

Figure 5.1 Example of Fuzzy Inference Process

5.2. Methodology

The laboratory tests provide data about coefficient of diffusion (D), coefficient of conductivity (K), biogas diffusive flux and convective flow rate, and the influence of environmental parameters: temperature (T), water content (WC), porosity (n), concentration gradient (∇C), and pressure gradient (∇P) for biogas transport within the hydrophobic polymer medium. The data (The experimental data on Tables: 3, 8, 9, 10, 11, 12, 13 in Appendix A1) were formulated as knowledge bases (input and output premises) (Qasaimeh et al. 2006a). The water content is negligible for hydrophobic medium and the porosity is kept fixed at 95%. The first step is to take the inputs and determine the degree to which they belong to each of the appropriate fuzzy sets via membership functions. In the Fuzzy Logic Toolbox (Matlab 6.5), the input is always a crisp numerical value limited to the universe of discourse of the input variable and the output is a fuzzy degree of membership in the qualifying linguistic set (interval between 0 and 1). Mamdani fuzzy inference system is applied in this research. Mamdani-type inference, expects the output membership functions to be fuzzy sets for each output variable and needs defuzzification.

5.3. Modeling

The data obtained from experimental tests for methane and carbon dioxide convective flow rates and diffusive flux in the hydrophobic polymer is being modeled in this section (Qasaimeh et al. 2006a). Fuzzy system incorporates gas transport rates according to the following sets:

$$G(u_i) = \begin{cases} u_i = o & \text{no flow} \quad (5.1) \\ u_i = f(K_i, \nabla P_i, T) & \text{convection} \quad (5.2) \\ u_i = f(D_i, \nabla C_i, T) & \text{diffusion} \quad (5.3) \end{cases}$$

where G (ui) is biogas transport rate for i gas (methane, carbon dioxide), K_i is the conductivity coefficient of biogas i, ∇P_i is the pressure gradient, T is the temperature, D_i is the diffusion coefficient of gas i, ∇C_i is the concentration gradient, u_i is the function f (K_i, ∇P_i, T) for convective flow, and function f (D_i, ∇C_i, T) for diffusive flux.

Fuzzy system modeled the diffusion transport and convection transport for carbon dioxide and methane in two sub-models according to the above-defined sets. Figure 5.2 shows a fuzzy sub-model that represents the methane and carbon dioxide diffusive flux within variable concentration gradient and temperature.

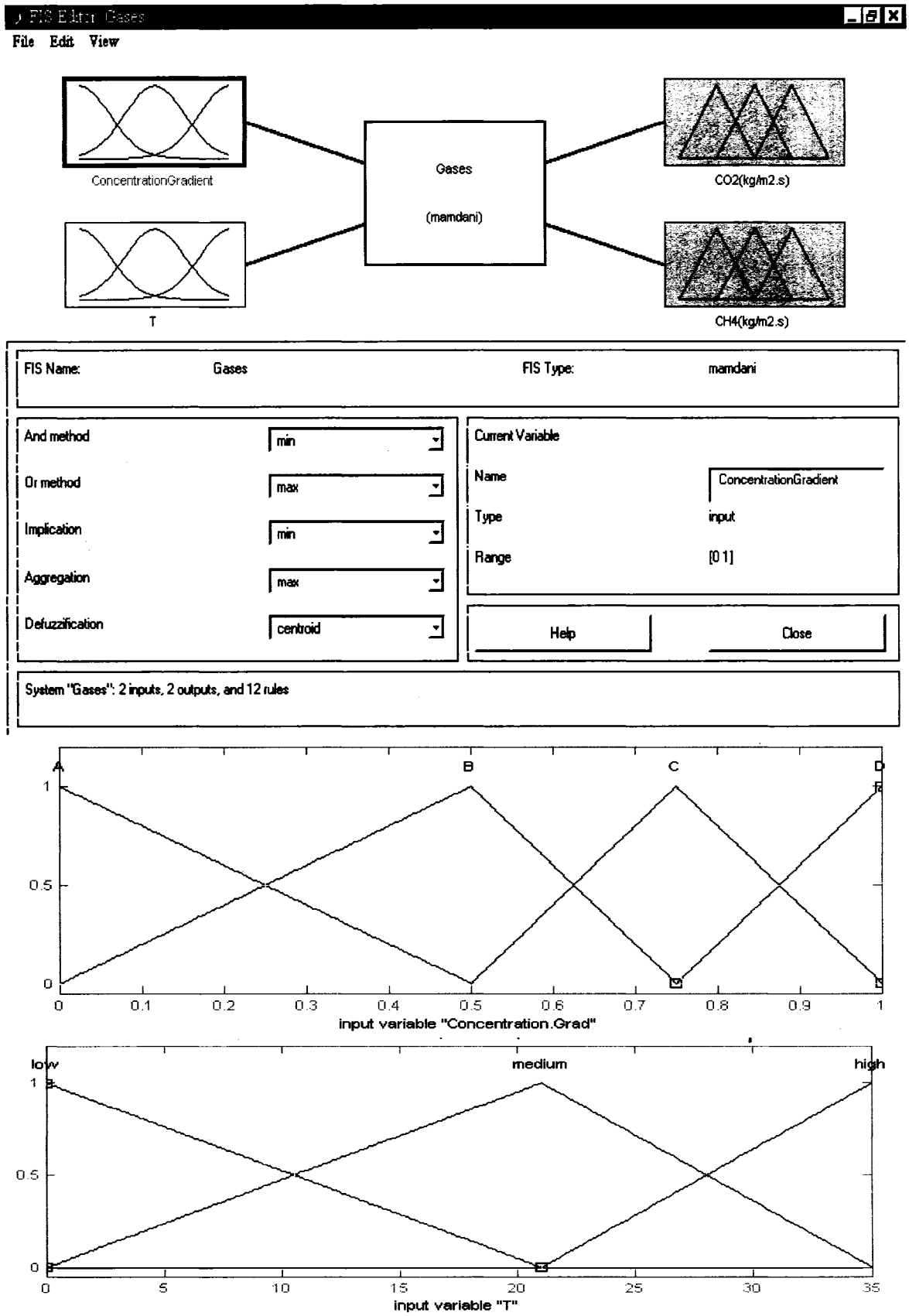
FIS Editor: Gases
File Edit View
ConcentrationGradient
T
Gases
(mamdani)
CO2(kg/m2.s)
CH4(kg/m2.s)
FIS Name: Gases
FIS Type: mamdani
And method min
Or method max
Implication min
Aggregation max
Defuzzification centroid
Current Variable
Name ConcentrationGradient
Type input
Range [0 1]
Help
Close
System "Gases": 2 inputs, 2 outputs, and 12 rules
A
B
C
D
input variable "Concentration.Grad"
low
medium
high
input variable "T"

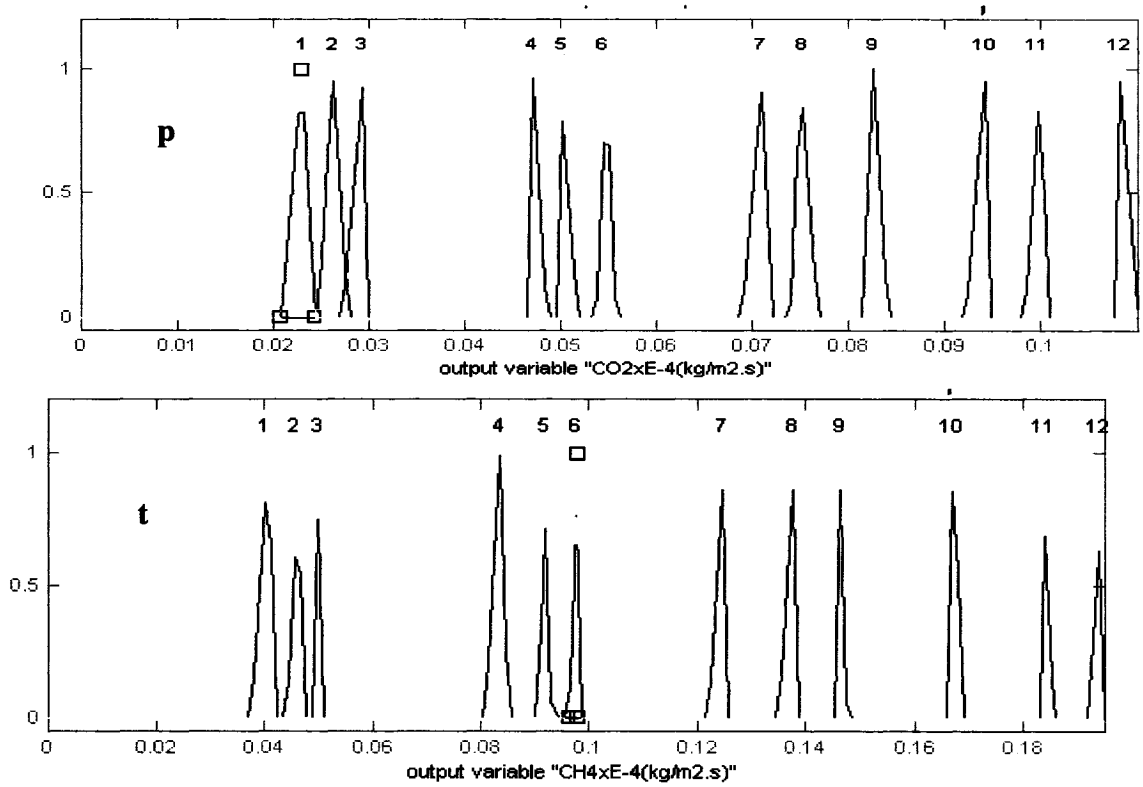

Figure 5.2 Fuzzy Model for Carbon Dioxide and Methane Diffusion within Variable Concentration Gradient and Temperature in Hydrophobic Polymer Material.

The knowledge obtained while performing laboratory tests and getting the experimental data drove to the need of expert knowledge while modeling, thus premises and rules were manually built. The following rules were applied:

1- If ∇C is (A) and T is (low) then CO_2 is (p_1) and CH_4 is (t_1)
2- If ∇C is (A) and T is (medium) then CO_2 is (p_2) and CH_4 is (t_2)
3- If ∇C is (A) and T is (high) then CO_2 is (p_3) and CH_4 is (t_3)
4- If ∇C is (B) and T is (low) then CO_2 is (p_4) and CH_4 is (t_4)
5- If ∇C is (B) and T is (medium) then CO_2 is (p_5) and CH_4 is (t_5)
6- If ∇C is (B) and T is (high) then CO_2 is (p_6) and CH_4 is (t_6)
7- If ∇C is (C) and T is (low) then CO_2 is (p_7) and CH_4 is (t_7)
8- If ∇C is (C) and T is (medium) then CO_2 is (p_8) and CH_4 is (t_8)
9- If ∇C is (C) and T is (high) then CO_2 is (p_9) and CH_4 is (t_9)
10- If ∇C is (D) and T is (low) then CO_2 is (p_{10}) and CH_4 is (t_{10})
11- If ∇C is (D) and T is (medium) then CO_2 is (p_{11}) and CH_4 is (t_{11})
12- If ∇C is (D) and T is (high) then CO_2 is (p_{12}) and CH_4 is (t_{12})

(Appendix (A2.1) provides all details about premises (inputs - outputs), operators, and rules).

With manually built fuzzy model, calibration takes place repeatedly until the correlation between the experimental data and fuzzy modeled data were very high and the squared difference was minimal. Verification of model was done on set of data other than data used in calibration.

Figure 5.3 shows the fuzzy inference system for two inputs (concentration gradient and temperature- two columns to the left) to find two output variables (CO_2 and CH_4 flux- two columns to the right) using implied operators, 12 rules, aggregation, and defuzzification to have final crisp values for CO_2 and CH_4 flux at the bottom to the right of the screen shot.

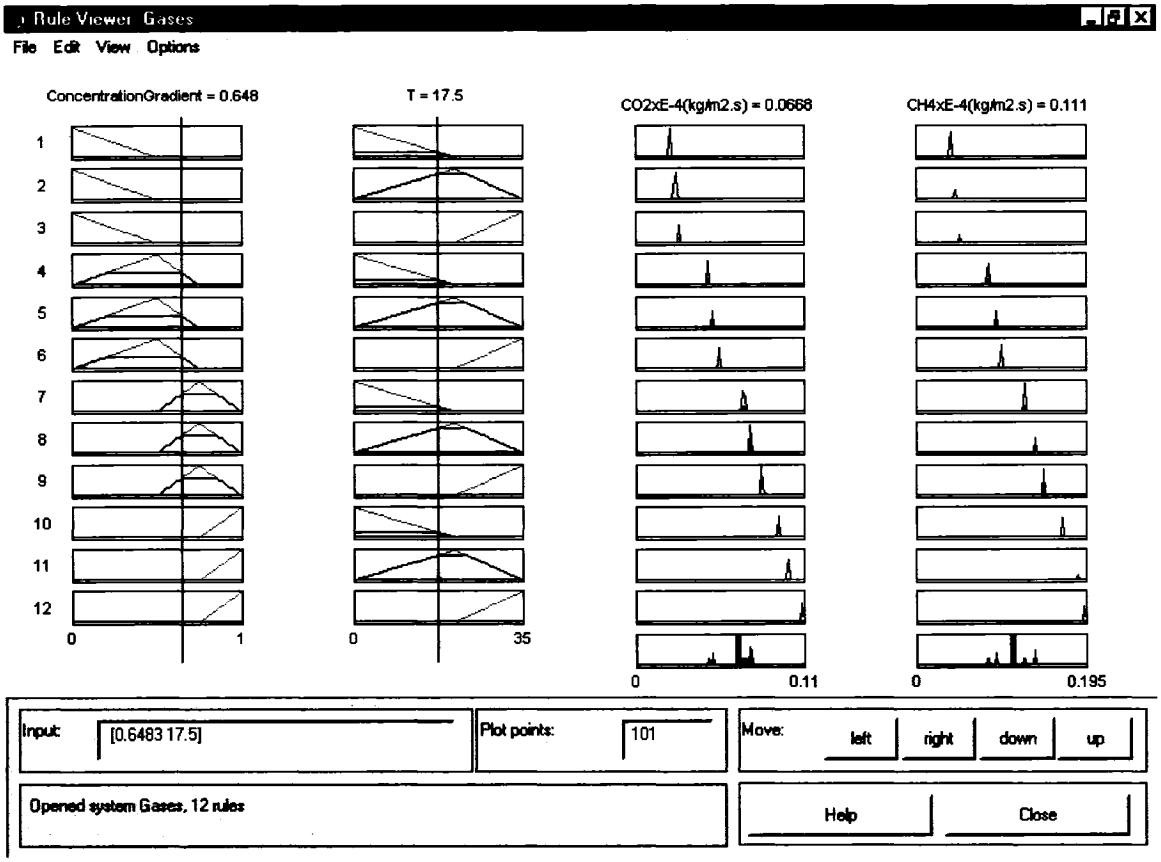

Figure 5.3 Process of Fuzzy Inference to Evaluate Methane and Carbon Dioxide Diffusion

Fuzzy logic approach gives the flexibility to find a value for any particular condition within the modeling range. Figure 5.4 and 5.5 show surfaces of the carbon dioxide and methane diffusive flux respectively for temperature ranges from 0 to 35 ^{o}C and concentration gradient from 0 to 1 kg/m^3.m (refer to Chap 2). Comparing to results calculated in a classical way (Figure 4.8), the use of a fuzzy system permit to evaluate an accurate biogas flux for any combination of temperature and concentration gradient.

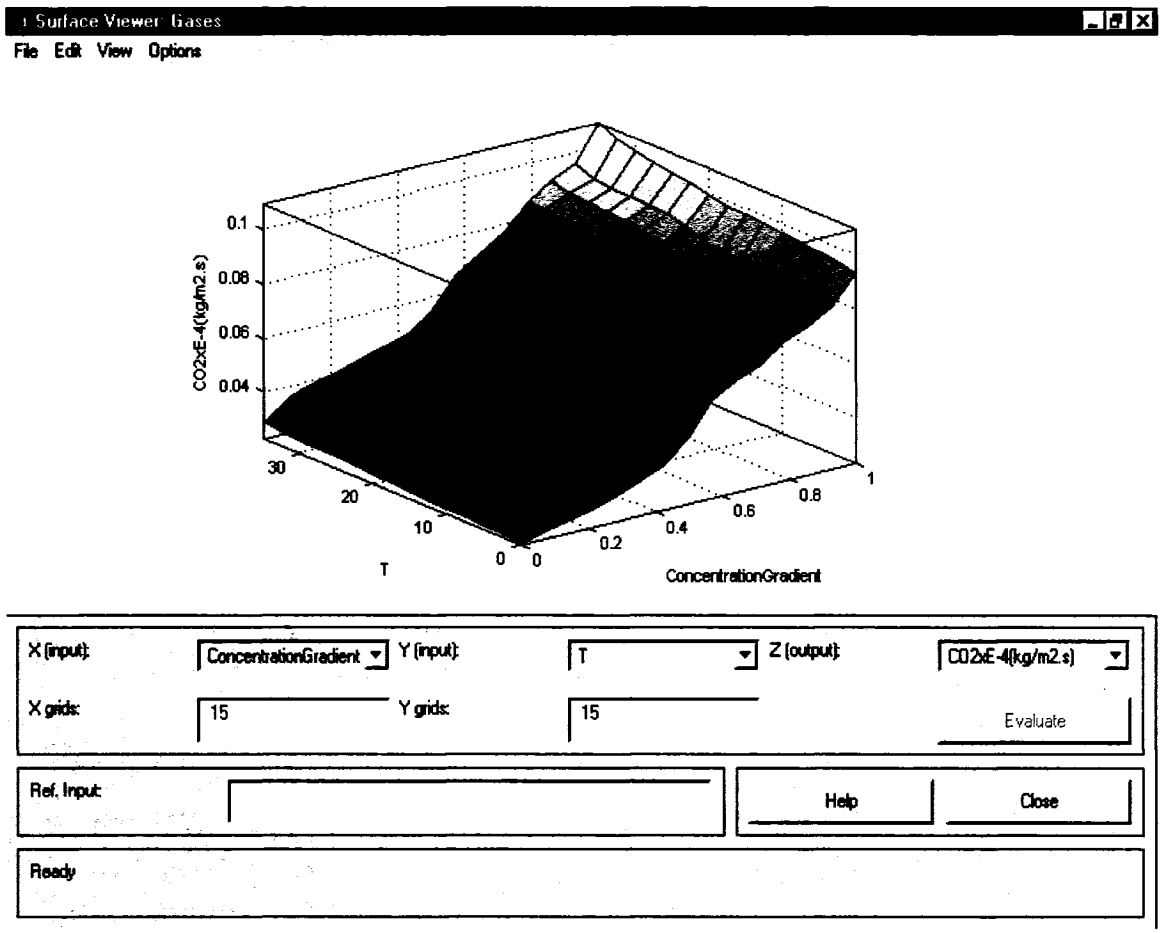

Figure 5.4 Surface of Carbon Dioxide Diffusion within Variable Carbon Dioxide Concentration Gradient and Variable Temperature.

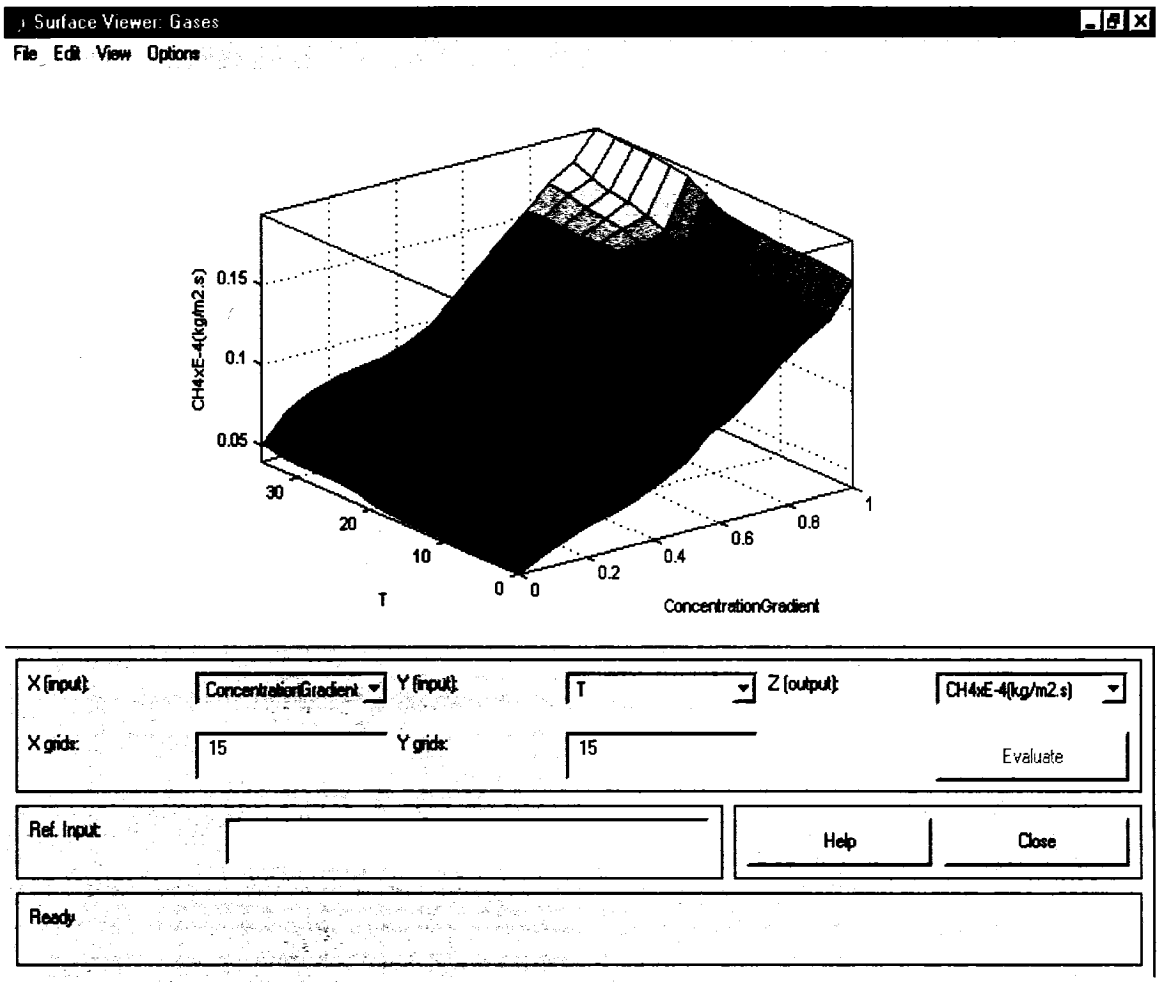

Figure 5.5 Surface of Methane Diffusion within Variable Methane Concentration Gradient and Variable Temperature.

For biogas convective transport in the polymer material, fuzzy system modeled the convection transport for both carbon dioxide and methane. Figure 5.6 shows a fuzzy model that describes the methane and carbon dioxide convective flow rates within variable pressure gradient and temperature.

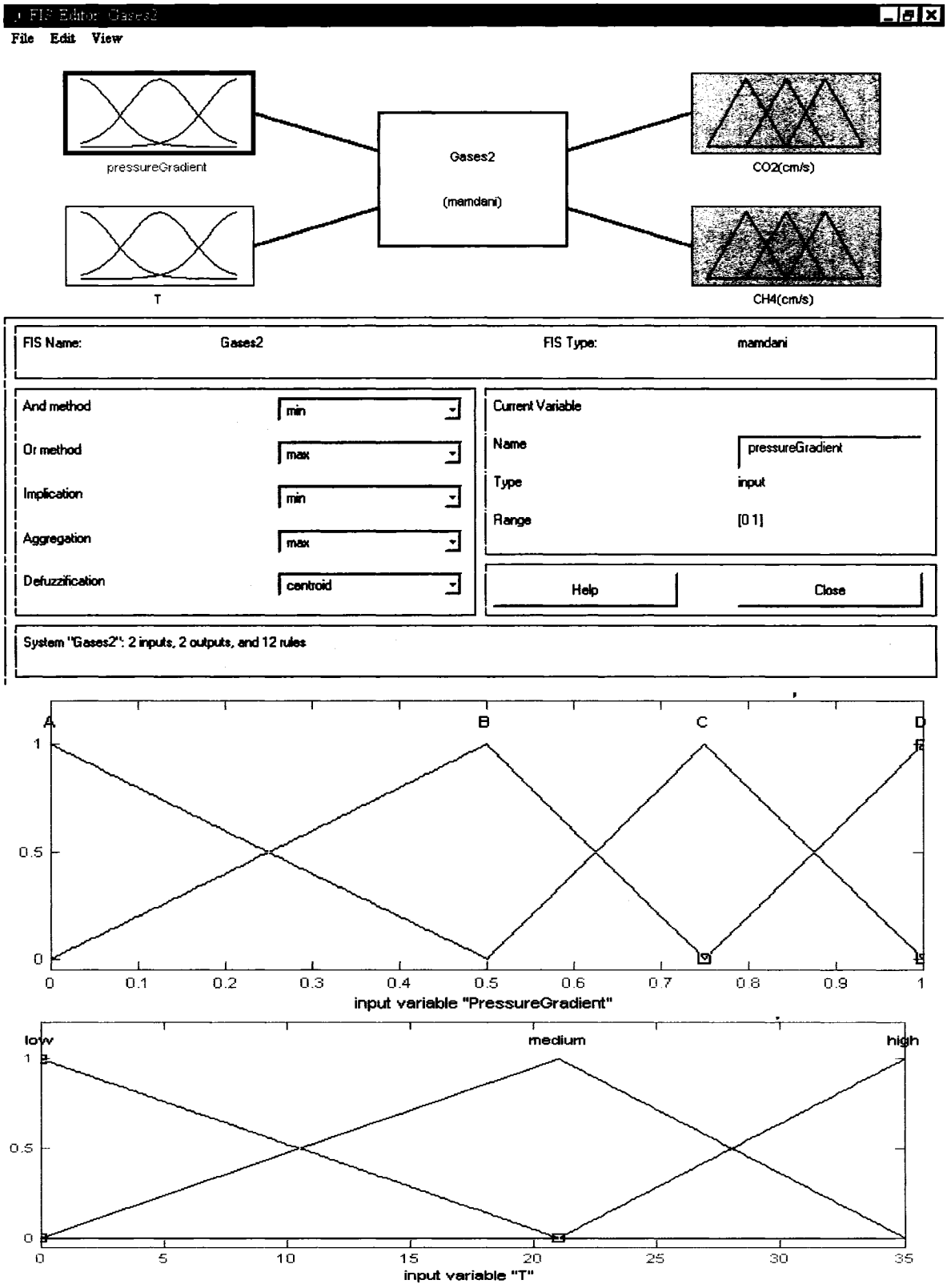
FIS Editor: Gases2
File Edit View
pressureGradient
T
Gases2
(mamdani)
CO2(cm/s)
CH4(cm/s)
FIS Name: Gases2
FIS Type: mamdani
And method min
Or method max
Implication min
Aggregation max
Defuzzification centroid
Current Variable
Name pressureGradient
Type input
Range [0 1]
Help
Close
System "Gases2": 2 inputs, 2 outputs, and 12 rules
A
B
C
D
input variable "PressureGradient"
low
medium
high
input variable "T"

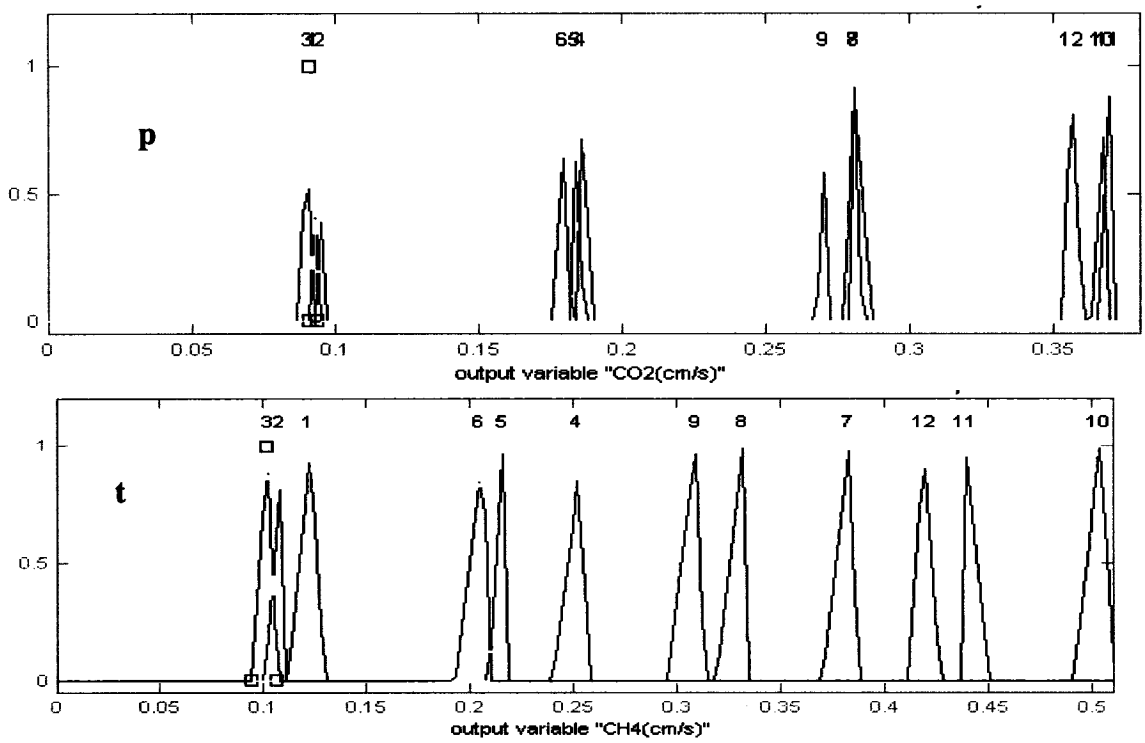

Figure 5.6 Fuzzy Model for Carbon Dioxide and Methane Convection within Variable Pressure Gradient and Temperature in Hydrophobic Permeable Polymer Material

The fuzzy inference process (Figure 5.7) includes pressure gradient and temperature as input-premises, two outputs that represent methane and carbon dioxide convection flow in polymer material, and 12 fuzzy rules. The fuzzy rules are described as the following:

1- If ∇P is (A) and T is (low) then CO_2 is (p_1) and CH_4 is (t_1)
2- If ∇P is (A) and T is (medium) then CO_2 is (p_2) and CH_4 is (t_2)
3- If ∇P is (A) and T is (high) then CO_2 is (p_3) and CH_4 is (t_3)
4- If ∇P is (B) and T is (low) then CO_2 is (p_4) and CH_4 is (t_4)
5- If ∇P is (B) and T is (medium) then CO_2 is (p_5) and CH_4 is (t_5)
6- If ∇P is (B) and T is (high) then CO_2 is (p_6) and CH_4 is (t_6)
7- If ∇P is (C) and T is (low) then CO_2 is (p_7) and CH_4 is (t_7)
8- If ∇P is (C) and T is (medium) then CO_2 is (p_8) and CH_4 is (t_8)
9- If ∇P is (C) and T is (high) then CO_2 is (p_9) and CH_4 is (t_9)
10- If ∇P is (D) and T is (low) then CO_2 is (p_{10}) and CH_4 is (t_{10})
11- If ∇P is (D) and T is (medium) then CO_2 is (p_{11}) and CH_4 is (t_{11})

12- If ∇P is (D) and T is (high) then CO_2 is (p12) and CH4 is (t12)

Appendix (A2.2) provides all details about building premises (inputs - outputs), operators, and rules.

An example on Figure 5.7 shows that when the temperature (T) equals 21.4 (°C) and pressure gradient equals 0.717 ($N/m^2.m$), then the unit area flow rate equals 0.266 (cm/s) for CO_2 and 0.31 (cm/s) for CH_4. Figure 5.8 and 5.9 show surfaces of carbon dioxide and methane flow rates respectively for any value of pressure gradient in the range from 0 to 1 ($N/m^2.m$) at any temperature in the range from 0 to 35 (°C).

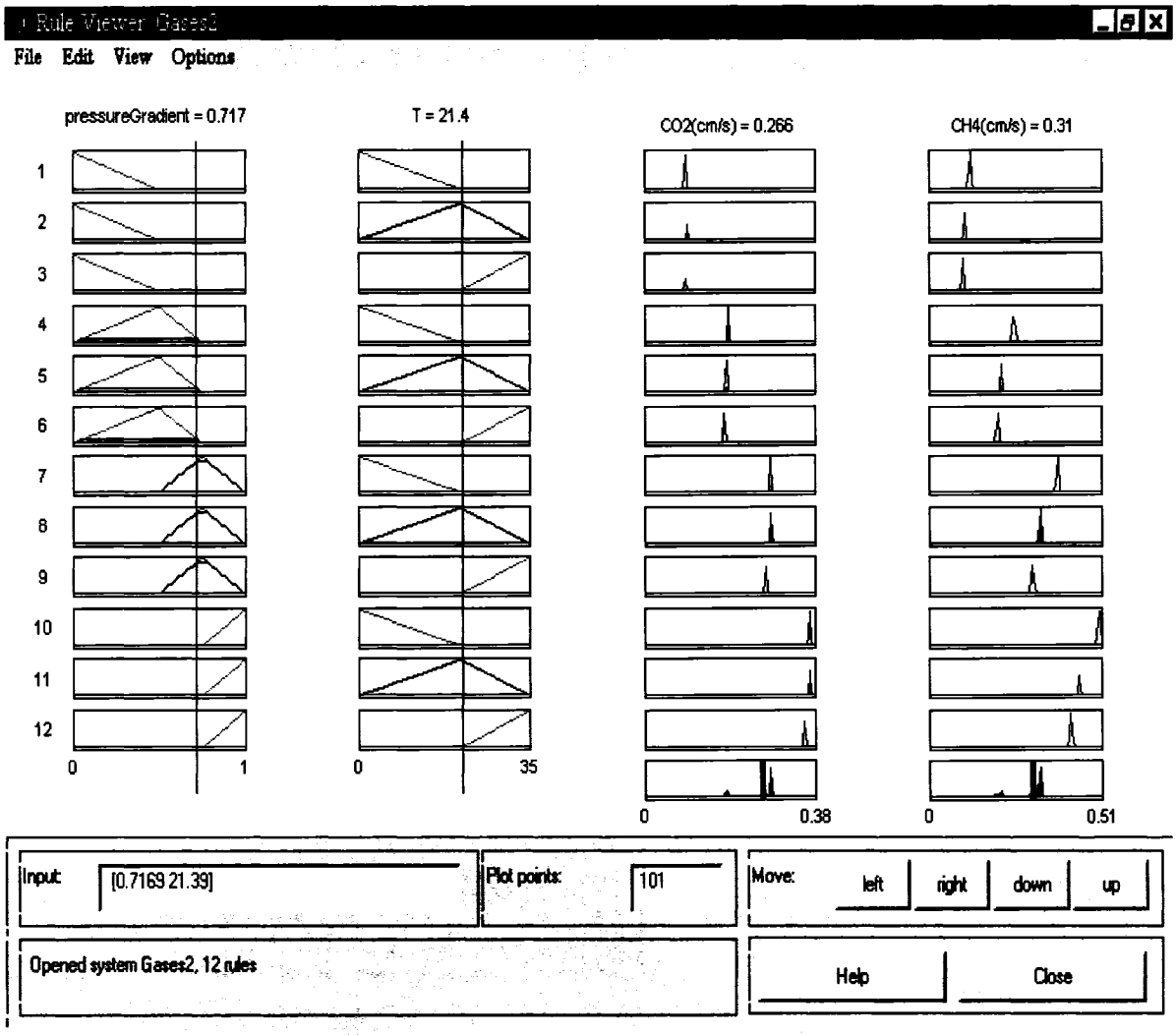

Figure 5.7 Process of Fuzzy Inference to Evaluate Methane and Carbon Dioxide Convection.

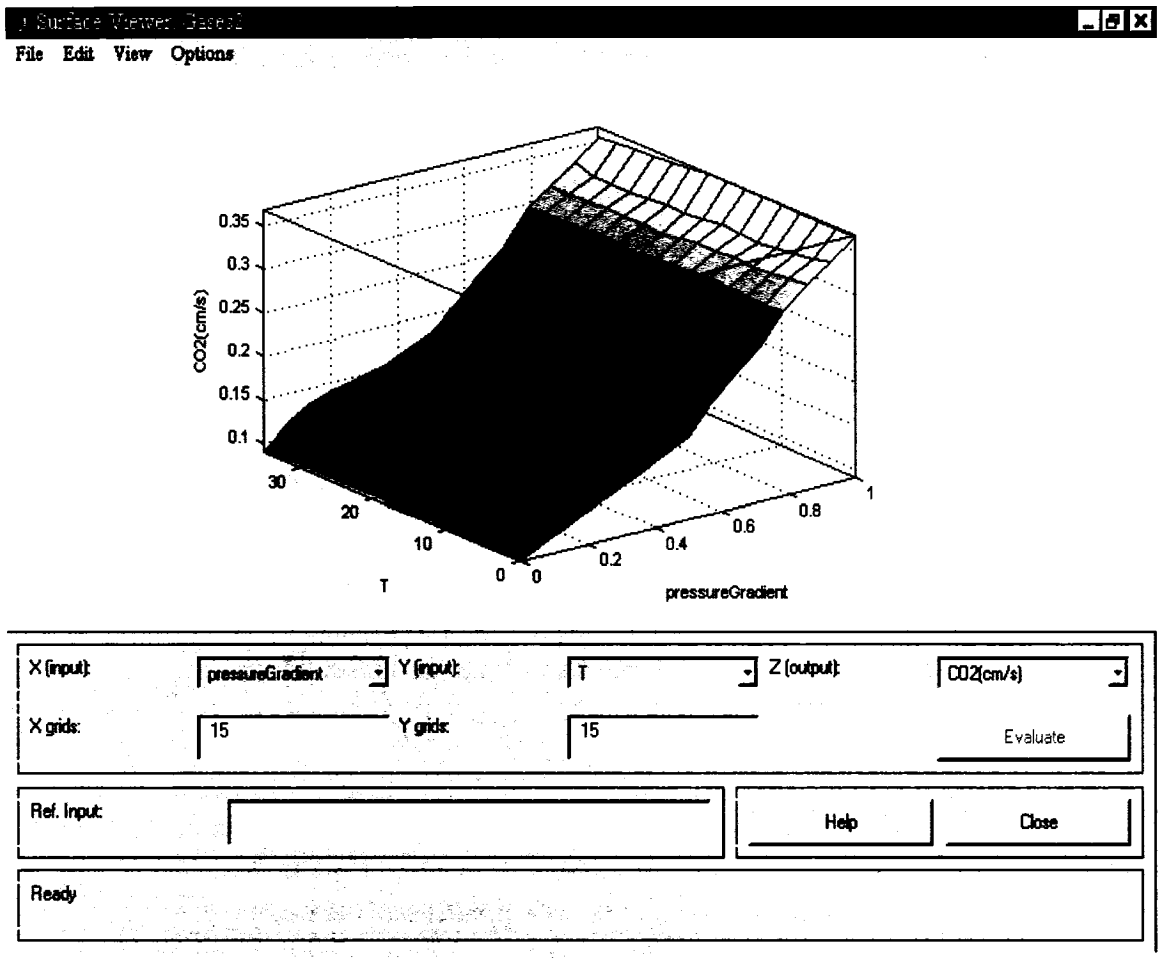

Figure 5.8 Surface of Carbon Dioxide Flow within Variable Pressure Gradient and Variable Temperature.

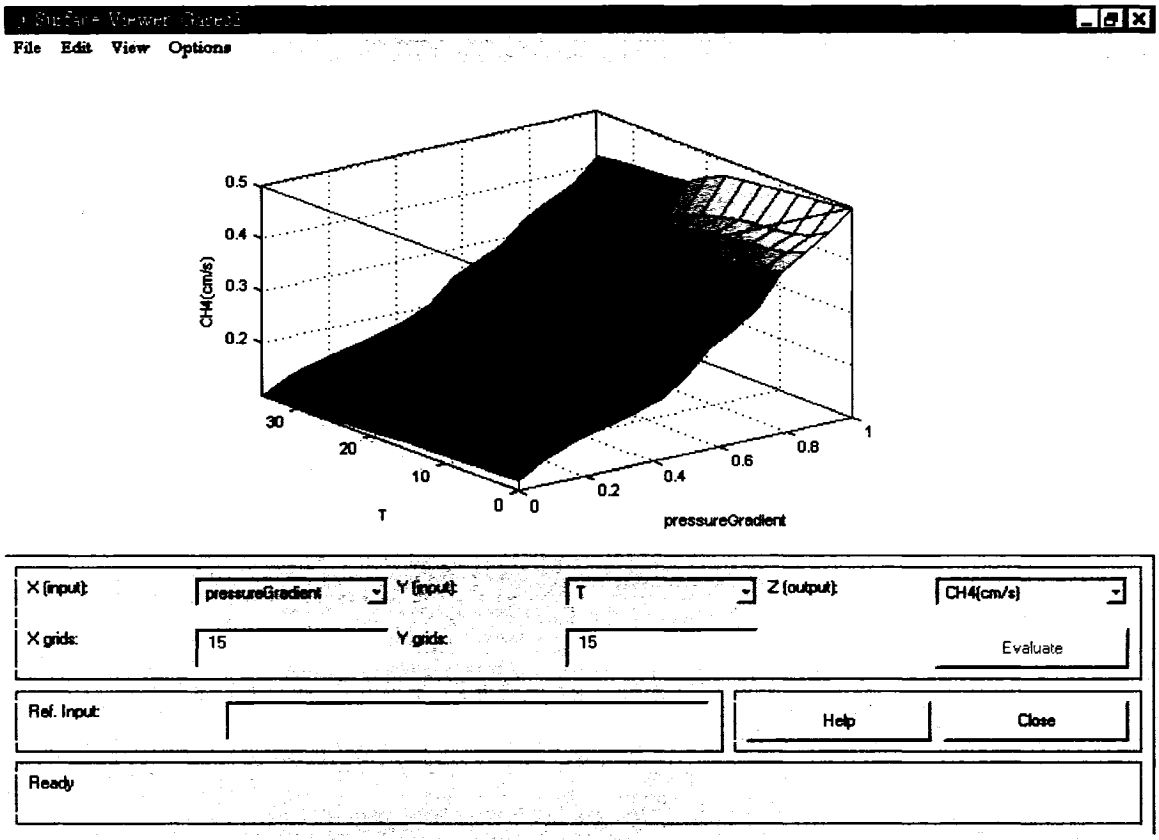

Figure 5.9 Surface of Methane Flow within Variable Pressure Gradient and Variable Temperature.

Diffusive flux for CH_4 and CO_2 in hydrophobic polymer medium is shown in Figure 5.10 and Figure 5.11 respectively, for experimental data (Exp), fuzzy modeled data (Fuzzy), and Fick's law data. Convective flow of CH_4 and CO_2 in hydrophobic polymer medium is shown in Figure 5.12 and Figure 5.13 respectively, for experimental data (Exp), fuzzy modeled data (Fuzzy), and convection formula.

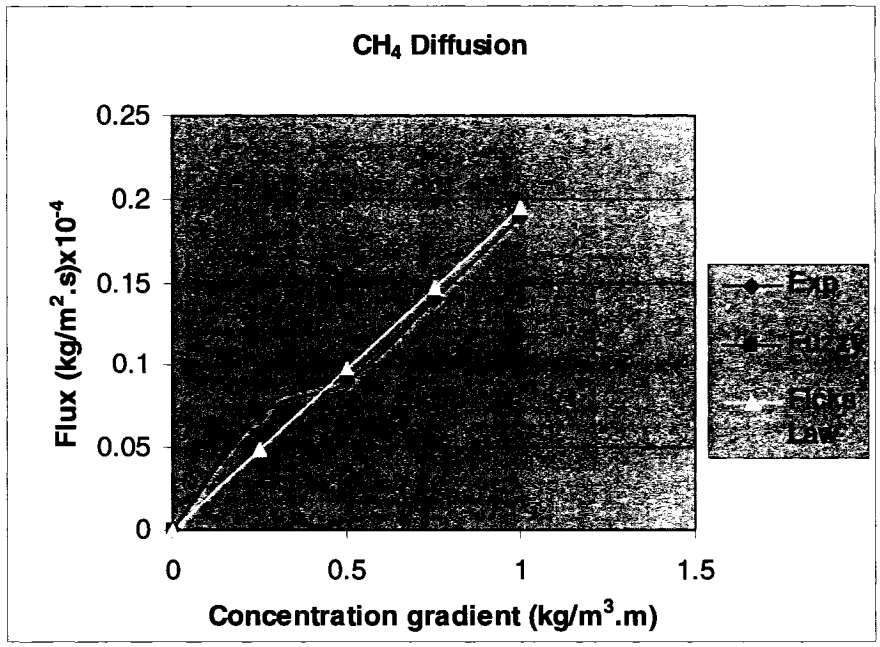

Figure 5.10 Flux of CH_4 vs. Concentration Gradient for Experimental Data (Exp), Fuzzy Modeled Data (Fuzzy), and Fick's Law Data for the CH_4 Diffusion in Hydrophobic Polymer Medium at 25 °C.

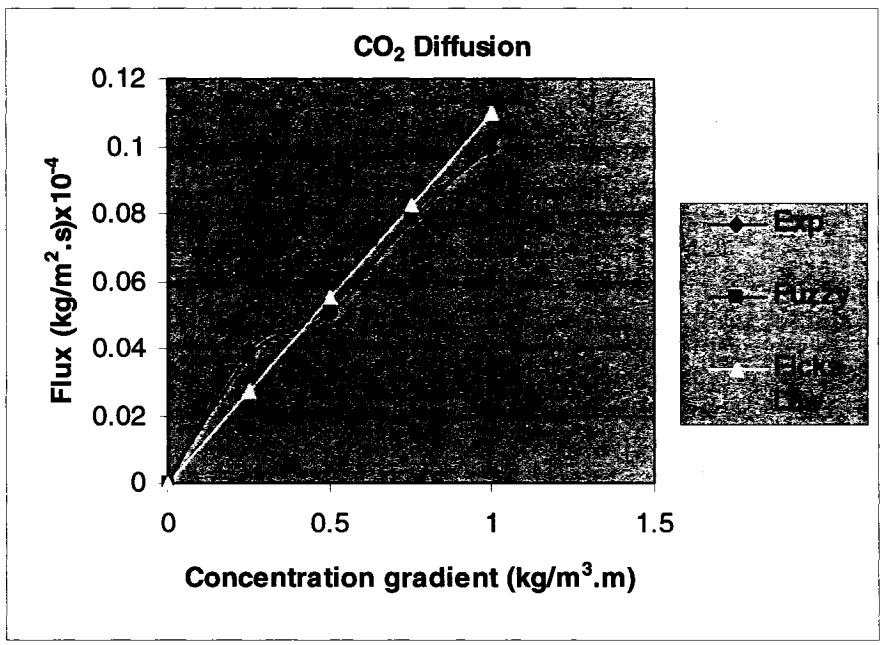

Figure 5.11 Flux of CO_2 vs. Concentration Gradient for Experimental Data (Exp), Fuzzy Modeled Data (Fuzzy), and Fick's Law Data for the CO_2 Diffusion in Hydrophobic Polymer Medium at 25 °C.

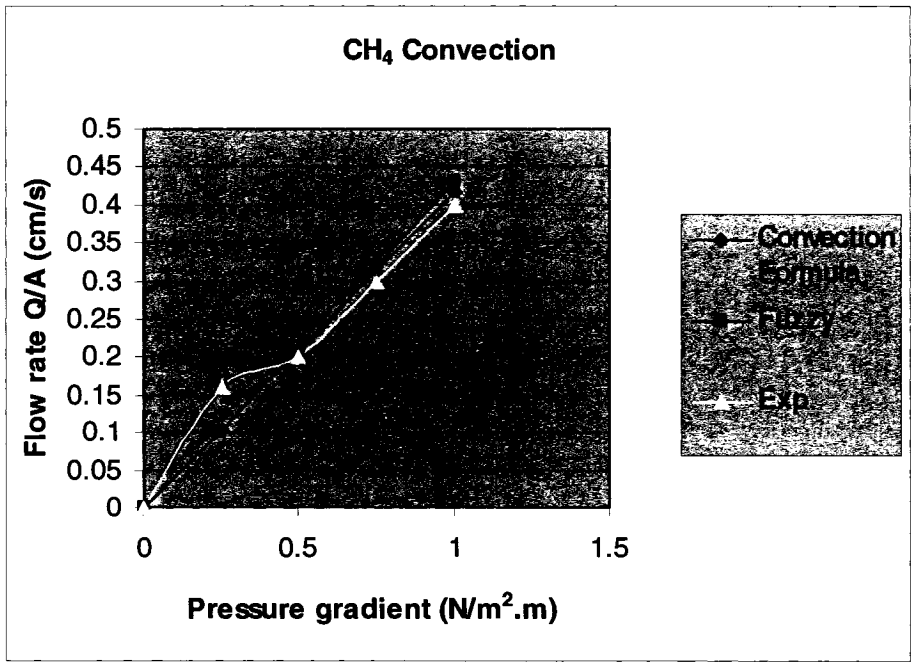

Figure 5.12 Flow of CH_4 vs. Pressure Gradient for Experimental Data (Exp), Fuzzy Modeled Data (Fuzzy), and Convection Formula Data for the CH_4 Convection in Hydrophobic Polymer Medium at 25 °C.

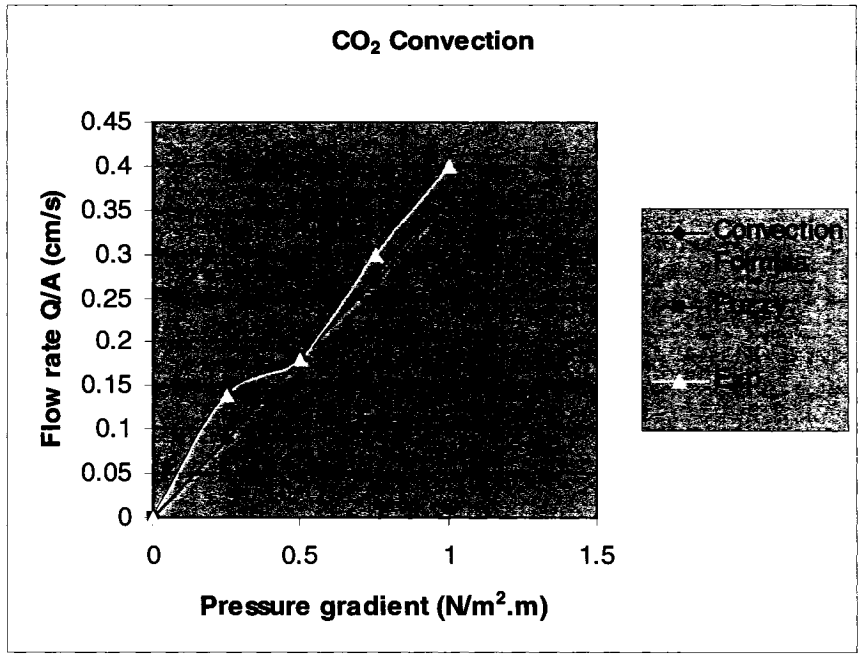

Figure 5.13 Flow of CO_2 vs. Pressure Gradient for Experimental Data (Exp), Fuzzy Modeled Data (Fuzzy), and Convection Formula Data for the CO_2 Convection in Hydrophobic Polymer Medium at 25 °C.

The experimental and fuzzy modeled data (Figures 5.10 - 5.13) for methane and carbon dioxide transport due to convection and diffusion in porous hydrophobic polymer medium show more than 99% correlation (see also Appendix A2.1 and A2.2).

5.4. Conclusion

Fuzzy logic is efficient to model ambiguous methane and carbon dioxide transport in the hydrophobic medium (Qasaimeh et al. 2006a). Fuzzy logic models in first set multi inputs (temperature and concentration gradient) and multi outputs (methane diffusion and carbon dioxide diffusion). Fuzzy logic models in second set multi inputs (temperature and pressure gradient) and multi outputs (methane convection and carbon dioxide convection). Methane and carbon dioxide transport in the hydrophobic medium would be difficult to model in classical modeling procedures (section 1.2.6). Results obtained in this work showed more than 99% correlation between experimental and fuzzy modeled data for methane and carbon dioxide transport via convection and diffusion in porous hydrophobic polymer medium. Still the biogas mass transfer of any biogas ratio in porous polymer medium is prone to difficulty; the next chapter will spot the light on it.

CHAPTER 6

Genetic Algorithm Optimization for Multi-Biogas Mass Transfer in Hydrophobic Polymer Medium

6.1. Introduction

Genetic algorithms are stochastic search method introduced in the 1970s by researchers such as John Holland (1975) and Ingo Rechenberg (1973). Genetic Algorithms (GA) are stochastic optimization techniques that are based on the analogy of the mechanics of biological genetics and imitate the phenomenon of selection of the fittest approach (Baron 1998). A GA is generally characterized by:

- Coding scheme for each possible solution, using a finite string of bits (called chromosome);
- Fitness value that provides the quality of each solution;
- Initial set of solutions to the problem, called initial population, randomly generated or chosen on a prior knowledge;
- A set of reproduction, mutation and natural selection operators, that allows the development of the population.

Based on simplifications of natural evolutionary processes, genetic algorithms operate on a population of solutions rather than a single solution. Each individual of a population is a potential knowledge base that is encoded before applying four operations: crossover, mutation, evaluation and natural selection, and decoding.

A. Crossover

The progression of the population is achieved by reproduction of the best individuals based on their ability to endure natural selection. Reproduction is mainly made by crossover of the genotype (chromosome) of two parents to produce the genotype of two children (Balazinski et al 2000).

B. Mutation

Mutation is a random inversion of a bit in the genotype of a new member of the population. Mutation allows trying completely different solutions.

C. Evaluation

The capacity of each individual to endure natural selection is evaluated by objective function. The objective function evaluates the capacity of the knowledge base to approximate the sampled data. This fitness value can be computed as the root mean square error method.

D. Natural Selection

Natural selection is performed on a population by keeping the most promising individuals based on their fitness. This is equivalent to using solutions that are the closest to the optimum (Balazinski et al 2000).

When the genetic algorithm is in steady state, a newly child replaces the worst genotype of the population in the process of creating child solution using genetic operators such as

crossover and/or mutation. This process of production is repeated until optimization criterion is met, which normally takes place when many of iterations have been accomplished. The population has often come together when the optimization criteria have been met up where the genotypes in the population are identical to each other (Ronald 1994).

Genetic algorithms (GA) can be applied to natural and real world problems. For instance, the fuzzy decision support system used the genetically generated fuzzy knowledge base to evaluate the capability of constructed wetland sediments to adsorb mercury, where decision cannot be ended up by human expert (Elektorowicz et al. 2003; Elektorowicz and Qasaimeh 2004). In this research, the genetic algorithm is used to optimize the biogas transfer rate in hydrophobic polymer medium that is proposed for the new MSW management system (QEJ bricks) in landfill. This approach is novel and for the first time is proposed for biogas transfer within polymer medium in landfill.

6.2. GA Optimization of Biogas Transfer

In the landfill, the important parameters (temperature, pressure, and biogas concentration) are variable. Therefore, biogas behavior is stochastic in addition to the variation of gas ratio in the emission. The experimental data in Figure 6.1 shows the biogas flux vs. different pressure gradients where each curve satisfies certain biogas ratio (see section 2.2.1.4), simulating a situation on landfill, particularly at different ages of the landfill. When polymer capacity at landfill is designed, the amount of gas should be taken in consideration, and hence an optimization should be conducted. Genetic algorithm has

been used to optimize the design for a micro-scale unit for biogas mass transfer rate ($\Delta F = dm/dt$) in the porous hydrophobic polymer medium (Fig. 6.2) in constructed landfill.

Genetic algorithm is used to characterize the dynamics of input-output data by identifying a dynamic transfer function, which is a mathematical representation of the relation between the input and output used in control theory. Transfer function is obtained by fitting a dynamic input-output data to the input-output solutions. Input-output data are encoded to chromosomes (1, 0 digits). These chromosomes are subjected to genetic processes as crossover and mutations. Then a process of evaluation takes place. The evaluation process entails an objective function that evaluates the squared difference between experimental and calculated values. After the chromosomes are being evaluated, they are either selected for more iteration or decoded to the solutions. The selection process is performed on non-optimal chromosomes by keeping the most promising individuals based on their fitness. The decoding process is performed on optimal chromosomes to obtain optimal solutions and required optimal transfer function.

Genetic algorithm is applied by means of TransGA 1.0 (©Angel Martin 2002) for optimizing the micro-scale biogas transfer rates in the porous hydrophobic medium.

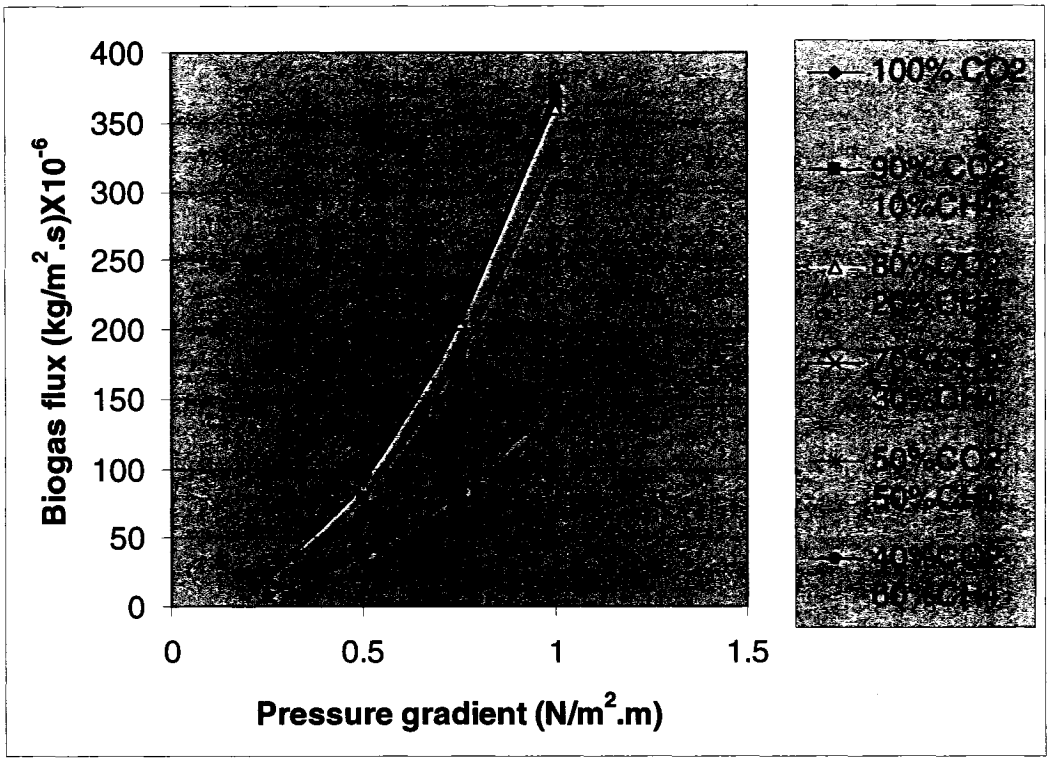

Figure 6.1 Biogas Flux for Different Percentages within Different Pressures (at average temperature 25 °C)

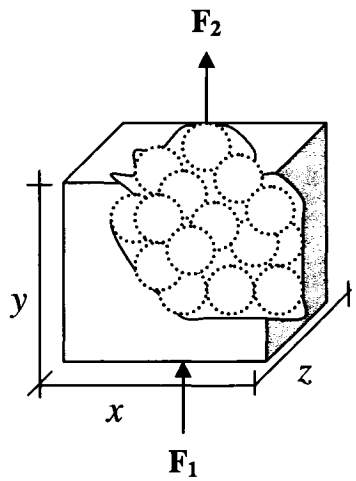

$$\Delta F = \frac{dm}{dt}$$

$\Delta F = F_2 - F_1$

F: mass flux (g/s)
m: mass (g)
t: time(s)

Figure 6.2 A Micro-Scale Unit of Porous Hydrophobic Polymer to be Optimized by (GA) for Biogas Mass Transfer (ΔF)

The genetic algorithm proceeds in iterative processes of reproduction and mutation as shown in Figure 6.3 to achieve the optimized solution that is being represented by transfer function for input/output solutions (Appendix A3). The transfer function represents the simulation of output values of biogas flux due to input values of biogas percentages during the landfill time.

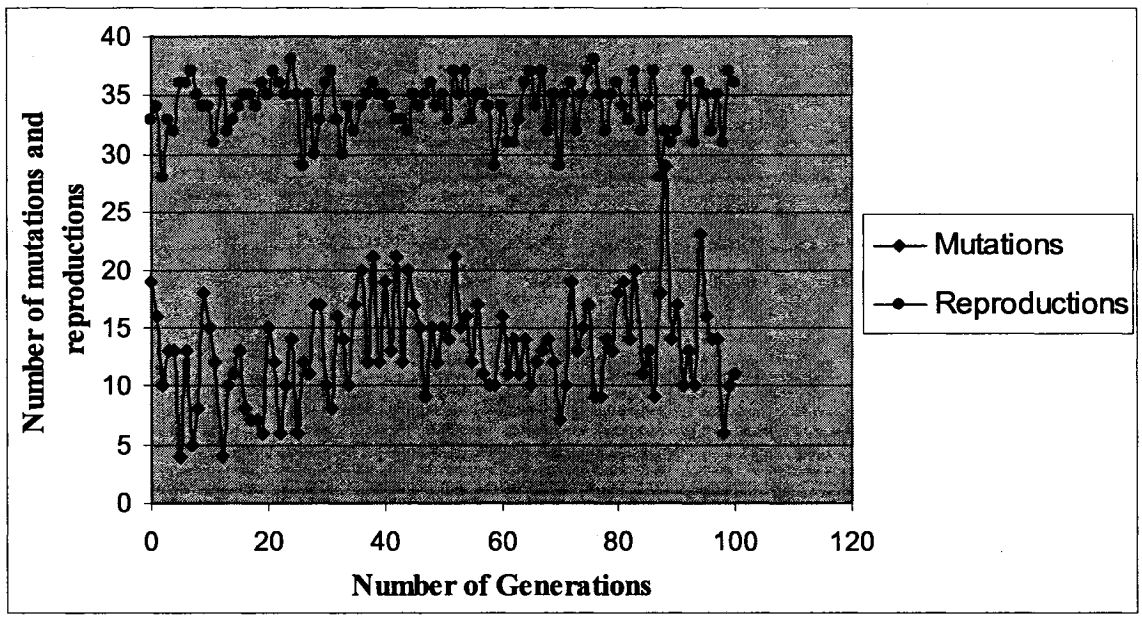

Figure 6.3 Mutation and Reproduction Processes Done during GA Optimization

The solutions were evaluated and optimized until steady state was achieved, where the genotypes in the population are very similar if not identical to each other. As shown in Figure 6.4, transfer functions from F1 to F5 represent the optimum phenotypes that are summarized as the following:

$$F1 = (z^2\text{-}0.242\ z\text{-}0.0868)/\ (z^2\text{-}1.13\ z\text{+}0.198) \qquad (6.1)$$

$$F2 = (z^2-0.242\ z-0.0868)/\ (z^2-1.14\ z+0.206) \quad (6.2)$$

$$F3 = (z^3-0.682\ z^2+0.0198\ z+0.0382)/\ (z^3-1.9\ z^2+1.07\ z-0.155) \quad (6.3)$$

$$F4 = (z^3-0.682\ z^2+0.0198\ z+0.0382)/\ (z^3-1.88\ z^2+1.03\ z-0.141) \quad (6.4)$$

$$F5 = (z+0.888)/\ (z-0.704) \quad (6.5)$$

The solution F5 in equation (6.5) is the most optimal solution, because it has the least objective function value. The objective function evaluates the capacity of the knowledge base to approximate the sampled data. This fitness value is computed as the root mean square error method. Thus the optimization process is done as minimization on the objective function. Therefore, F5 is used as a representative transfer function for simulation and design of the biogas mass transfer through the porous hydrophobic polymer medium.

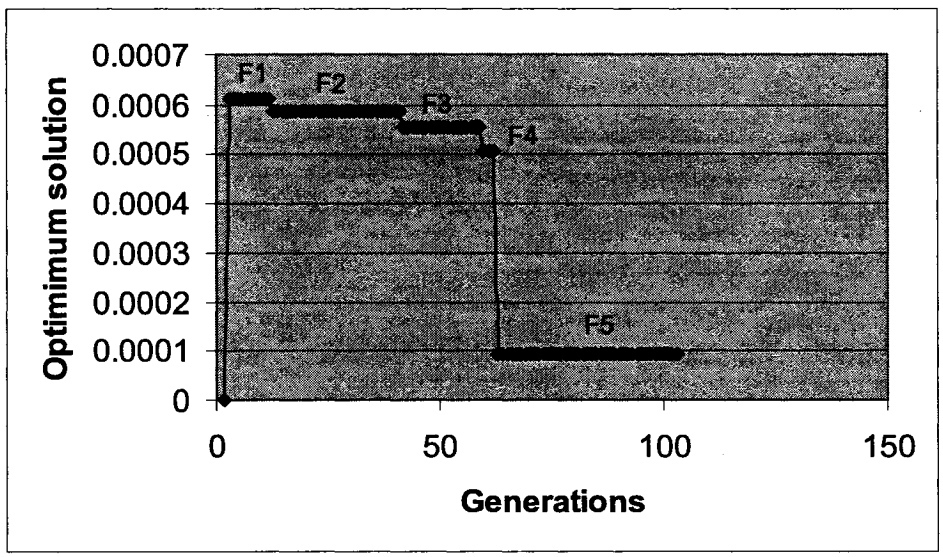

Figure 6.4 Optimum Solutions vs. Iterative Generations

The transfer function which represents the biogas transfer through the permeable hydrophobic polymer is used for QEJ bricks design. As shown in Figure 6.5, the output of the transfer function is adjusted by the factor (**K**) to have the output [f (u) = **K** × u] scaled up to the field. The **K** factor depends on the pressure gradient as it is represented by curve shown in Figure 6.6.

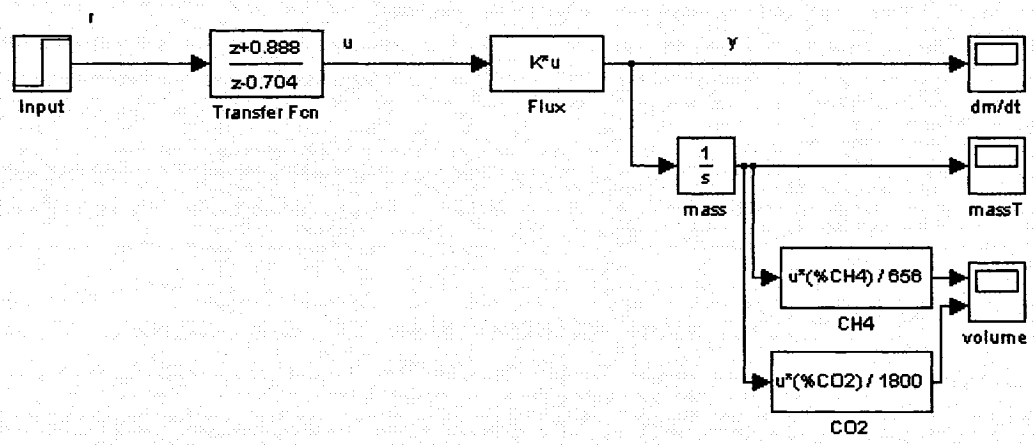

Figure 6.5 A Scheme for Finding Daily Biogas Mass Transfer Rates, Masses, and Volumes Using Optimum Transfer Function

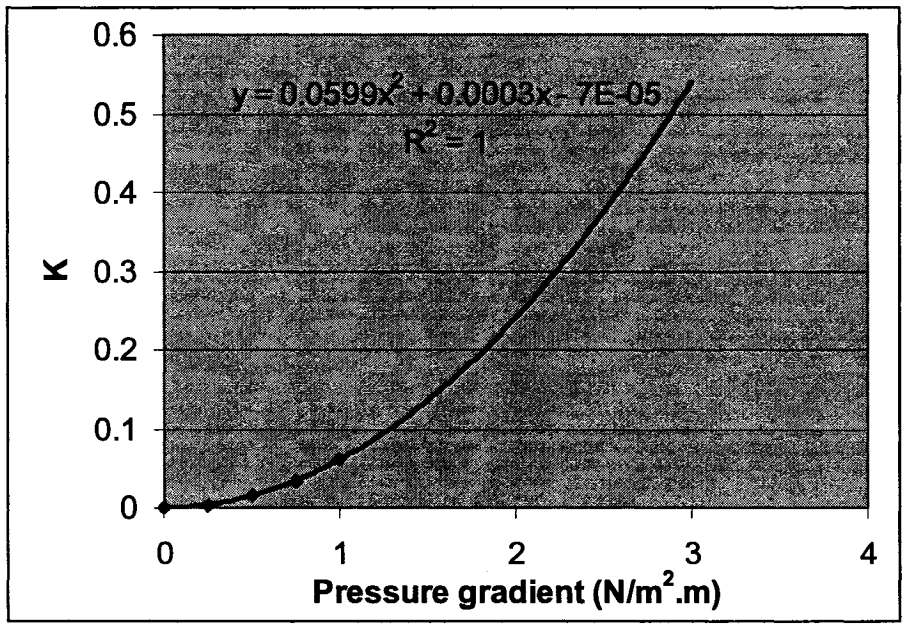

Figure 6.6 K Factor that Adjusts the Output of Transfer Function to Filed Scale within Variable Pressure Gradient

The results obtained from simulation on Figure 6.5, provides a scheme to find daily biogas mass transfer rates (dm/dt), mass, and volume. The mass transfer rate shown in Figure 6.7 is used to find the total daily mass and volume of biogas as shown in Figure 6.8 and Figure 6.9 respectively that are used for QEJ bricks system.

Figure 6.10 shows design volumes and percentages for biogas mixture (CH_4, CO_2) in QEJ bricks landfill during 40 years. The capacity and the properties of hydrophobic porous polymer used in QEJ bricks landfill should withstand the biogas mixture volumes and mass transfer requirements.

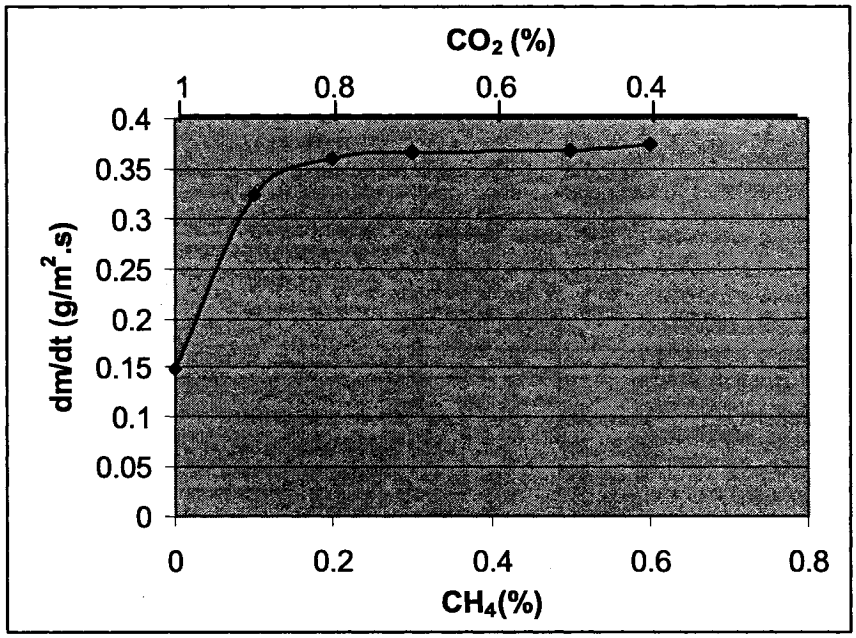

Figure 6.7 Biogas Mass Transfer Rate (dm/dt) vs. Different Biogas Percentages at Pressure Gradient 1 $N/m^2.m$ (within 40 years and average temperature 25 °C)

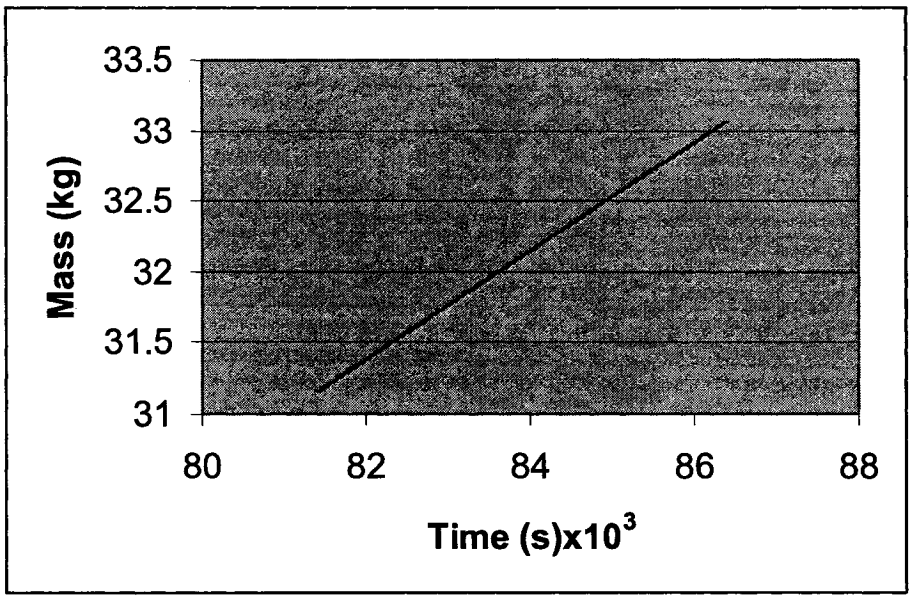

Figure 6.8 Total Mass of Biogas Mixture (40% CO_2, 60% CH_4) in Landfill per Day per Unit Area (at pressure gradient 1 $N/m^2.m$ and average temperature 25 °C)

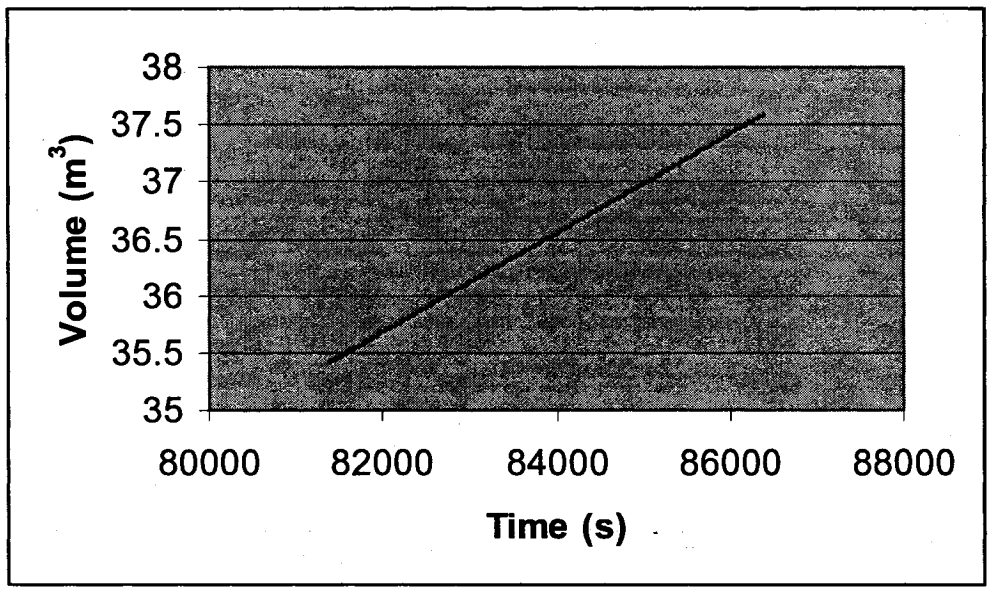

Figure 6.9 Total Volume of Biogas Mixture in Landfill per Day per Unit Area (at pressure gradient 1 $N/m^2.m$ and average temperature 25 °C)

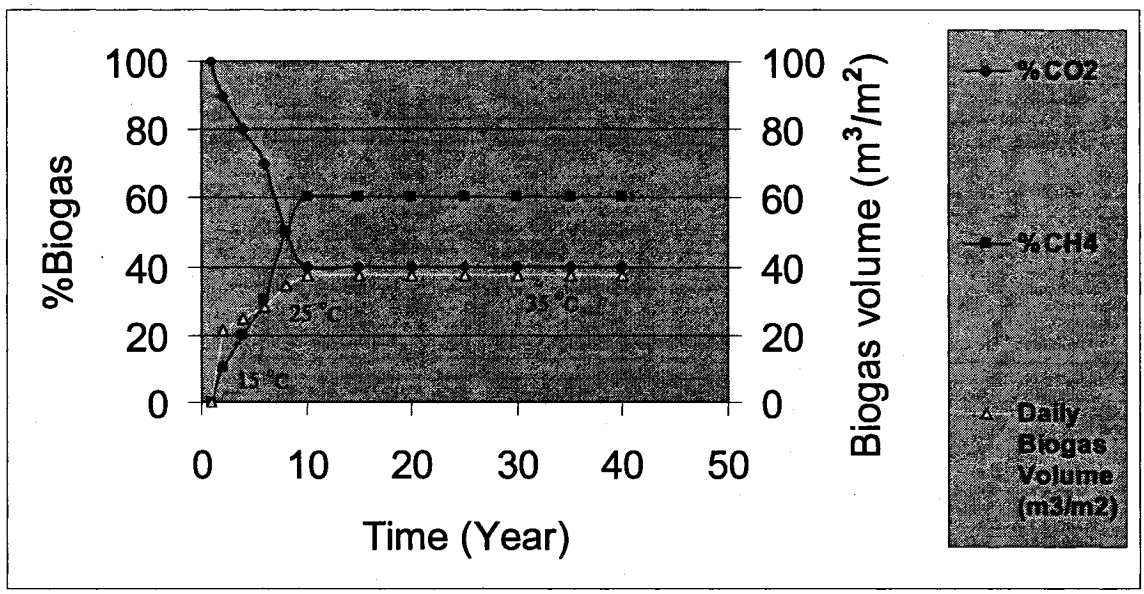

Figure 6.10 Biogas Design Volumes in the New MSW System during 40 Years Age

6.3. Conclusion

Genetic algorithm is used to optimize a transfer function that represents input of biogas percentages and output solutions for daily mass transfer rates for biogas mixture from which mass and volume of biogases within the landfill time of service are used for design of the selected hydrophobic porous polymer that transfers and conveys the biogas in QEJ bricks landfill system.

CHAPTER 7

Intelligent Fuzzy Control Approach for Biogas Evacuation in the QEJ Bricks System

7.1. Introduction

As previously described in Chapter 5, fuzzy logic modeled the uncertain multi transport of biogas in hydrophobic polymer medium. Fuzzy logic will also be applied here to control evacuation and collection processes of biogas within the hydrophobic polymer medium of the new intelligent QEJ bricks system proposed in this research.

7.2. Methodology

The methodology of this section of research is applied using the Fuzzy Logic Toolbox in MATLAB 6.5. The graphical user interface (GUI) in the Fuzzy Logic Toolbox: the Fuzzy Inference System (FIS) Editor, the Membership Function Editor, the Rule Editor, the Rule Viewer, and the Surface Viewer are dynamically linked, such that changes made to the FIS can affect other GUIs. Once having fuzzy controller built using the graphical editors, work is saved with its specifications in the Matlab workspace. The fuzzy controller is then available to be used in the Fuzzy Controller block in a Simulink diagram, and hence using it in a simulated environment (Qasaimeh et al. 2006b).

7.3. Control System

Fuzzy control is being used in this research for controlling biogas evacuation process. The biogas moves in porous hydrophobic polymer due to convection and/or diffusion,

eventually biogas are to be collected. Valves that are linked to blowers regulate the ports for gas collection. Fuzzy controllers regulate the valves, so that the collection processes are controlled.

In this work, biogas is characterized by two parameters: the pressure and the flow velocity, which are the inputs of the fuzzy system. The output of the fuzzy system is the valve opening, which controls the gas outflow rates (Qasaimeh et al. 2006b).

After having fuzzy inference system built for biogas characteristics using the graphical editors as it is shown in Figure 7.1, work is saved with its specification in the Matlab workspace. The fuzzy inference system is then available to be used in the Fuzzy Controller block in a Simulink diagram to control biogas collection processes. The Simulink diagram as shown in Figure 7.2 implies intelligent fuzzy system that includes sensors/meters to measure pressure head and velocity for biogas in the hydrophobic polymer in QEJ bricks system (see Chapter 3 - Figure 3.7). Collected information by meters is conveyed to data acquisition system, which in turn sends information to *fuzzy logic controller* that takes inputs to specify output to control the valve at collection ports. The *fuzzy logic controller* used in this design is combined with instant rule viewer to show process of fuzzy inference system (Qasaimeh et al. 2006b).

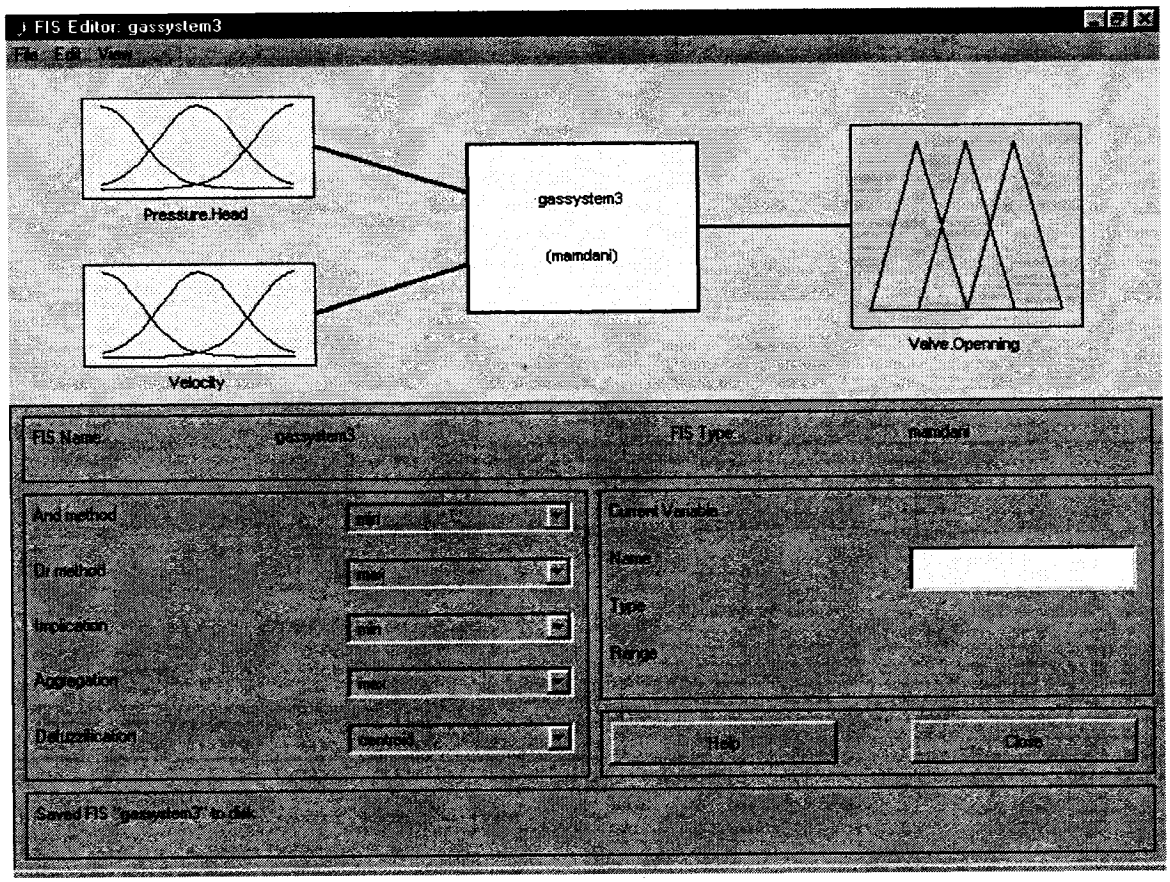

Figure 7.1 Fuzzy System for Biogas Evacuation Control in MATLAB

The input premises and a consequence output premise in the above-described fuzzy system are formulated as membership functions. These premises are shown in the following demonstration:

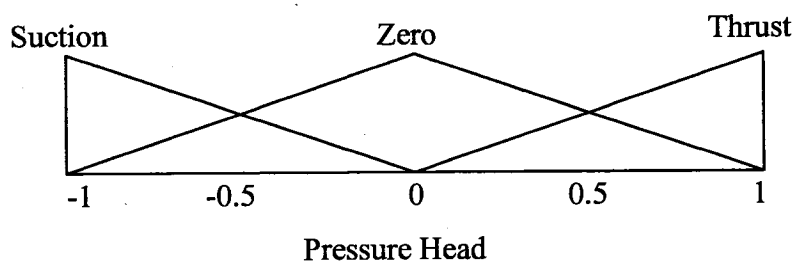

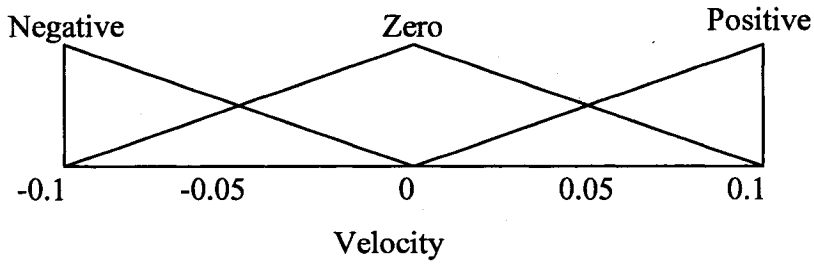

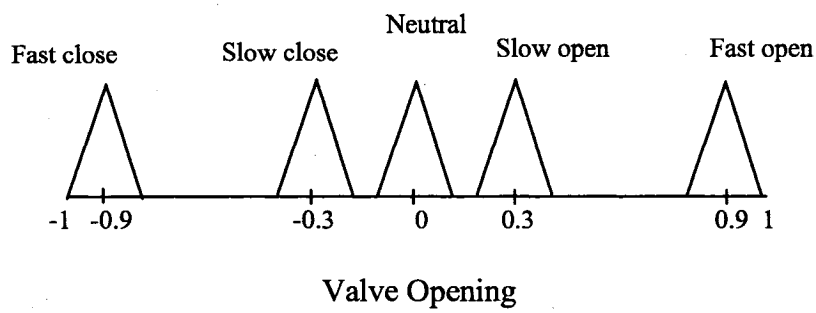

The if-then rule statements used to formulate the statements that comprise fuzzy system are specified as the following:

1. If biogas pressure head is thrust then valve is opened fast (for biogas convective flow);
2. If biogas pressure head is suction, then valve is closed fast;
3. If pressure head is zero and biogas velocity is zero, then valve is neutral
4. If pressure head is zero and biogas velocity is positive, then valve is opened slowly (for diffusive flow);

5. If pressure head is zero and velocity is negative, then valve is closed slowly (*detailed information on premises, operators and rules available in Appendix A2.3*).

The pressure head and velocity data was provided by sensors/metres. Each sensor was calibrated to certain range as shown in the input premises. These ranges will be scaled up to the actual values once outputs are analyzed.

Fuzzy logic controller in Figure 7.2 implies the required biogas fuzzy inference system that evaluates outputs (valve opening) for the inputs (pressure head and velocity). The fuzzy inference process within the *Fuzzy logic controller* is interpreted by Simulink as shown in Figure 7.3.

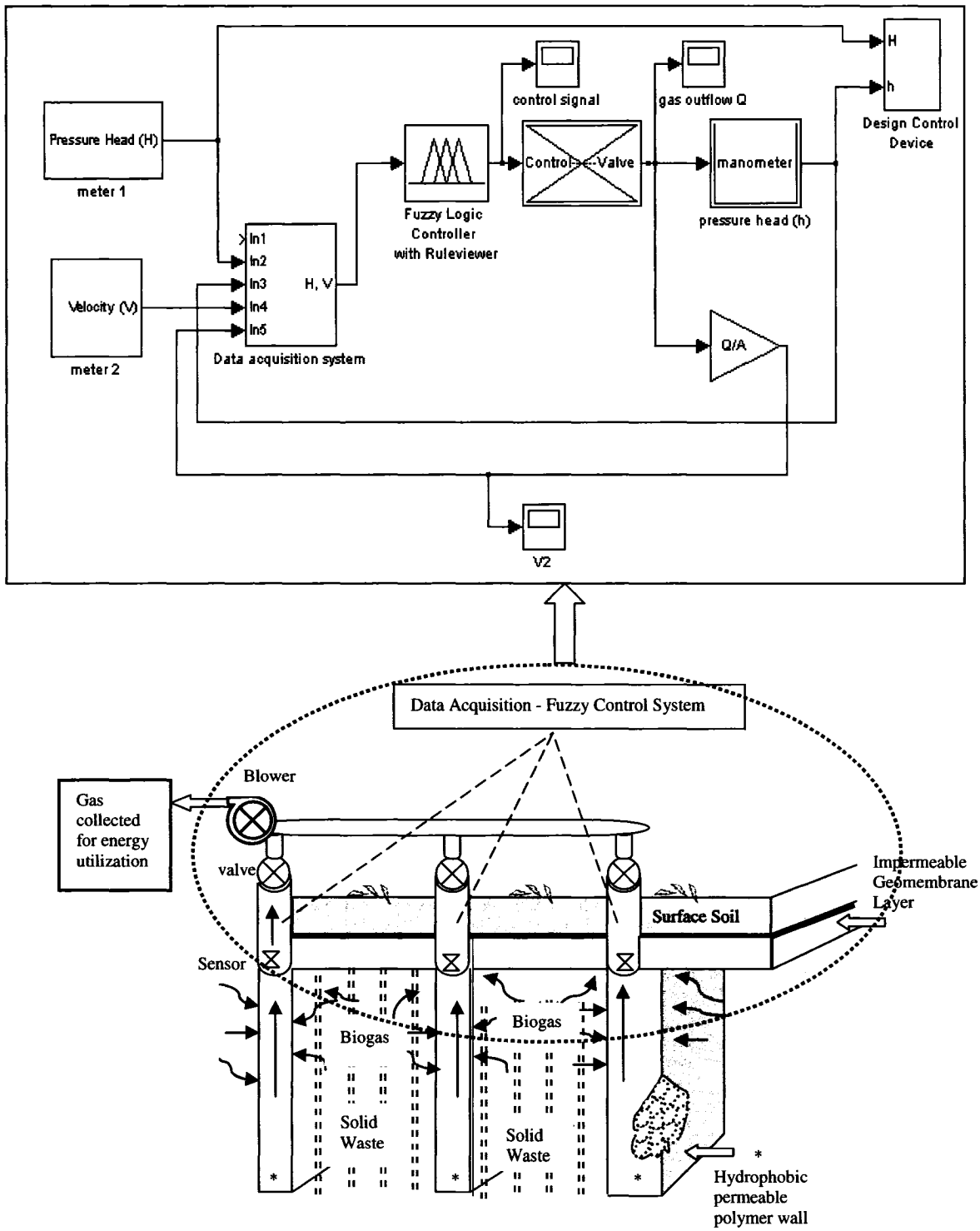

Figure 7.2 Data Acquisition-Fuzzy Control System for Controlling Biogas Evacuation Processes in QEJ Bricks System (Simulink Design)

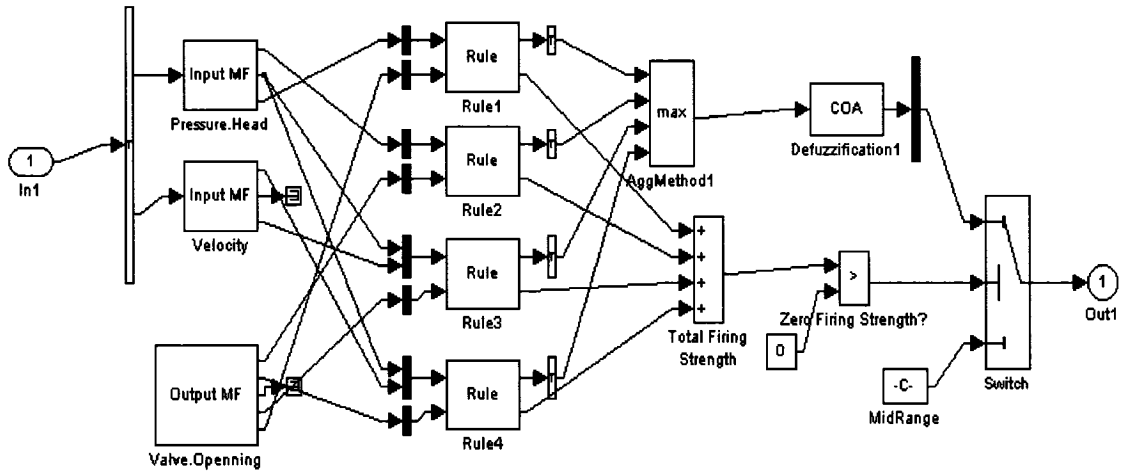

Figure 7.3 Fuzzy Inference System within the Fuzzy Logic Controller

Once the *fuzzy logic controller* ends up with defuzzified output, this output (valve opening) goes to the *valve* block to adjust it. Figure 7.4 shows the valve opening with time due to the fuzzy control.

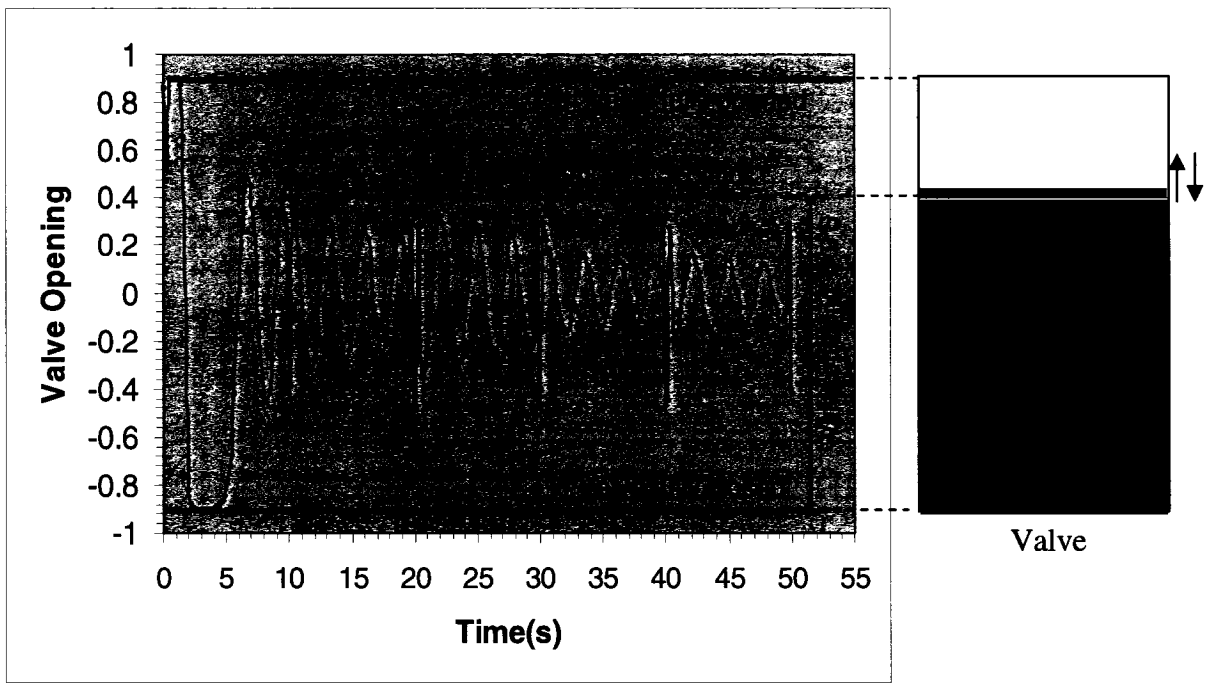

Figure 7.4 Schedule of Valve Opening due to Fuzzy Controller

The *valve* block involves transfer function (Fcn) as shown in Figure 7.5 that uses the control output to estimate values that are integrated within definite upper/lower limits (saturation) to obtain scale up of biogas outflow rates that should be released.

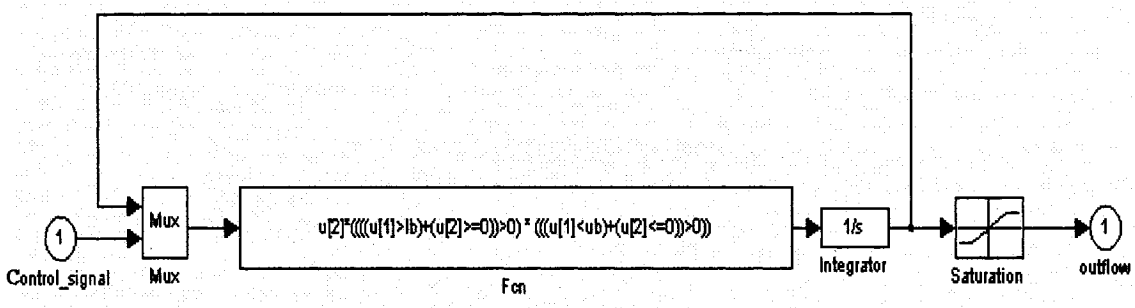

Figure 7.5 Control Signal Conversion Function Implied at Valve Block to Evaluate Biogas Outflow

The output of *valve* block as shown in Figure 7.6 indicates the scale up of biogas outflow rate that should be released for collection as a result of fuzzy control. The output of *valve* block becomes input to the block of manometer that gives the outflow pressure head. As shown in Figure 7.7, the pressure head governed by fuzzy controller, and the pressure head measured from pressure head meter/sensor represent design pressure heads to be used by collection control device. *Collection control device* block represents the device that could be installed to use the design pressure heads to control collection/evacuation processes. Figure 7.8 shows the simulation run of the intelligent data acquisition-fuzzy control system described in Figure 7.2 for biogas collection processes with fuzzy rule

viewer and control device viewer showing how valve is opening and closing due to fuzzy control according to biogas pressure and velocity.

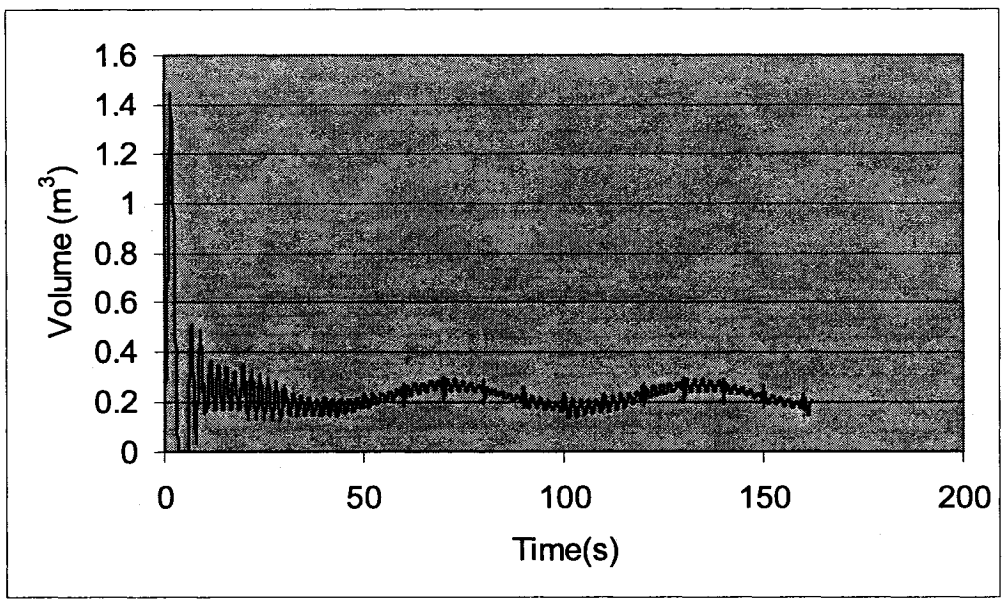

Figure 7.6 Schedule of Gas Outflow Rate as a Result of Fuzzy Controller (Fig. 7.2)

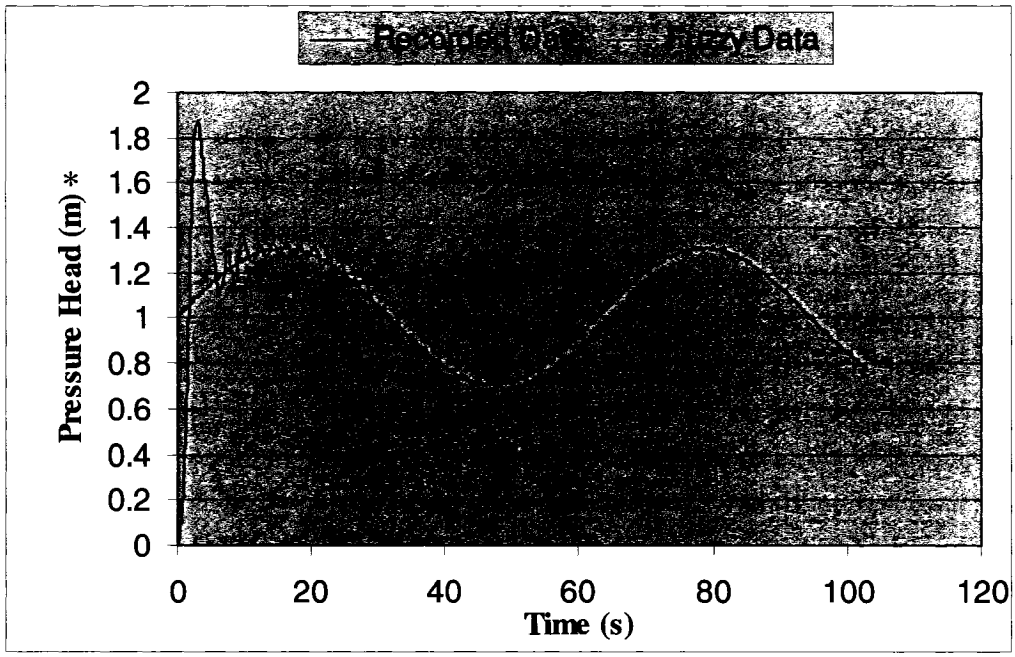

Figure 7.7 Design Pressure Heads vs. Time for Recorded Data and Fuzzy Simulated Data (results from design control device block in Fig. 7.2)

* Atmospheric pressure is included

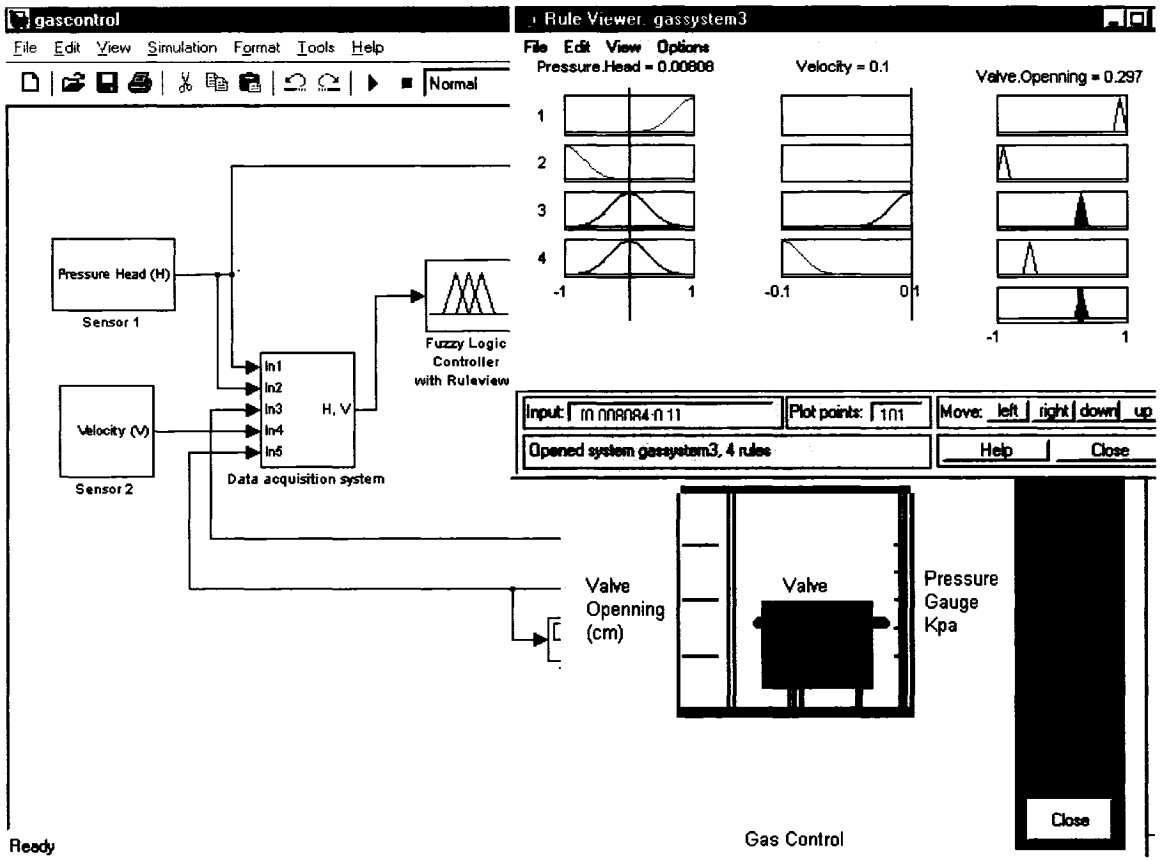

Figure 7.8 Simulation Run of Data Acquisition-Fuzzy Control System for Biogas Collection Processes with Rule and Control Device Viewer

7.4. Conclusion

Intelligent data acquisition-fuzzy control system was designed for biogas evacuation in the developed QEJ bricks system (Qasaimeh et al. 2006b). Fuzzy logic was used to adapt valves in collection processes depending on variable biogas pressure and velocity. Fuzzy logic provided automatic evacuation process to control biogas release with time.

CHAPTER 8

Conclusions and Research Contributions

8.1. Conclusions

This research provides a novel MSW management system for biogas control in landfill. The MSW management system proposed in this research (Intelligent QEJ Bricks) provides new approaches on: management and operation, material medium for biogas collection, biogas transport modeling, biogas mass transfer optimization, design configuration, and automatic intelligent control system for biogas evacuation. The new operation of the developed system includes series of cells with porous bricks built sequentially to form walls confining the waste. This approach implies integrated operation system that combines waste disposal, biogas evacuation, and biogas control. The control concept in this research entails three parts: i) the control incorporated from the new configuration of the system that surrounds and captures all available biogas, ii) the control of the polymer medium that makes the gas move in least resistant path i.e. within the polymer medium, iii) the fuzzy logic control for evacuation-collection processes for available biogas that is being delivered for storage and utilization.

In this research a recyclable hydrophobic polymer medium (styrofoam) was tested at laboratory to check its functioning to work as a permeable medium for biogas collection and therefore the test procedure on polymer medium entailed the following findings: i) the permeability of polymer medium, ii) the conductivity and diffusion coefficients of carbon dioxide and methane within the polymer medium, iii) carbon dioxide and methane convective flow rate through polymer medium, iv) carbon dioxide and methane diffusive

flux through polymer medium, v) the influence of parameters such as water content, porosity, temperature, pressure gradient, concentration gradient on gas movement due to diffusion and convection.

The permeability test showed that the polymer medium (styrofoam) used in this research has the highest permeability since it had a minimal head loss due to high porosity (95 % air voids) and due to minimal water content (hydrophobic polymer medium). The polymer coefficient of permeability was obtained to equal 5.4×10^{-8} m^2. This coefficient shows that the polymer material is an excellent permeable medium for biogas collection.

The coefficient of diffusion of methane is higher 1.8 times than that of carbon dioxide at 15 °C. On the other hand the coefficient of conductivity of methane is less 2.3 times than that of carbon dioxide at 15 °C. In addition, as the temperature increases the coefficient of diffusion increases for both methane (from 0.17 to 0.19 cm^2/s) and carbon dioxide (from 0.09 to 0.11 cm^2/s) when the temperature increases from 0 °C to 25 °C. However as the temperature increases the coefficient of conductivity decreases for both methane (from 4 to 2.5 cm/s) and carbon dioxide (from 8 to 6 cm/s) when the temperature increases from 0 °C to 25 °C.

As the porosity of the polymer medium increases the coefficient of conductivity and diffusion increases. On the other hand, as the water content increases in the polymer medium, the coefficient of conductivity and diffusion decreases. For the hydrophobic polymer in this research, porosity is kept to the level of 95 % air voids. Water content

was minimal because of polymer hydrophobicity; the most important parameter was the temperature. The other important parameters are concentration gradient and pressure gradient for diffusion and convection respectively.

Temperature affects the coefficients of conductivity and diffusion. The temperature and the concentration gradient affect the biogas flux due to diffusion. The temperature and the pressure gradient affect the biogas flow due to convection. There is a higher biogas flow rate at lower temperatures when it is moving due to convection. On the contrary, there is a higher biogas flux at higher temperatures when it is moving due to diffusion. The average ratio of methane transport rate to carbon dioxide transport rate is 1.8 for diffusion and 1.3 for convection. The previously mentioned parameters are variable and bring the biogas transport in polymer to ambiguity.

Biogas modeling is complex process in the landfill. Major part of biogas modeling done in the past depended on empirical modeling that needed many parameters. These models are classical formulas and have complicated procedures. The complexity of the biogas transport in porous media in landfill can be solved using natural language that takes the real data to the flexible artificial computing.

Fuzzy logic was able to model ambiguous methane and carbon dioxide transport in the hydrophobic medium. The author successfully adapted fuzzy logic to integrated multi inputs (temperature and concentration gradient) and multi outputs (diffusion of methane and carbon dioxide) in one model and multi inputs (temperature and pressure gradient)

and multi outputs (convection of methane and carbon dioxide) in second model. This approach was impossible using classical modeling procedures. Results obtained in this work showed more than 99% correlation between experimental and fuzzy modeled data for methane and carbon dioxide transport via convection and diffusion in porous hydrophobic polymer medium.

Genetic algorithm was successfully used to optimize a transfer function that represents solutions for biogases mixture transfer rates. From transfer rates, mass and volume of biogases, within the landfill time of service, are determined for design of the polymer of QEJ bricks for any ratio of biogas.

Intelligent Fuzzy control system has been successfully applied for biogas collection processes. Biogas is being evacuated from the porous medium to storage and utilization, the process of evacuation is linked to valves that are connected to blowers. The valves are controlled by fuzzy logic system that is fed by meters-data acquisition system. The output of automatic intelligent fuzzy system is dependent on the input data from the meters-data acquisition system.

8.2. Research Contributions

This research fruitfully contributed to the domain of waste management and biogas transport in porous media. This research developed the following:

- New waste management and operation system;
- Application of new hydrophobic material medium for biogas collection;

- New landfill construction design.

This research work contributed to:

- Finding the conductivity coefficient of carbon dioxide and methane within hydrophobic porous polymer medium;
- Finding the diffusion coefficient of carbon dioxide and methane within hydrophobic porous polymer medium;
- Finding the carbon dioxide and methane convective flow rate through hydrophobic porous polymer medium;
- Finding the carbon dioxide and methane diffusive flux through hydrophobic porous polymer medium;
- Finding the influence of parameters (temperature, water content, porosity, concentration gradient, and pressure gradient) on gas movement (diffusion and convection) in polymer medium.

This research integrated a novel approach by applying:

- Intelligent fuzzy automatic control system for biogas evacuation;
- Genetic algorithm to optimize multi-biogas transfer rates required for hydrophobic bricks design in landfill;
- Recyclable hydrophobic polymer into environmental design.

8.3. Recommendations and the Future Work

The recommendations and future work can be summarized in the following points:

- Performing experimental tests of permeability, conductivity, and diffusion on biogas transport in different hydrophobic composites and for various technical parameters;
- Conducting tests of mechanical properties of hydrophobic polymer;
- Testing the polymer longevity;
- Testing Intelligent QEJ Bricks system in a pilot scale or in the field;
- Investigating prospective advantages of Intelligent QEJ Bricks.

REFERENCES

Adams R.S, Ellis R. (1969). Some Physical and Chemical Changes in the Soil Brought about by Saturation with Natural Gas. In Proc. Soil Sci. Soc. Am. 24: 41-44

Agren G.I. (1985). Limits to Plant Production. Journal of Theoretical Biology 113: 89-92

Andreottola G., Cossu R. (1988). Mathematical Model of Biogas Production. Rifituti Solidi 2 (6): 473

Anthony C. (1986). Bacterial Oxidation Of Methane And Methanol. Adv. Microb. Physiol. 27: 113-209

Arp, W.J., Drake, B.G., Pockman, W.T., Curtis, P.S, Whigham, D.F. (1993). Interactions between C_3 and C_4 Salt Marsh Plant Species during Four Years of Exposure to Elevated Atmospheric CO_2. Vegetatio 104: 133-143

ATSDR- Agency for Toxic Substances and Disease Registry (2001). Landfill Gas Primer- An Overview for Environmental Health Professionals. Department of Health and Human Services, Atlanta, U.S

Aubertin M., Aachib M., Authier K. (2000). Evaluation of Diffusive Gas Flux through Covers with a GCL. Geotextiles and Geomembranes 18: 215-233

Augenstein D., Pacey J. (1991). Modeling landfill Methane Generation. Proceedings Sardinia 91. Third international landfill Symposium, CISA Publisher, Cagliari, Sardinia

Augustein D., Yazdani R, Moore R., Dahl K. (1997). Yolo County Controlled Landfill Demonstration Project. Proceedings from the 2nd Annual Landfill Symposium, the Solid Waste Association of North America 3 – 39

Baath E. (1989). Effects of Heavy Metals in Soil on Microbial Processes and Populations (a review). Water Air Soil Pollut. 47: 335-379

Babich H., Stozky G. (1980). Environmental Factors that Influence the Toxicity of Heavy Metals and Gaseous Pollutants to Microorganisms. CRC Crit. Rev. Microbiol 8: 99-145

Bagchi A. (2004). Design of Landfills and Integrated Solid Waste Managenment. 3rd Ed. John Wiley & Sons Inc. NJ, USA

Bagchi A. (1994). Design, Construction, and Monitoring of Landfills. 2nd Ed. John Wiley & Sons Inc. NY, USA

Baggsa E.M., Blum H. (2004). CH_4 Oxidation and Emissions of CH_4 and N_2O from Lolium Perenne Swards under Elevated Atmospheric CO_2. Soil Biology & Biochemistry 36: 713–723

Bailey J.E., Ollis D.F. (1986). Biochemical Engineering Fundamentals. 2nd Ed. McGraw-Hill Book Company, New York

Baille M, Romero AR., Baille A. (1996). Gas-Exchange Responses of Rose Plants to CO_2 Enrichment and Light. Journal of Horticultural Science, 71 (6): 945–956

Balazinski M., Jemielniak K. (1998). Tool Conditions Monitoring Using Fuzzy Decision Support Systems. Proceeding of 5th International Conference on Monitoring and Automatic Supervision in Manufacturing, Warsaw, Poland pp. 115-122

Balazinski M., Achiche S., Baron L., (2000). Influences of Optimization and Selection Criteria on Genetically-Generated Fuzzy Knowledge Bases, (CAMT2000), Proceeding of International Conference on Advanced Manufacturing Technology, Johor Bahru, Malaysia pp. 159-164

Bardossy, A., & Duckstein, L. (1993). The Use of Fuzzy Rules for the Description of Natural Systems. In Proceedings of First European Congress on Fuzzy and Intelligent Technology. Aachen: Verlag Mainz, Wissenschaftsverlag.

Baron L. (1998). Genetic Algorithm for Line Extraction, Rapport Technique EPM/RT-98/06, École Polytechnique de Montréal

Barta TM., Hanson RS. (1993). Genetics of Methane and Methanol Oxidation in Gram-Negative Methylotrophic Bacteria. Antonie Van Leeuwenhoek 64:109–120

Bear J. (1972). Dynamics of Fluids in Porous Media. American Elsevier, NY, U.S.A

Bender M., Conrad R. (1992). Kinetics of CH_4 Oxidation in Oxic Soils Exposed to Ambient Air or High CH_4 Mixing Ratios. FEMS Microbiol. Ecol. 101:261-270

Bender M., Conrad R. (1994). Microbial Oxidation of Methane, Ammonium, Carbon Monooxide, and Turnover of Nitrous Oxide and Nitric Oxide in Soils. Biogeochemistry 27:97-112

Boeckx P., Van Cleemput O. (1996). Methane Oxidation in a Neutral Landfill Cover Soil: Influence of Moisture Content, Temperature, and Nitrogen Turnover. J. Environ. Qual. 25:178-183

Boeckx P., Van Cleemput O., Villaralvo I. (1996). Methane Emission from a Landfill and the Methane Oxidizing Capacity of Its Covering Soil. Soil Biol. Biochem. 28:1397-1405

Bogner J., Spokas K., Burton E.A. (1997). Kinetics of Methane Oxidation in a Landfill Cover Soil: Temporal Variations, a Whole-Landfill Oxidation Experiment, and Modeling of Net CH_4 Emissions. Environ. Sci. Technol. 31:2504-2514

Bogner J., Spokas K., Burton E., Sweeney R., Corona V. (1995). Landfills as Atmospheric Methane Sources and Sinks. Chemosphere. 31:4119-4130

Bonan G.B., Pollard D., Thompson S.L., (1992). Effects of Boreal Forest Vegetation on Global Climate. Nature 359: 716-718

Bonde A., (2000). Fuzzy Logic Basics, GTE Government Systems Corp, Needham, MA02194, (retrieved 2002) on the *World Wide Web at URL: http://www.austinlinks.com/Fuzzy/basics.html*

Börjesson G., Svensson B.H. (1997). Seasonal and Diurnal Methane Emissions from a Landfill and Their Regulation by Methane Oxidation. *Waste Manage. Res.* 15:33-54

Borri Dino, Concilio Grazia, and Conte Emilia (1998). A Fuzzy Approach for Modeling Knowledge In Environmental Systems Evaluation. Comput., Environ. And Urban Systems, Vol. 22, No. 3, Pp 299-313

Bouazza Abdelmalek, and Vangpaisal Thaveesak (2003). An apparatus to measure gas permeability of geosynthetic clay liners. Geotextiles and Geomembranes 21: 85–101

Bowden RD., Newkirk, KM., Rullo GM. (1998). Carbon Dioxide and Methane Fluxes by a Forest Soil under Laboratory-Controlled Moisture and Temperature Conditions, Soil Biol. Biochem. 30 (12): 1591-1597

Burrows KJ, Cornish A, Scott D, Higgins IJ (1984). Substrate Specificities of the Soluble and Particulate Methane Mono-Oxygenases of Methylosinus Trichosporium OB3b. J Gen Microbiol 130: 3327–3333

Cannell M.G.R., Milne R., Sheppard L.J., Unsworth M.H., (1987). Radiation Interception and Productivity of Willow. Journal of Applied Ecology 24: 261-278

Carman P.C. (1956). Flow of Gases through Porous Media. Academic Press, New York, 182p

Castro M. S., Melillo J. M., Steudler P. A., Chapman J. W. (1994). Soil Moisture as a Predictor of Methane Uptake by Temperate Forest Soils. Canadian Journal of Forest Research 24: 1805-1810

Castro M. S., Steudler P. A., Melillo J. M., Aber J. D., Bowden R. D. (1995). Factors Controlling Atmospheric Methane Consumption by Temperate Forest Soils. Global Biogeochemical Cycles 9: 1-10

Chan G.Y.S., Chu L.M., Wong M.H. (2002). Effects of Leachate Recirculation on Biogas Production from Landfill Co-Disposal of Municipal Solid Waste, Sewage Sludge and Marine Sediment. Environmental Pollution.118: 393–399

Chan G.Y.S., Chu L.M., Wong M.H. (1997). Influence of Landfill Factors On Plants and Soil Fauna an Ecological Perspective. Environmental Pollution. 97 (1-2): 39-44

Chen D.X., Coughenour M.B., Eberts D., Thullen J.S. (1994). Interactive Effects of CO_2 Enrichment and Temperature on the Growth of Dioecious Hydrilla Verticillata. Environ. Exp. Bot. 34: 345-353

Christophersen M., Linderød L., Jensen PE. (2000). Methane Oxidation at Low Temperatures in Soil Exposed to Landfill Gas. Journal of Environmental Quality 29 (6): 1989-97

Chugh S., Clarke W., Pullammanappallil P., Rudolph V. (1998). Effect of Recirculated Leachate Volume on MWS Degradation. Waste Management and Research 16: 564–573

Coleman J.S., Bazzaz F.A., (1992). The Effects of CO_2 and Temperature on Growth and Resource Use of Co-Occurring C_3 and C_4 Annuals. Ecology 73: 1244-1259

Coughenour M.B., Chen D.X. (1997). An Assessment of Grassland Ecosystem Responses to Atmospheric Change Using Linked Ecophysiological and Soil Process Models. Ecological Applications 7: 802-827

Crank J. (1975). The Mathematics of Diffusion, 2nd Edition. Clarendon Press, Oxford, UK.

Cure J.D., (1985). Carbon dioxide doubling responses: a crop survey. In: B.R. Strain and J.D. Cure (Editors), Direct Effects of Increasing Carbon Dioxide on Vegetation. U.S. Department of Energy, Washington, DC, pp. 99-116.

Cureton P.M., Groenvelt P.H., McBride R.A. (1991). Landfill Leachate Recirculation: Effects on Vegetation Vigour and Clay Surface Cover Infiltration. Journal of Environmental Quality 20: 17–24

Czepiel P.M., Mosher B., Crill P. M., Harris R. C. (1996). Quantifying the Effect of Oxidation on Landfill Methane Emissions. J. Geophys. 101:16721-16729

DeLucia EH., Hamilton JG., Naidu SL., Thomas RB., Andrews JA., Finzi A., Lavine M., Matamala R., Mohan JE., Hendrey GR. (1999). Net Primary Production of a Forest Ecosystem with Experimental CO_2 Enrichment. Science 284:1177-1179

Diamadopoulous E. (1994). Characterization and Treatment of Recirculation- Stabilized Leachate. Water Research. 28: 2439–2445

Didier G., Bouazza A., Cazaux D. (2000). Gas Permeability of Geosynthetic Clay Liners. Geotextiles and Geomembranes 18: 235-250

Dunfield P., Knowles R., Dumont R., Moore T.R. (1993). Methane Production and Consumption in Temperate and Subartic Peat Soils: Response to Temperature and pH. Soil Biol. Biochem. 25:321-326

Duxbury J.M. (1994). The Significance of Agricultural Sources of Greenhouse Gases. Fertilizer Research 38: 151-163

Elektorowicz M., Qasaimeh A. (2004). Fuzzy Modeling Estimation of Mercury Removal by Wetland Components. Fuzzy Information Processing NAFIPS '04, IEEE Annual Meeting. 1:37- 40

Elektorowicz M., Balazinski M., Qasaimeh A. (2003). Assessment of the Capacity of Metal Sorption to Sediments of Natural Systems Using Fuzzy Knowledge, Proceeding of CSCE Canadian Society for Civil Engineering 31st Annual Conference, Moncton, NB, Canada

Elektorowicz M., Balazinski M., Qasaimeh A., (2002). Application of the Artificial Intelligence to Estimate the Constructed Wetland Response to Heavy Metal Removal. Proceedings of Joint CSCE/ASCE International Conference on Environmental Engineering, Niagara Falls, ON, Canada

El-Fadel, M., Findikakis, A., Leckie, J., (1989). A Numerical Model for Methane Production in Managed Sanitary Landfills. Waste Manage. Res. 7: 31-42

El-Fadel M. (1991). Modeling Gas and Heat Generation and Transport in Sanitary Landfills. PhD Thesis, UMI Dissertation Services

El-Fadel M., Findikakis A., Leckie J. (1996). Numerical Modeling of Generation and Transport of Gas and Heat in Landfills I. Model Formulation, Waste Management & Research 14: 483–504

El-Fadel M. (1999). Leachate Recirculation Effects on Settlement and Biodegradation Rates in MSW Landfills. Environmental Technology. 20: 121–133

EMCON Associates (1980). Methane Generation and Recovery from Landfills. Ann Arbor, MI: Ann Arbor Science Publishers.

Engineered Textile Products, ETP Inc. (2004). Biogas Collection Covers. Retrieved 2004 on the World Wide Web at URL: http://www.etpinfo.com/biogas.htm

Enoch H Z. (1990). Crop Response to Aerial Carbon Dioxide. Acta Horticulturae 268: 17–32

EPA (1991). U. S. Environmental Protection Agency. Air Emissions from Municipal Solid Waste Landfills: Background Information for Proposed Standards and Guidelines. EPA-450/3-90/011a. March 1991

Fierro A., Tremblay N., Gosselin A. (1993). CO_2 Enrichment and Supplementary Lighting Improve Growth and Yield of Tomato and Pepper Transplants. HortScience 29 (3): 152-154

Findikakis, A., Leckie, J., (1979). Numerical Simulation of Gas Flow in Sanitary Landfills. J. Environ Eng. 115: 927-945

Fox P. (1996) Landfill Cover Systems in the United States. In Alternative Dichtungsmaterialien im Deponiebau und in der Altlastensicherung, Burkhardt & Egloffstein (Eds), Schriftenreihe Angew. Geol. Karlsruhe 41: 2.1-2.24

Fredlund D.G., Rahardjo H., (1993). Soils Mechanics for Unsaturated Soils. Wiley-Interscience Publication. 517 pp.

Galloway J.N., Schlesinger W.H., Levy H., Michaels A., Schnoor J.L. (1995). Nitrogen Fixation: Anthropogenic Enhancement-Environmental Response. Global Biogeochemical Cycles 9: 235-252

Gardner, N., B. Manley and J. Pearson. (1993). "Gas Emission from Landfills and their Contributions to Global Warming". Applied Energy, 44:165-174.

Gen M., Cheng R. (1997). Genetic Algorithms and Engineering Design. Wiley, New York.

Geomembrane Technologies Inc. GTI, (2004). Gas Collection Cover Systems, Retrieved 2004 on the World Wide Web at URL: http://www.adi.ca/GTI/floatingcovers.html

Geosyntec Consultants (1998a). Guidance Manual – Tire Shreds As Gas Collection Material At Municipal Solid Waste Landfills, Prepared For The California Integrated Waste Management Board

Geosyntec Consultants (1998b). Test Pad Demonstration Program – Tire Shreds As Cover Foundation, Leachate Drainage, and Operations Layer Material at Municipal Solid Waste Landfills, Prepared For the California Integrated Waste Management Board

Green J., Prior SD., Dalton H. (1985). Copper Ions as Inhibitors of Protein C of Soluble Methane Monooxygenase of Methylococcus Capsulatus (Bath). Eur J Biochem 153:137-144

Groffman P. M., Gold A. J., Simmons R. C. (1992). Nitrate Dynamics in Riparian Forests: Microbial Studies. Journal of Environmental Quality 21: 666-671

Gulley N., Roger J. S. (1995). Fuzzy Logic Toolbox User's Guide, The Mathworks, Inc., Natick, Mass., USA

Hand DW. (1984). Crop Response to Winter and Summer CO_2 Enrichment. Acta Horticulturae 162: 45–64

Hanson R. S., Hanson T. E. (1996). Methanotrophic bacteria. Microbiol. Rev. 60: 439-471

Hellebrand H. J., Scholz V. (2000): Influence of Plants and Fertilisation Level on the Microbial Uptake of Methane in Soils. In: Abstracts 272 und P5101 (CD-ROM XIV) of *Memorial CIGR World Congress 2000*, Tsukuba, Japan

Hillel D., (1980). Fundamentals of Soil Physics. Academic Press, New York

Holland J. (1975). Adaptation in Natural and Artificial Systems. The University of Michigan Press, Ann Arbor

Houghton J.T., Filho L.G.M., Callandar B.A., Harriss N., Kattenberg A., Maskell K., (1996). Technical Summary. *In*: Houghton J.T., Filho L.G.M., Callandar B.A., Harriss N., Kattenberg A., Maskell K. (Eds.), Climate Change (1995). The Science of Climate Change. Cambridge University Press, Cambridge, pp. 1-49

Houghton J.T., Jenkins G.J., Ephraumas J.J. (1990). Climate Change - The PCC Scientific Assessment. Cambridge Univ. Press. Cambridge

Hutsch B.W. (1998). Methane Oxidation in Arable Soil as Inhibited by Ammonium, Nitrite and Organic Manure with Respect to Soil pH. Biology and Fertility of Soils 28: 27–35

Huber A., Wohnlich S. (1999). Gas Collection Layers. Proceedings Sardinia 99, Seventh International Waste Management and Landfill Symposium S. Margherita Di Pula, Cagliari, Italy

Hunt H.W., Trlica M.J., Redente E.F., Moore J.C., Delting J.K., Kittel T.G.F., Walter D.E., Fowler M.C., Klein D.A., Elliott E.T. (1991). Simulation Model for the Effects of Climate Change on Temperate Grassland Ecosystems. Ecol. Model. 53: 205-246

Isebrands JG., Karnosky DF. (2001). Environmental Benefits of Poplar Culture. In: Dickmann DI., Isebrands JG., Eckenwalder JE., Richardson J. editors. Poplar Culture in North America. Ottawa, Ontario, Canada: NRC Research Press; p. 207–218

Jaffrin A., Bentounes N., Joan A.M., Makhlouf S. (2003). Landfill Biogas for heating Greenhouses and providing Carbon Dioxide Supplement for Plant Growth, Biosystems Engineering 86 (1): 113–123

Jahng D., Wood T. K. (1996). Metal Ions and Chloramphenicol Inhibition of Soluble Methane Monooxygenase from Methylosinus Trichosporium OB3b, Appl. Microbiol. Biotechnol. 45:744–749

Jaques, A., F. Neitzert, P. Boileau (1997). Trends in Canada's Greenhouse Gas Emissions (1990- 1995). Pollution Data Branch, Air Pollution Prevention Directorate, Environment Canada, April 1997.

Jia-ying Xin, Jun-ru Cui, Jian-zhong Niu, Shao-feng Hua, Chun-gu Xia, Shu-ben Li, Li-min Zhu (2004). Production of Methanol from Methane by Methanotrophic Bacteria, Biocatalysis and Biotransformation 22 (3): 225-229

Jones H.A., Nedwell D.B. (1993). Methane Emission and Methane Oxidation in Landfill Cover Soil. FEMS Microbiol. Ecol. 102:185-195

Kalaykov I. (2000). From Numbers to Fuzzy Values – the Direct Jump. Proceeding of ESIT 2000, Aachen, Germany pp. 201-206

Kantrowitz M., Horstkotte E., Joslyn C. (1993). Fuzzy Logic/Part1, What is a Fuzzy Expert System, retrieved 2002 on the World Wide Web at URL: http://www-2.cs.cmu.edu/Groups/AI/html/faqs/ai/fuzzy/part1/faq-doc-4.html

Kartalopoulos S. V., (1996). Understanding Neural Networks and Fuzzy Logic: Basic Concepts and Applications. IEEE Press, the Institute of Electrical and Electronics Engineers, Inc., New York, USA

Keeling C.D., Bacastow R.B., Whorf T.P. (1982). Measurements of the Concentration of Carbon Dioxide at Maunaloa Observatory, Hawaii, p 377-385. In W.C. Clark (ed.) Carbon dioxide review. Oxford University Press, New York.

Kightley D., Nedwell D.B., Cooper M. (1995). Capacity for Methane Oxidation in Landfill Cover Soils Measured in Laboratory-Scale Microcosms. Appl. Environ. Microbiol. 61: 592-601

Kimball B.A. (1983). Carbon Dioxide and Agricultural Yield: An Assemblage and Analysis of 430 Prior Observations. Agron. J. 75:779-788

Kimball B.A. (1997). Influence of Increasing CO_2 Concentration on Photosynthetic Stimulation of Selected Weeds. Photosynth. Res. 54: 199-208

King G. M. (1992). Ecological Aspects of Methane Oxidation, a Key Determinant of Global Methane Dynamics, p. 431–468. *In* K. C. Marshall (ed.), Advances in Microbial Ecology. Plenum Press, New York, N.Y.

King, G.M., and P.S. Adamsen. (1992). Effect of Temperature on Methane Consumption in a Forest Soil and in Pure Cultures of the Methanotroph Methylomonas Rubra. Appl. Environ. Microbiol. 58:2758-2763

King, G.M., Schnell, S., (1994). Effect of Increasing Atmospheric Methane Concentration on Ammonium Inhibition of Soil Methane Consumption. Nature 370: 282-284

Kinman, R.N., Nutini, D.L., Walsh, J.J., Vogt, W.G., Stamm, J., Rickabaugh, J., (1987). Gas Enhancement Techniques in Landfill Simulators. Waste Management and Research 5: 13–25

Klir, George J., Ute H. St.Clair and Bo Yuan (1997). Fuzzy Set Theory, Prentice Hall, Upper Saddle River, NJ

Kravchenko, I., Boeckx, P., Galchenko, V., Van Cleemput, O., (2002). Short- and Medium-Term Effects of NH_4 on CH_4 and N_2O Fluxes in Arable Soils with a Different Texture. Soil Biology and Biochemistry 34: 669-678

Kriofske, K., Poly-Flex, Inc., Grand Prairie, Tx. (1998). The Use of Polyethylene Geomembranes in Lining and Gas Collection Covers for Manure Lagoons, Manure Management Conference Proceedings, Ames, Iowa. Retrieved 2004 on the World Wide Web at URL:
http://www.ctic.purdue.edu/Core4/Nutrient/ManureMgmt/Paper102.html

Kumaraswamy, S., Ramakrishnan, B., Sethunathan, N. (2001). Methane Production and Oxidation in an Anoxic Rice Soil as Influenced by Inorganic Redox Species, J. Environ. Qual. 30:2195–2201

LaDeau SL., Clark JS. (2001). Rising CO_2 Levels and the Fecundity of Forest Trees. Science 292:95-98

Lang, R., Tchobanoglus, G., (1989). Modeling Emissions of Trace Gases from Landfills. 82nd Annual Meeting and Exhibition, Anaheim, pp. 1-14

Le Mer, J., Roger, P., (2001). Production, Oxidation, Emission and Consumption of Methane by Soils: A Review. European Journal of Soil Biology 37: 25–50

Leach, A. (1990) Landfill gas abstraction, Proceedings of International Conference on Landfill Gas: Energy and Environment 90, Bournemouth, U.K. pp. 204–222

Lee TD., Tjoelker MG., Ellsworth DS., Reich PB. (2001). Leaf Gas Exchange Responses of 13 Prairie Grassland Species to Elevated CO_2 and Increased Nitrogen Supply. New Phytol. 150:405-418

Leita, L., De Nobil M., Muhlbachova, G., Mondini, C., Marchiol, L., and Zerbi, G. (1995). Bioavailability and Effects of Heavy Metals on Soil Microbial Biomass Survival during Laboratory Incubation. Biol. Fertil. Soils. 19: 103-108

Lemna Technologies Inc. (2004). Gas Collection Cover, Retrieved 2004 on the World Wide Web at URL:
http://www.lemnatechnologies.com/supportpages/products/gasCollectionCovers.htm

Lemos S., Yuan H., Collins M., Antholine W. (2002). Review of Multifrequency EPR of Copper in Particulate Methane Monooxygenase. Current Topics in Biophysics 26(1): 43-48

Lessard R., Rochette P., Topp E., Pattey E., Desjardins R. L. and Beaumont G. (1994) Methane and Carbon Dioxide Fluxes from Poorly Drained Adjacent Cultivated and Forest Sites. *Canadian Journal of Soil Science* 73, 139-146

Lindhout, P. and G. Pet. (1990). Effects of CO_2 Enrichment on Young Plant Growth of 96 Genotypes of Tomato *(Lycopersicon Esculentum).* Euphytica 51(2): 191-196

Los Angeles County Sanitation Districts (2005). Retrived (2006) on URL web: http://www.lacsd.org

Luxmoore R.J., Norby R.J., O'Neill E.G. (1986). Seedling Tree Responses to Nutrient Stress Under Atmospheric CO_2 Enrichment. 18th IUFRO World Congr. Forest Plants and Forest Protection. Div. 2. 1:178-183

Manley, B. (1997) Landfill Gas Control and Utilisation in the UK - The Next Ten Years. In Neue Aspekte bei der Deponiegasnutzung. Rettenberger & Stegmann (Eds), Trierer Berichte zur Abfallwirtschaft, Economica, Bonn 11: 98-109

Manna, L., Zanetti, M., Genon, G. (1999). Modeling Biogas Production at Landfill Site. Resources Conservation and Recycling 26: 1-14
Marshall, T.J. (1959). The Diffusion of Gases through Porous Media. J. Soil. Sci. 10:79–82

Matthews, E., (1994). Nitrogenous Fertilizers: Global Distribution of Consumption and Associated Emissions of Nitrous Oxide and Ammonia. Global Biogeochemical Cycles 8: 411-439

Maurice, C., Ettala, M., Lagerkvist, A. (1999). Effects of Leachate Irrigation on Landfill Vegetation and Subsequent Methane Emissions. Water, Air, and Soil Pollution. 113: 203–216

McBean E., Rovers F., Farquhar G. (1995). Solid Waste Landfill Engineering and Design, Prentice Hall PTR, NJ, USA

McCarty, P., (1965). Thermodynamics of Biological Synthesis and Growth. Proceedings of Second International Water Pollution Research Conference, New York. Pergamon Press: 169-187

McCarty, P., Tong, X., Smith, L., and Bae, J., (1986). Mechanisms of Bacterial Hydrolysis of Lignocellulosic Materials. Draft Annual Report, Contract No. PL-86-1, Department of Civil Eng., Stanford University, CA, U.S.A.

McGrath and Masonnn (2004). An Observational Method for the Assessment of Biogas Production from an Anaerobic Waste Stabilization Pond treating Farm Dairy Wastewater. Biosystems Engineering 87 (4): 471–478

Metcalfe, D., Farquhar, G., (1987). Modeling Gas Migration through Soils from Waste Disposal Sites. Water, Air, Soil Pollut. 32: 247-259

Mishra, S. R., Bharati, K., Sethunathan, N., and Adhya, T. K. (1999). Effects of Heavy Metals on Methane Production in Tropical Rice Soils. Ecotoxicol. Environ. Saf. 44: 129-136

Mohanty, S. R., K. Bharati, N. Deepa, V. R. Rao, and T. K. Adhya (2000). Influence of Heavy Metals on Methane Oxidation in Tropical Rice Soils. Ecotoxicology and Environmental Safety. 47: 277-284

Mohsen, M., Farquhar, G., Kouwen, N., (1980). Gas Migration and Vent Design at Landfill Sites. Water, Air, Soil Pollut. 13: 79-97

Moldrup P., Olesen T., Gamst J., Schjonning P., Yamaguchi T., Rolston D.E. (2000). Predicting the Gas Diffusion Coefficient in Repacked Soil: Water-Induced Linear Reduction Model. Soil Sci. Soc. Am. J. 64:1588–1594

Moore, C., Rai, I., Alzaydi, A., (1979). Methane Migration around Sanitary Landfills. J. Geotech. Eng. Div. 2: 131-144

Mortensen, L.M. (1987). Review: CO_2 enrichment in greenhouses. Crop Responses. Scientia Hort. 33:1-25

Mostafa, A.W., Walied, Z., Neeraj, G., (1999). Effect of Leachate Recirculation on Municipal Solid Waste Biodegradation. Journal of Canada Water Quality Research. 34: 267–280

Murrell JC., McDonald IR., Gilbert B. (2000). Regulation of Expression of Methane Monooxygenases by Copper Ions. Trends Microbiol. 8: 221-225

Nastev, M., Therrien, Lefebvre, R., and Gélinas, P. (2001). Gas Production and Migration in Landfills and Geological Materials. Journal of Contaminant Hydrology 52: 187-211

Nguyen H., Shiemke AK., Jacobs SJ., Hales BJ., Lidstrom ME., Chan SI. (1994). The Nature of The Copper Ions in The Membranes Containing the Particulate Methane Monooxygenase from *Methylococcus Capsulatus* (Bath). Jour. Biol Chem 269: 14995-15005

Nielsen AK., Gerdes K., Murrell JC. (1997). Copper-Dependent Reciprocal Transcriptional Regulation of Methane Monooxygenase Genes in Methylococcus Capsulatus and Methylosinus Trichosporium. Mol. Microbiol. 25: 399-409

Niklaus PA., Wohlfender M., Siegwolf R., Krner C. (2001). Effects of Six Years of Atmospheric CO_2 Enrichment on Plant, Soil and Soil Microbial C of a Calcareous Grassland. Plant Soil 233:189-202

Nozhevnikova A., Lifshitz A.B., Lebedev V.S., Zavarzin G.A. (1993). Emission of Methane into the Atmosphere from Landfills in the Former USSR. Chemosphere 26:401-417

Oren R., Ellsworth DS., Johnsen KH., Phillips N., Ewers BE., Maler C., Schafer KVR., McCarthy H., Hendrey G., McNulty SG. (2001). Soil Fertility Limits Carbon Sequestration by Forest Ecosystems in a CO_2 -Enriched Atmosphere. Nature 411:469-472

Pacey, J. (1986). "Factors Influencing Landfill Gas Production". Proceeding of Joint UK/US Engineering Conference. Solihull, 28-31 October: 51-59.

Paradise C. J., Cyr R. J. (1995). Carbon Dioxide Uptake in Plants: A Computer-Aided Experimental System I*n:* Tested studies for laboratory teaching, 16: 99–114 (C. A. Goldman, Editor). Proceedings of the 16th Workshop/Conference of the Association for Biology Laboratory Education (ABLE), 273 pages.

Park, J. and Shin, H. (2001). Surface Emission of Landfill Gas from Solid Waste Landfill, Atmosphere Environment 35: 3445-3451

Pearce, B. (1993). Evaluating Land Use Planning: The Importance of Impact Research. In A. Khakee, K. Eckerberg (Eds.). Process & Policy Evaluation in Structure Planning, (pp. 132-148). Stockholm: Byggforskningsradet.

Permavoid Ltd (2002). Virtual Curtain System retrieved 2006 at: http://www.virtual-curtain.com/index.htm

Peter John W. J., Melillo J. M., Steudler P. A., Newkirk K. M., Bowles F. P. and Aber J. D. (1994). Responses of Trace Gas Fluxes and N Availability to Experimentally Elevated Soil Temperatures. Ecological Applications 4: 617-625

Phelps PA., Agarwal SK., Speitel GE., Georgiou G. (1992). Methylosinus Trichosporium OB3b Mutants Having Constitutive Expression of Soluble Methane Monooxygenase in The Presence of High Levels of Copper. Appl. Environ. Microbiol. 58:3701-3708

Popov, V., and Power, H., (1999). DRM-MD Approach for the Numerical Solution of Gas Flow in Porous Media, with Application to Landfill. Engineering Analysis with Boundary Elements 23: 175-188

Prather, M., Derwent, R., Ehalt, D., Fraser, P., Sanhueza, E., Zhau, X., (1996). Other Trace Gases and Atmospheric Chemistry. In: Houghton, J.T., Filho, L.G.M., Callandar, B.A., Harriss, N., Kattenberg, A., Maskell, K. (Eds.), Climate Change 1995. The Science of Climate Change. Cambridge University Press, Cambridge, pp. 77-126.

Priemé, A., and S. Christensen. (1997). Seasonal and Spatial Variation of Methane Oxidation in a Danish Spruce Forest. Soil Biol. Biochem. 29:1165-1172

Qasaimeh A. (2003). Application of the Artificial Intelligence to the Design of Constructed Wetlands for Heavy Metal Removal, M.A.Sc. Thesis, Concordia University, Canada

Qasaimeh Ahmad, Elektorowicz Maria, Jasiuk Iwona (2006a). Investigation and Fuzzy Regime for Biogas Transport in Hydrophobic Permeable Polymer. North American Fuzzy Information Processing Society NAFIPS 2006, Montréal, Canada, June 3-6, 2006

Qasaimeh Ahmad, Elektorowicz Maria, and Jasiuk Iwona (2006b). Intelligent Fuzzy Control for Biogas in Hydrophobic Polymer System. International Symposium on Industrial Electronics ISIE 2006, ETS - Downtown Montréal, Canada, July 9-13, 2006

Radoglou K.M., Aphalo P., Jarvis P.G. (1992). Response of Photosynthesis, Stomatal Conductance and Water Use Efficiency to Elevated CO_2 and Nutrient Supply in Acclimated Seedlings of Phaseolus Vulgaris L. Ann. Bot. 70:257-264

Rechenberg, I. (1973). Evolutionsstrategie: Optimierung technischer Systeme nach Prinzipien der biologischen evolution ("Evolution Strategy: The Optimization of Technical Systems According to The Principles of Biological Evolution"). Stuttgart: Frommann-Holzboog Verlag.

Reible D. (1999). Fundamentals of Environmental Engineering. CRC Press LLC, Lewis Publishers USA

Reinhart, D.R., (1996). Full-scale Experience with Leachate Recirculating Landfills: Case Studies. Waste Management and Research. 14: 347-365

Reinhart, D.R., Al-Yousfi, A.B., (1996). The Impact of Leachate Recirculation on Municipal Solid Waste Landfill Operating Characteristics. Waste Management and Research. 14: 337-346

Richards, K. M., Aitchinson, E. M. (1990). Landfill Gas: Energy and Environmental Themes, Proceedings of the International Conference on Landfill Gas: Energy and Environment 90, Bournemouth, U.K., pp. 21–44.

Richards, L. A. (1931). Capillary Conduction of Liquids in Porous Mediums. Physics (1) 318

Roger Jang, J.-S. (1995). Chap 3: Fuzzy Rules and Fuzzy Reasoning (retrieved 2006) on the URL: http://www.cs.nthu.edu.tw/~jang

Ronald, S. P., (1994). Preserving Diversity in Routing Genetic Algorithms: Comparisons with Hash Tagging. Technical Report, The University of South Australia, Department of Computer and Information Science, Australia

Sasek, T.W., DeLucia, E.H., Strain, B.R. (1985). Reversibility of Photosynthetic Inhibition in Cotton after Long-Term Exposure to Elevated CO_2 Concentrations. Plant Physiol. 78(3): 619-622

Scanlon B., Nicot J., Massmann J. (2002). Soil Gas Movement in Unsaturated Systems. Soil Physics Companion. CRC Press LLC. pp 297- 341

Schachermayer, E., Baumeler, A., Kisliakova, A. (1999). Reduktion von Treibhausgasen durch Optimierung der Abfallwirtschaft. *Müll und Abfall* 2: 64-73

Scotford, I.M., Williams, A. G. (2001). Practicalities, Costs and Effectiveness of a Floating Plastic Cover to Reduce Ammonia Emissions from a Pig Slurry Lagoon. Jour. Agric. Engng Res. 80 (3): 273-281

Sellers, P.J., Hall, F.G., Margolis, H., Kelly, B., Baldocchi, D., den Hartog, G., Cihlar, J., Ryan, M., Goodison, B., Crill, P., Ranson, J., Lettenmaier, D., Wickland, D. (1995). Boreal Ecosystem Atmosphere Study (BOREAS): An Overview and Early Results from the 1994 Field Year. Bull. Am. Meteorol. Soc. 76: 1549-1577

Shekdar, A. V. (1997). A Strategy for the Development of Landfill Gas Technology in India. Waste Management & Research 15: 255-266

Sionit, N., Strain, B.R., Beckford, H.A. (1981). Environmental Controls on the Growth and Yield of Okra. I. Effects of Temperature and CO_2 Enrichment at Cool Temperatures. Crop Sci. 21: 855-888

Sitaula, B.K., Bakken, L.R., Abrahamsen, G., (1995). CH_4 Uptake by Temperate Forest Soil: Effect of N Input and Soil Acidification. Soil Biology and Biochemistry 27: 871-880

Smith DS., Huxman TE., Zitzer SF., Charlet TN., Housman DC., Coleman JS., Fenstermaker LK., Seemann JR., Nowak RS. (2000). Elevated CO_2 Increases Productivity and Invasive Species Success in an Arid Ecosystem. Nature 408:79-82

Soltani F. (1997). Etude de l'e'coulement de gaz a` travers les ge'osynthetiques bentonitiques utilise's en couverture des centres de stockage de de'chets. These de Doctorat. INSA Lyon, France

Sommerfeld, R.A., Mosier, A.R., Musselman, R.C. (1993). CO_2, CH_4 and N_2O Flux through a Wyoming Snowpack and Implications for Global Budgets. Nature 361:140-142

Stein, V. B., Hettiaratchi, J. P. A. (2001). Methane Oxidation in Three Alberta Soils: Influence of Soil Parameters and Methane Flux Rates. Journal of Environmental Technology 22: 101-111

Steinkamp R., Butterbach-Bahl K., Papen H. (2001). Methane Oxidation by Soils of an N Limited and N Fertilized Spruce Forest in the Black Forest, Germany. Soil Biology & Biochemistry 33: 145-153

Stephens D. (1996). Vadose Zone Hydrology. CRC Press Inc. Lewis Publishers USA

Steudler, P.A., Bowden, R.D., Melillo, J.M., Aber, J.D., (1989). Influence of Nitrogen Fertilization on Methane Uptake in Temperate Forest Soils. Nature 341: 314-316

Strain, B.R. and Bazzaz, F.A. (1983). Terrestrial Plant Communities. In: E.R. Lemon (Editor), CO_2 and Plants. AAAS Selected Symposia Series, Westview, Boulder, CO, pp. 177-222.

Strosher, M., (1996). Investigations of flare gas emissions in Alberta. Final report to: Enviornment Canada Conservation and Protection, Alberta Energy and Utilities Board, and Canadian Association of Petroleum Producers. Alberta Research Council, Canada

Sulisti, Watson-Craik I.A., Senior E., (1996). Studies on The Co-Disposal of O-Cresol with Municipal Refuse. Journal of Chemical Technology and Biotechnology. 65: 72–80

Sundh I., Borga P., Nilsson M., Svensson B. H. (1995a). Estimation of Cell Numbers of Methanotrophic Bacteria in Boreal Peatlands on Analysis of Specific Phospholipid Fatty Acids. FEMS Microbiol. Ecol. 18:103-112

Sundh, I., C. Mikkela, M. Nilsson, and B. H. Svensson. (1995b). Potential Aerobic Methane Oxidation in A Sphagnum-Dominated Peatland-Controlling Factors and Relation to Methane Emission. Soil Biol. Biochem. 27: 829–837

Takeguchi M., Okura I. (2000). Role of Iron and Copper in Particulate Methane Monooxygenase of *Methylosinus Trichosporium* OB3b. Catal. Surv. Jpn. 4: 51-13

Thomas J.F., C.D. Raper Jr., Anderson C.E., Downs R.J. (1975). Growth of Young Tobacco Plants as Affected By Carbon Dioxide and Nutrient Variables. Agron. Jour. 67:685-689

Tlustos, P., Willison, T.W., Baker, J.C., Murphy, D.V., Pavlikova, D., Goulding, K.W.T., Powlson, D.S. (1998). Short-Term Effects of Nitrogen on Methane Oxidation in Soils. Biology and Fertility of Soils 28: 64-70

Topp, E. and Hanson, R.S. (1991). "Methane Oxidizing Bacteria," in Microbial Production and Consumption of Greenhouse Gases: Methane, Nitrogen Oxides, and Halomethanes. John E. Rogers and William B. Whitman, Eds.; American Society for Microbiology, Washington D.C.

Topp, E., Pattey, E., (1997). Soils as Sources and Sinks for Atmospheric Methane. Canadian Journal of Soil Science 77: 167-178

Tremblay Nicolas and Gosselin André (1998). Effect of Carbon Dioxide Enrichment and Light, HortTechnology October-December 1998 8(4)

Tremblay N., Yelle S., Gosselin A. (1987). Effects of CO_2 Enrichment, Nitrogen and Phosphorus Fertilization during Transplant Production on Growth and Yield of Celery. HortScience 22(5): 875-876

Tuskan GA., Walsh ME. (2001). Short Rotation Woody Crop Systems, Atmospheric Carbon Dioxide, and Carbon Management: AUS Case Study. Forestry Chronicle 77(2): 259–64

United States Environmental Protection Agency. US EPA (1996). Turning a Liability into an Asset: A Landfill Gas-to- Energy Project Development Handbook. Washington: EPA.

Uprety, D.C., Dwivedi, N., Mohan, R. (1998). Characterization of CO_2 Responsiveness in a *Brassica Oxycamp* Interspecific Hybrid. J. Agron. and Crop Sci. 180: 7-13

Uprety, D.C., Dwivedi, N., Jain, V., Mohan., R. (2002). Effect of Elevated Carbon Dioxide on the Stomatal Parameters of Rice Cultivars. Photosynthetica 40 (2): 315-319

Uprety, D.C., Garg, S.C., Tiwari, M.K., Mitra, A.P. (2000a). Crop Responses to Elevated CO_2: Technology and Research (Indian Studies). Global Environ. Res. (Japan). 3(2): 155-167

Uprety, D.C., Kumari, S., Dwivedi, N., Mohan, R. (2000b). Effect of Elevated CO_2 on the Growth and Yield of Rice Variety 'Pusa 834'. Ind. Jour. Pl. Physiol. 5 (1): 105-107

Uprety, D.C., Mishra, R.S., Abrol, Y.P. (1995). Effect of Elevated CO_2 and Moisture Stress on the Photosynthesis and Water Relation in *Brassica* Species. Jour. Agron. and Crop Sci. (Germany) 175: 231-237

Urban L. (1994). Effect of High-Pressure Mist and Daytime Continuous CO_2 Enrichment on Leaf Diffusive Conductance, CO_2 Fixation and Production of Rosa Hybrida Plants Grown on Rockwool. Acta Horticulturae 361: 317–324

Valsaraj, K., (1995). Elements of Environmental Engineering: Thermodynamics and Kinetics. Lewis Publishers, CRC Press, Inc. USA

Van Der Nat F., De Brouwer J., Middelburg J., Laanbroek H. (1997). Spatial Distribution and Inhibition by Ammonium of Methane Oxidation in Intertidal Freshwater Marshes. Applied and Environmental Microbiology 63 (12): 4734-4740

Wand S., Midgley G., Jones M., Curtis P. (1999). Responses of Wild C_4 and C_3 Grass (Poaceae) Species to Elevated Atmospheric CO_2 Concentration: A Meta-Analytic Test of Current Theories and Perceptions. Global Change Biology 5: 723-741

Warith, A., Zekry, W., Gawri, N., (1999). Effect of Leachate Recirculation on Municipal Solid Waste Biodegradation. Journal of Canada Water Quality Research. 34: 267–280

Westlake, K. (1995). Landfill In: Hester, R.E., Harrison, R.M. (Eds.), Waste Treatment and Disposal. The Royal Society of Chemistry, Herts, Cambridge

Whalen, S.C., Reeburgh, W.S., Sandbeck, K.A. (1990). Rapid Methane Oxidation in a Landfill Coversoil. Appl. Environ. Microbiol. 56:3405-3411

Wheless, E., Wiltsee, G. (2001). Demonstration Test of the Capstone Microturbine on Landfill Gas. In Proceedings 24th SWANA Annual Landfill Gas Symposium, Dallas, Texas

Wikipedia (2006). Fuzzy Sets retrieved (2006) on the URL: http://en.wikipedia.org/wiki/Fuzzy_sets

Wilson S., Shuttleworth A. (2002). Design and Performance of a Passive Dilution Gas Migration Barrier. Ground Engineering (retrieved 2004) at: http://www.epg-ltd.co.uk/paperge2002/papergroundeng2002.htm

Wong, S.C. (1979). Elevated Atmospheric Partial Pressure of CO_2 and Plant Growth. I. Interaction of Nitrogen Nutrition and Photosynthetic Capacity in C_3 and C_4 Plants. Oecologia 44: 68-74

Woodrow L., Liptay A., Grodzinski B. (1987). The Effects of CO_2 Enrichment and Ethephon Application on The Production of Tomato Transplants. Acta Hort. 201:133-140

Yager, R. R., & Filev, D. P. (1994). Essentials of fuzzy modeling and control, New York: Wiley.

Zak, D.R., Pregitzer, K.S., Curtis, P.S., Terri, J.A., Fogel, R., Randlet, D.L., (1993). Elevated Atmospheric CO_2 and Feedback between Carbon and Nitrogen Cycles. Plant Soil 151: 105-117

APPENDIX

A1. EXPERIMENTAL DATA AND ANALYSIS

Table 1: Data and Average Error on Figure 4.1

$Q(cm^3/s)$	$H_{Lsoil}(cm)$	$H_{Lsand}(cm)$	$H_{Lpolymer}(cm)$	$H_{Lcoarse}(cm)$
0	0	0	0	0
2.23	0.8	0.9	0.1	0.2
4.45	2.4	3.5	0.15	0.25
6.68	6.5	7.5	0.25	0.4
8.9	13	16	0.3	0.5
11.13	14	17	0.35	0.6
Avg Error	0.2	0.2	0.02	0.02

Table 2: Data and Average Error on Figure 4.2

∇PH(cm/cm)	Q/A(cm/s)
0	0
6.25E-03	0.029
9.38E-03	0.0375
1.56E-02	0.049
1.88E-02	0.0578
Avg Error	0.002

Table 3: Data and Average Error on Figure 4.3

T (°C)	K CO_2	KCH_4	DCH_4	DCO_2
0	7.2	3.6	0.167	0.094
15	6.8	2.9	0.184	0.1
25	6.35	2.69	0.195	0.11
Avg Error	0.02	0.02	0.002	0.002

Table 4: Data and Average Error on Figure 4.4

Porosity	KCH_4	KCO_2
0.8	1.96	4.6
0.85	2.13	5
0.9	2.3	5.4
0.95	2.48	5.8
0.98	2.58	6.1
Avg Error	0.02	0.02

Table 5: Data and Average Error on Figure 4.5

Water Content %	KCH_4	KCO_2
0.2	2.33	5.47
0.3	2.32	5.45
0.5	2.3	5.42
1	2.26	5.32
3	2.09	4.93
Avg Error	0.021	0.05

Table 6: Data and Average Error on Figure 4.6

Porosity	DCH_4	DCO_2
0.8	0.167	0.09
0.85	0.18	0.1
0.9	0.195	0.11
0.95	0.21	0.118
Avg Error	0.005	0.005

Table 7: Data and Average Error on Figure 4.7

Water content %	DCO_2	DCH_4
0.1	0.11	0.196
0.2	0.11	0.195
0.3	0.109	0.194
0.5	0.108	0.193
1	0.106	0.189
3	0.099	0.175
10	0.07	0.13
Avg Error	0.005	0.007

Table 8: Calculated Data on Figure 4.8

	FLUX					
∇C	T25 (CH_4)	T15 (CH_4)	T0 (CH_4)	T25 (CO_2)	T15 (CO_2)	T0 (CO_2)
0	0	0	0	0	0	0
0.25	0.04875	0.046	0.04175	0.0275	0.025	0.0235
0.5	0.0975	0.092	0.0835	0.055	0.05	0.047
0.75	0.1463	0.138	0.1253	0.0825	0.075	0.0705
1	0.195	0.184	0.167	0.11	0.1	0.094

Table 9: Calculated Data on Figure 4.9

	FLOW					
∇P	T25 (CH_4)	T15 (CH_4)	T0 (CH_4)	T25 (CO_2)	T15 (CO_2)	T0 (CO_2)
0	0	0	0	0	0	0
0.25	0.1046	0.1088	0.1275	0.089	0.0927	0.0932
0.5	0.209	0.2175	0.255	0.1799	0.1855	0.1865
0.75	0.3138	0.326	0.383	0.26998	0.2783	0.2797
1	0.418	0.435	0.51	0.3599	0.371	0.373

A2. FUZZY PERMISES AND RULES

A2.1. Biogas Diffusion Modeling

[System]
Name='Gases'
Type='mamdani'
Version=2.0
NumInputs=2
NumOutputs=2
NumRules=12
AndMethod='min'
OrMethod='max'
ImpMethod='min'
AggMethod='max'
DefuzzMethod='centroid'

[Input1]
Name='Conc.Grad'
Range=[0 1]
NumMFs=4
MF1='A':'trimf',[0 0 0.5]
MF2='D':'trimf',[0.75 1 1]
MF3='B':'trimf',[0 0.5 0.75]
MF4='C':'trimf',[0.5 0.75 1]

[Input2]
Name='T'
Range=[0 35]
NumMFs=3
MF1='low':'trimf',[0 0 21]
MF2='medium':'trimf',[0 21 35]
MF3='high':'trimf',[21 35 35]

[Output1]
Name='CO2xE-4(kg/m2.s)'
Range=[0 0.11]
NumMFs=12
MF1='1':'trimf',[0.0208068783068783 0.023 0.0243]
MF2='2':'trimf',[0.0247 0.0262 0.0277910052910053]
MF3='3':'trimf',[0.0272 0.0295 0.029537037037037]
MF4='4':'trimf',[0.0467 0.047 0.0484523809523809]
MF5='5':'trimf',[0.0495910052910053 0.0496910052910053 0.0516910052910053]
MF6='6':'trimf',[0.0536910052910053 0.0546910052910053 0.0556910052910053]
MF7='7':'trimf',[0.0688227513227513 0.0711 0.0718]
MF8='12':'trimf',[0.108074074074074 0.108074074074074 0.110074074074074]
MF9='11':'trimf',[0.0982 0.0999 0.100542328042328]
MF10='10':'trimf',[0.0920910052910053 0.0940910052910053 0.0944910052910053]
MF11='9':'trimf',[0.0813 0.0825 0.0839550264550264]
MF12='8':'trimf',[0.0738910052910053 0.0748910052910053 0.0766910052910053]

[Output2]
Name='CH4xE-4(kg/m2.s)'
Range=[0 0.195]
NumMFs=12
MF1='6':'trimf',[0.0962103174603175 0.0979 0.0979]
MF2='5':'trimf',[0.090084126984127 0.092884126984127 0.093184126984127]
MF3='7':'trimf',[0.122003968253968 0.125 0.125]
MF4='8':'trimf',[0.134900793650794 0.138 0.138]
MF5='3':'trimf',[0.048784126984127 0.050184126984127 0.050884126984127]
MF6='2':'trimf',[0.0441071428571429 0.0464 0.0468]
MF7='10':'trimf',[0.165853174603175 0.167 0.169]
MF8='4':'trimf',[0.0807 0.0834 0.0848611111111111]
MF9='9':'trimf',[0.145388888888889 0.146388888888889 0.147388888888889]
MF10='11':'trimf',[0.183547619047619 0.183547619047619 0.185547619047619]
MF11='1':'trimf',[0.0374 0.0407 0.0420436507936508]
MF12='12':'trimf',[0.192547619047619 0.193547619047619 0.194547619047619]

[Rules]
1 1, 1 11 (1) : 1
1 2, 2 6 (1) : 1
1 3, 3 5 (1) : 1
3 1, 4 8 (1) : 1
3 2, 5 2 (1) : 1
3 3, 6 1 (1) : 1
4 1, 7 3 (1) : 1
4 2, 12 4 (1) : 1
4 3, 11 9 (1) : 1
2 1, 10 7 (1) : 1
2 2, 9 10 (1) : 1

2 3, 8 12 (1) : 1

Table 1: CH_4 Diffusion at T = 25 °C on Figure 5.10

∇C (kg/m^3.m)	Fick's Law	Fuzzy Data	Experimental Data
0	0	0	0
0.25	0.04875	0.074	0.07
0.5	0.0975	0.094	0.09
0.75	0.1463	0.14	0.14
1	0.195	0.19	0.19

Correlation (Fuzzy: Exp) = 0.999554

Table 2: CO_2 Diffusion at T = 25 °C on Figure 5.11

∇C (kg/m^3.m)	Fick's Law	Fuzzy Data	Experimental Data
0	0	0	0
0.25	0.0275	0.0376	0.04
0.5	0.055	0.0525	0.05
0.75	0.0825	0.0778	0.08
1	0.11	0.102	0.1

Correlation (Fuzzy: Exp) = 0.998325

A2.2. Biogas Convection Modeling

```
[System]
Name='Gases2'
Type='mamdani'
Version=2.0
NumInputs=2
NumOutputs=2
NumRules=12
AndMethod='min'
OrMethod='max'
ImpMethod='min'
AggMethod='max'
DefuzzMethod='centroid'

[Input1]
Name='PressureGradient'
Range=[0 1]
NumMFs=4
MF1='A':'trimf',[0 0 0.5]
MF2='D':'trimf',[0.75 1 1]
```

MF3='B':'trimf',[0 0.5 0.75]
MF4='C':'trimf',[0.5 0.75 1]

[Input2]
Name='T'
Range=[0 35]
NumMFs=3
MF1='low':'trimf',[0 0 21]
MF2='medium':'trimf',[0 21 35]
MF3='high':'trimf',[21 35 35]

[Output1]
Name='CO2(cm/s)'
Range=[0 0.38]
NumMFs=12
MF1='1':'trimf',[0.0909275132275132 0.0912275132275132 0.0940275132275132]
MF2='2':'trimf',[0.093005291005291 0.093405291005291 0.096005291005291]
MF3='3':'trimf',[0.0878201058201058 0.0898201058201058 0.0918201058201058]
MF4='4':'trimf',[0.185063492063492 0.186063492063492 0.189063492063492]
MF5='5':'trimf',[0.181978306878307 0.181978306878307 0.186478306878307]
MF6='6':'trimf',[0.177005291005291 0.178005291005291 0.182005291005291]
MF7='7':'trimf',[0.277116402116402 0.281116402116402 0.283116402116402]
MF8='12':'trimf',[0.353 0.356 0.36]
MF9='11':'trimf',[0.36542328042328 0.37 0.37]
MF10='10':'trimf',[0.363005291005291 0.369005291005291 0.369005291005291]
MF11='9':'trimf',[0.268 0.269 0.271931216931217]
MF12='8':'trimf',[0.278957671957672 0.279957671957672 0.286957671957672]

[Output2]
Name='CH4(cm/s)'
Range=[0 0.51]
NumMFs=12
MF1='6':'trimf',[0.192480952380952 0.206080952380952 0.208680952380952]
MF2='5':'trimf',[0.208603174603175 0.215603174603175 0.215603174603175]
MF3='7':'trimf',[0.369793650793651 0.382793650793651 0.386793650793651]
MF4='8':'trimf',[0.318650793650794 0.331650793650794 0.332650793650794]
MF5='3':'trimf',[0.0937698412698413 0.101469841269841 0.105969841269841]
MF6='2':'trimf',[0.100350793650794 0.109350793650794 0.110350793650794]
MF7='10':'trimf',[0.490460317460317 0.504460317460317 0.510460317460317]
MF8='4':'trimf',[0.2394 0.2544 0.2554]
MF9='9':'trimf',[0.294698412698413 0.308698412698413 0.312698412698413]
MF10='11':'trimf',[0.438655555555556 0.438655555555556 0.449955555555556]
MF11='1':'trimf',[0.111468888888889 0.122688888888889 0.128888888888889]
MF12='12':'trimf',[0.410853968253968 0.418553968253968 0.426353968253968]

[Rules]
1 1, 1 11 (1) : 1
1 2, 2 6 (1) : 1
1 3, 3 5 (1) : 1
3 1, 4 8 (1) : 1
3 2, 5 2 (1) : 1
3 3, 6 1 (1) : 1
4 1, 7 3 (1) : 1
4 2, 12 4 (1) : 1
4 3, 11 9 (1) : 1
2 1, 10 7 (1) : 1
2 2, 9 10 (1) : 1
2 3, 8 12 (1) : 1

Table 3: CH_4 Convection at T = 25 °C on Figure 5.12

∇P ($N/m^2.m$)	Convection Formula	Fuzzy Data	Experimental Data
0	0	0	0
0.25	0.1046	0.158	0.16
0.5	0.209	0.208	0.2
0.75	0.3138	0.319	0.3
1	0.418	0.43	0.4

Correlation (Fuzzy: Exp) = 0.999367

Table 4: CO_2 Convection at T = 25 °C on Figure 5.13

∇P ($N/m^2.m$)	Convection Formula	Fuzzy Data	Experimental Data
0	0	0	0
0.25	0.089	0.142	0.14
0.5	0.1799	0.182	0.18
0.75	0.26998	0.279	0.3
1	0.3599	0.364	0.4

Correlation (Fuzzy: Exp) = 0.998219

A2.3. Intelligent Fuzzy Control

[System]
Name='gassystem3'
Type='mamdani'
Version=2.0
NumInputs=2
NumOutputs=1

```
NumRules=5
AndMethod='min'
OrMethod='max'
ImpMethod='min'
AggMethod='max'
DefuzzMethod='centroid'

[Input1]
Name='Pressure.Head'
Range=[-1 1]
NumMFs=3
MF1='suction':'gaussmf',[0.6 -2]
MF2='zero':'gaussmf',[0.6 0]
MF3='thrust':'gaussmf',[0.6 2]

[Input2]
Name='Velocity'
Range=[-0.1 0.1]
NumMFs=3
MF1='negative':'gaussmf',[0.03 -0.1]
MF2='zero':'gaussmf',[0.03 0]
MF3='positive':'gaussmf',[0.03 0.1]

[Output1]
Name='Valve.Openning'
Range=[-1 1]
NumMFs=5
MF1='close-fast':'trimf',[-1 -0.9 -0.8]
MF2='close-slow':'trimf',[-0.594708994708995 -0.494708994708995 -
0.394708994708995]
MF3='neutral':'trimf',[-0.1 0 0.1]
MF4='open-slow':'trimf',[0.2 0.3 0.4]
MF5='open-fast':'trimf',[0.8 0.9 1]

[Rules]
3 0, 5 (1) : 1
1 0, 1 (1) : 1
2 3, 4 (1) : 1
2 1, 2 (1) : 1
2 2, 3 (1) : 1
```

A3. GENETIC ALGORITHM OPTIMIZATION

Report generated on 12/26/05 at 02:06:38

ALGORITHM PARAMETERS:
Population: 80
Generations: 100
Selection Type: Sigma Scaling
Elitism: 5
Mutation Probability: 0.001
Reproduction Probability: 0.85
Selection Probability: 0.7
Regeneration Period: 10
Regeneration Percent: 10

EVOLUTION:

Generation	Mean	Std. Deviation	Mutations	Reproductions
0	-325.01	103.16	19	33
1	-309.38	126.49	16	34
2	-9.99E+70	2.00E+71	10	28
3	-287.76	150.26	13	33
4	-235.3	141.18	13	32
5	-180.77	114.03	4	36
6	-187.28	109.9	13	36
7	-155.11	78.061	5	37
8	-159.26	76.03	8	35
9	-151.67	75.31	18	34
10	-175.39	103.65	15	34
11	-155.56	87.813	12	31
12	-175	102.94	4	36
13	-156.67	82.598	10	32
14	-142.11	70.676	11	33
15	-139.29	67.142	13	34
16	-150.99	81.567	8	35
17	-153.23	88.999	7	35
18	-143.11	71.081	7	34
19	-149.19	78.686	6	36
20	-163.17	99.367	15	35
21	-144.78	75.982	12	37
22	-124.65	44.926	6	36
23	-127.15	48.777	10	35
24	-136.77	62.553	14	38
25	-148.54	76.777	6	35
26	-142.43	70.489	12	29
27	-139.66	64.004	11	35
28	-137.29	61.718	17	30

29	-137.04	65.687	17	33
30	-154.17	88.498	10	36
31	-131.82	55.804	8	37
32	-127.54	50.213	16	33
33	-143.08	75.384	14	30
34	-135.85	63.425	10	34
35	-137.29	68.147	17	32
36	-145.62	78.195	20	34
37	-149.13	78.947	12	35
38	-142.86	71.688	21	36
39	-134.43	61.967	12	35
40	-158.34	88.732	19	35
41	-162.91	103.12	13	34
42	-166.67	103.95	21	33
43	-155	91.355	12	33
44	-139.69	70.404	20	32
45	-135.6	63.822	17	35
46	-147.37	81.202	15	34
47	-153.23	89	9	35
48	-160	95.624	15	36
49	-146.27	77.114	12	34
50	-155.08	84.228	15	35
51	-158.07	93.284	14	33
52	-151.57	86.755	21	37
53	-1.22E+72	2.43E+72	15	35
54	-191.67	127.4	16	37
55	-173.14	113.02	12	33
56	-147.55	83.988	17	35
57	-151.57	91.666	11	35
58	-168.75	115.67	10	34
59	-186.44	131.15	10	29
60	-182.26	126.76	16	34
61	-176.12	115.33	11	31
62	-159.33	100.23	14	31
63	-162.72	108.12	11	33
64	-154.84	93.495	14	36
65	-139.07	70.684	10	37
66	-144.29	79.585	12	34
67	-173.02	117.77	13	37
68	-171.88	116.37	14	32
69	-157.82	99.106	12	35
70	-6.98E+145	1.40E+146	7	29
71	-228.58	160.12	10	35
72	-183.61	117.05	19	36
73	-166.67	101.07	13	32
74	-156.14	92.23	15	35
75	-175	108.82	17	37
76	-145.62	74.937	9	38

77	-146.67	75.932	9	35
78	-143.08	69.999	14	32
79	-133.88	58.857	13	35
80	-158.91	86.72	18	36
81	-144.29	75.734	19	34
82	-150.82	86.394	14	33
83	-147.62	78.34	20	37
84	-144.27	75.245	11	32
85	-148.08	81.07	13	34
86	-150	79.999	9	37
87	-139.4	66.666	18	28
88	-155.11	87.245	29	32
89	-150	81.818	14	31
90	-168.66	99.864	17	32
91	-150	80.327	10	34
92	-159.33	92.051	13	37
93	-145.17	75.515	10	31
94	-137.71	65.355	23	36
95	-130.16	54.48	16	35
96	-4.80E+157	9.59E+157	14	32
97	-5.13E+157	1.03E+158	14	35
98	-5.88E+164	1.18E+165	6	31
99	-1.13E+158	2.21E+158	10	37
100	-8.24E+157	1.63E+158	11	36

Generation	Optimum Fenotype	Optimum Solution
0	1 z^2+-0.242 z^1+-0.0868/1 z^2+-1.13 z^1+0.198 //	0.000609
1	1 z^2+-0.242 z^1+-0.0868/1 z^2+-1.13 z^1+0.198 //	0.000609
2	1 z^2+-0.242 z^1+-0.0868/1 z^2+-1.13 z^1+0.198 //	0.000609
3	1 z^2+-0.242 z^1+-0.0868/1 z^2+-1.13 z^1+0.198 //	0.000609
4	1 z^2+-0.242 z^1+-0.0868/1 z^2+-1.13 z^1+0.198 //	0.000609
5	1 z^2+-0.242 z^1+-0.0868/1 z^2+-1.13 z^1+0.198 //	0.000609
6	1 z^2+-0.242 z^1+-0.0868/1 z^2+-1.13 z^1+0.198 //	0.000609
7	1 z^2+-0.242 z^1+-0.0868/1 z^2+-1.13 z^1+0.198 //	0.000609
8	1 z^2+-0.242 z^1+-0.0868/1 z^2+-1.13 z^1+0.198 //	0.000609
9	1 z^2+-0.242 z^1+-0.0868/1 z^2+-1.13 z^1+0.198 //	0.000609

10	1 z^2+-0.242 z^1+-0.0868/1 z^2+-1.14 z^1+0.206 //	0.000588
11	1 z^2+-0.242 z^1+-0.0868/1 z^2+-1.14 z^1+0.206 //	0.000588
12	1 z^2+-0.242 z^1+-0.0868/1 z^2+-1.14 z^1+0.206 //	0.000588
13	1 z^2+-0.242 z^1+-0.0868/1 z^2+-1.14 z^1+0.206 //	0.000588
14	1 z^2+-0.242 z^1+-0.0868/1 z^2+-1.14 z^1+0.206 //	0.000588
15	1 z^2+-0.242 z^1+-0.0868/1 z^2+-1.14 z^1+0.206 //	0.000588
16	1 z^2+-0.242 z^1+-0.0868/1 z^2+-1.14 z^1+0.206 //	0.000588
17	1 z^2+-0.242 z^1+-0.0868/1 z^2+-1.14 z^1+0.206 //	0.000588
18	1 z^2+-0.242 z^1+-0.0868/1 z^2+-1.14 z^1+0.206 //	0.000588
19	1 z^2+-0.242 z^1+-0.0868/1 z^2+-1.14 z^1+0.206 //	0.000588
20	1 z^2+-0.242 z^1+-0.0868/1 z^2+-1.14 z^1+0.206 //	0.000588
21	1 z^2+-0.242 z^1+-0.0868/1 z^2+-1.14 z^1+0.206 //	0.000588
22	1 z^2+-0.242 z^1+-0.0868/1 z^2+-1.14 z^1+0.206 //	0.000588
23	1 z^2+-0.242 z^1+-0.0868/1 z^2+-1.14 z^1+0.206 //	0.000588
24	1 z^2+-0.242 z^1+-0.0868/1 z^2+-1.14 z^1+0.206 //	0.000588
25	1 z^2+-0.242 z^1+-0.0868/1 z^2+-1.14 z^1+0.206 //	0.000588
26	1 z^2+-0.242 z^1+-0.0868/1 z^2+-1.14 z^1+0.206 //	0.000588
27	1 z^2+-0.242 z^1+-0.0868/1 z^2+-1.14 z^1+0.206 //	0.000588
28	1 z^2+-0.242 z^1+-0.0868/1 z^2+-1.14 z^1+0.206 //	0.000588
29	1 z^2+-0.242 z^1+-0.0868/1 z^2+-1.14 z^1+0.206 //	0.000588
30	1 z^2+-0.242 z^1+-0.0868/1 z^2+-1.14 z^1+0.206 //	0.000588
31	1 z^2+-0.242 z^1+-0.0868/1 z^2+-1.14 z^1+0.206 //	0.000588
32	1 z^2+-0.242 z^1+-0.0868/1 z^2+-1.14 z^1+0.206 //	0.000588
33	1 z^2+-0.242 z^1+-0.0868/1 z^2+-1.14 z^1+0.206 //	0.000588
34	1 z^2+-0.242 z^1+-0.0868/1 z^2+-1.14 z^1+0.206 //	0.000588
35	1 z^2+-0.242 z^1+-0.0868/1 z^2+-1.14 z^1+0.206 //	0.000588
36	1 z^2+-0.242 z^1+-0.0868/1 z^2+-1.14 z^1+0.206 //	0.000588

37	1 z^2+-0.242 z^1+-0.0868/1 z^2+-1.14 z^1+0.206 //	0.000588
38	1 z^2+-0.242 z^1+-0.0868/1 z^2+-1.14 z^1+0.206 //	0.000588
39	1 z^3+-0.682 z^2+0.0198 z^1+0.0382/1 z^3+-1.9 z^2+1.07 z^1+-0.155 //	0.000554
40	1 z^3+-0.682 z^2+0.0198 z^1+0.0382/1 z^3+-1.9 z^2+1.07 z^1+-0.155 //	0.000554
41	1 z^3+-0.682 z^2+0.0198 z^1+0.0382/1 z^3+-1.9 z^2+1.07 z^1+-0.155 //	0.000554
42	1 z^3+-0.682 z^2+0.0198 z^1+0.0382/1 z^3+-1.9 z^2+1.07 z^1+-0.155 //	0.000554
43	1 z^3+-0.682 z^2+0.0198 z^1+0.0382/1 z^3+-1.9 z^2+1.07 z^1+-0.155 //	0.000554
44	1 z^3+-0.682 z^2+0.0198 z^1+0.0382/1 z^3+-1.9 z^2+1.07 z^1+-0.155 //	0.000554
45	1 z^3+-0.682 z^2+0.0198 z^1+0.0382/1 z^3+-1.9 z^2+1.07 z^1+-0.155 //	0.000554
46	1 z^3+-0.682 z^2+0.0198 z^1+0.0382/1 z^3+-1.9 z^2+1.07 z^1+-0.155 //	0.000554
47	1 z^3+-0.682 z^2+0.0198 z^1+0.0382/1 z^3+-1.9 z^2+1.07 z^1+-0.155 //	0.000554
48	1 z^3+-0.682 z^2+0.0198 z^1+0.0382/1 z^3+-1.9 z^2+1.07 z^1+-0.155 //	0.000554
49	1 z^3+-0.682 z^2+0.0198 z^1+0.0382/1 z^3+-1.9 z^2+1.07 z^1+-0.155 //	0.000554
50	1 z^3+-0.682 z^2+0.0198 z^1+0.0382/1 z^3+-1.9 z^2+1.07 z^1+-0.155 //	0.000554
51	1 z^3+-0.682 z^2+0.0198 z^1+0.0382/1 z^3+-1.9 z^2+1.07 z^1+-0.155 //	0.000554
52	1 z^3+-0.682 z^2+0.0198 z^1+0.0382/1 z^3+-1.9 z^2+1.07 z^1+-0.155 //	0.000554
53	1 z^3+-0.682 z^2+0.0198 z^1+0.0382/1 z^3+-1.9 z^2+1.07 z^1+-0.155 //	0.000554
54	1 z^3+-0.682 z^2+0.0198 z^1+0.0382/1 z^3+-1.9 z^2+1.07 z^1+-0.155 //	0.000554
55	1 z^3+-0.682 z^2+0.0198 z^1+0.0382/1 z^3+-1.9 z^2+1.07 z^1+-0.155 //	0.000554

56	1 z^3+- 0.682 z^2+0.0198 z^1+0.0382/1 z^3+- 1.9 z^2+1.07 z^1+-0.155 //	0.000554
57	1 z^3+- 0.682 z^2+0.0198 z^1+0.0382/1 z^3+- 1.88 z^2+1.03 z^1+-0.141 //	0.000504
58	1 z^3+- 0.682 z^2+0.0198 z^1+0.0382/1 z^3+- 1.88 z^2+1.03 z^1+-0.141 //	0.000504
59	1 z^3+- 0.682 z^2+0.0198 z^1+0.0382/1 z^3+- 1.88 z^2+1.03 z^1+-0.141 //	0.000504
60	1 z^1+0.888/1 z^1+-0.704 //	9.30E-05
61	1 z^1+0.888/1 z^1+-0.704 //	9.30E-05
62	1 z^1+0.888/1 z^1+-0.704 //	9.30E-05
63	1 z^1+0.888/1 z^1+-0.704 //	9.30E-05
64	1 z^1+0.888/1 z^1+-0.704 //	9.30E-05
65	1 z^1+0.888/1 z^1+-0.704 //	9.30E-05
66	1 z^1+0.888/1 z^1+-0.704 //	9.30E-05
67	1 z^1+0.888/1 z^1+-0.704 //	9.30E-05
68	1 z^1+0.888/1 z^1+-0.704 //	9.30E-05
69	1 z^1+0.888/1 z^1+-0.704 //	9.30E-05
70	1 z^1+0.888/1 z^1+-0.704 //	9.30E-05
71	1 z^1+0.888/1 z^1+-0.704 //	9.30E-05
72	1 z^1+0.888/1 z^1+-0.704 //	9.30E-05
73	1 z^1+0.888/1 z^1+-0.704 //	9.30E-05
74	1 z^1+0.888/1 z^1+-0.704 //	9.30E-05
75	1 z^1+0.888/1 z^1+-0.704 //	9.30E-05
76	1 z^1+0.888/1 z^1+-0.704 //	9.30E-05
77	1 z^1+0.888/1 z^1+-0.704 //	9.30E-05
78	1 z^1+0.888/1 z^1+-0.704 //	9.30E-05
79	1 z^1+0.888/1 z^1+-0.704 //	9.30E-05
80	1 z^1+0.888/1 z^1+-0.704 //	9.30E-05
81	1 z^1+0.888/1 z^1+-0.704 //	9.30E-05
82	1 z^1+0.888/1 z^1+-0.704 //	9.30E-05
83	1 z^1+0.888/1 z^1+-0.704 //	9.30E-05
84	1 z^1+0.888/1 z^1+-0.704 //	9.30E-05
85	1 z^1+0.888/1 z^1+-0.704 //	9.30E-05
86	1 z^1+0.888/1 z^1+-0.704 //	9.30E-05
87	1 z^1+0.888/1 z^1+-0.704 //	9.30E-05
88	1 z^1+0.888/1 z^1+-0.704 //	9.30E-05
89	1 z^1+0.888/1 z^1+-0.704 //	9.30E-05
90	1 z^1+0.888/1 z^1+-0.704 //	9.30E-05
91	1 z^1+0.888/1 z^1+-0.704 //	9.30E-05
92	1 z^1+0.888/1 z^1+-0.704 //	9.30E-05
93	1 z^1+0.888/1 z^1+-0.704 //	9.30E-05
94	1 z^1+0.888/1 z^1+-0.704 //	9.30E-05
95	1 z^1+0.888/1 z^1+-0.704 //	9.30E-05
96	1 z^1+0.888/1 z^1+-0.704 //	9.30E-05
97	1 z^1+0.888/1 z^1+-0.704 //	9.30E-05

98	1 z^1+0.888/1 z^1+-0.704 //	9.30E-05
99	1 z^1+0.888/1 z^1+-0.704 //	9.30E-05
100	1 z^1+0.888/1 z^1+-0.704 //	9.30E-05

OPTIMUM SOLUTION:
Input 1: 1 z^1+0.888/1 z^1+-0.704
Objective Function = 9.30E-05